Dissertation zur Erlangung des Doktorgrades
der Fakultät für Chemie und Pharmazie
der Ludwig-Maximilians-Universität München

Development of an Oxidation Stress Testing Workflow for High-Throughput Liquid Formulation Screening of Therapeutic Antibodies

Paulina Luisa Fischer
aus
Kaiserslautern
2025

Erklärung

Diese Dissertation wurde im Sinne von § 7 der Promotionsordnung vom 28. November 2011 von Herrn / Frau Prof. Dr. Olivia Merkel betreut.

Eidesstattliche Versicherung

Diese Dissertation wurde eigenständig und ohne unerlaubte Hilfe erarbeitet.

Ludwigshafen, 21. März 2025

_____

Paulina Luisa Fischer

Dissertation eingereicht am:	28.03.2025
1.Gutachterin:	Prof. Dr. Olivia Merkel
2.Gutachter:	Prof. Dr. Wolfgang Frieß
Mündliche Prüfung am:	16.05.2025

TABLE OF CONTENT

LIST OF ABBREVIATIONS 1

II. OXIDATION OF THERAPEUTIC ANTIBODIES & HIGH THROUGHPUT SCREENING APPROACHES 5

1. Preface: Therapeutic Antibody Products 5
2. Oxidation of therapeutic antibody products 6
   - 2.1. Causes of oxidation, mechanisms and biological consequences 6
   - 2.2. Forced oxidation studies 9
   - 2.3. Analytical techniques for oxidation detection 10
   - 2.4. Mitigation strategies 11
   - 2.5. Prediction models 12
3. Formulation development of biologics 13
   - 3.1. High throughput screening (HTS) 13
   - 3.2. Integration of oxidation stress testing in HTS: advantages and challenges 15
4. References 17

III. AIM OF THIS THESIS 23

IV. OPTIMIZATION OF ANALYTICAL TECHNIQUES FOR OXIDATION DETECTION IN A HIGH THROUGHPUT WORKFLOW 25

1. Introduction 25
2. Materials 27
3. Methods 27
   - 3.1. Proteolytic digest 27
   - 3.2. Preparation of oxidized samples 29
   - 3.3. Reversed-Phase Chromatography (RP) 29
   - 3.4. Size Exclusion Chromatography (SEC) 29
   - 3.5. HT Analytical Protein A Chromatography 29
4. Results & Discussion 31
   - 4.1. Optimization of proteolytic digestion step 31
   - 4.2. Protein A – HTS conditions 36
5. Conclusion 39
6. References 40

V. DETERMINATION OF HIGH THROUGHPUT OXIDATION SCREENING PARAMETERS 43

1. Introduction 43
2. Materials 44
3. Methods 45
   - 3.1. Preparation of oxidized samples 45
   - 3.2. Quenching of oxidation reactions 46
   - 3.3. Reversed-Phase Chromatography Subunit Analysis (RP) 46
   - 3.4. Size Exclusion Chromatography (SEC) 47
   - 3.5. Cation Exchange Chromatography (CEX) 47
   - 3.6. Protein A Chromatography 47
4. Results & Discussion 48
   - 4.1. HTS suitable approach for oxidation quenching 48
   - 4.2. Selection of oxidation levels 49
   - 4.3. Peroxide-based oxidation stress 50
   - 4.4. Free radical oxidation assay (AAPH) 52
   - 4.5. Visible light and UV-A radiation assays 53
   - 4.6. Metal catalyzed oxidation assay (MCO) 54
   - 4.7. Assay variability 56
5. Conclusion 58
6. References 59

VI. DEVELOPMENT OF A HIGH-THROUGHPUT OXIDATION PROFILING STRATEGY FOR MONOCLONAL ANTIBODY PRODUCTS 61

Abstract 61

1. Introduction 62
2. Materials 64
3. Methods 65
   - 3.1. Preparation of oxidized samples 65
   - 3.2. High throughput analytical methods 66
4. Results 70
   - 4.1. Aggregation and fragmentation 70
   - 4.2. Charge isoforms 71
   - 4.3. Oxidation of methionine and tryptophan residues 71
   - 4.4. Modification of Fc and Fab subunits 74

5. Discussion 77
5.1. Selection of HT screening methods 77
5.2. Impact of oxidation 79
6. Conclusion 83
7. References 84

VII. ANTIBODY OXIDATION AND IMPACT OF FORMULATION: A HIGH THROUGHPUT SCREENING APPROACH 89
Abstract 89
1. Introduction 90
2. Materials 92
3. Methods 92
3.1. Experimental design 92
3.2. Preparation of drug substance and excipient stock solutions 93
3.3. Formulation compounding 94
3.4. Oxidation stress 94
3.5. Size Exclusion Chromatography (SEC) 95
3.6. Reversed-Phase Chromatography Subunit Analysis (RP) 95
3.7. Polysorbate Quantitation by AEX/RP mixed mode HPLC with charged aerosol detection (CAD) 96
3.8. LC/MS peptide Mapping 96
3.9. Data evaluation, oxidation scoring and formulation ranking 97
4. Results & Discussion 99
4.1. Impact of buffer and pH 99
4.2. Impact of protein concentration 104
4.3. Impact of surfactant 106
4.4. Impact of additional excipients 107
4.5. Evaluation of formulation impact in high throughout data sets 109
5. Conclusion 112
6. References 113
7. Supplementary data 117

VIII. SUMMARY OF THE THESIS 121

LIST OF ABBREVIATIONS

AAPH - 2,2'-Azobis(2-amidinopropane) dihydrochloride

ADCC - Antibody-dependent cellular cytotoxicity

AEX - Anion Exchange Chromatography

AGC - Automatic Gain Control

CAD - Charged aerosol detection

CD - Circular Dichroism

CDR - Complementarity-determining region

CEX - Cation Exchange Chromatography

CP – Citrate phosphate

CQA - Critical quality attributes

DAD – Diode array detector

DTT - Dithiothreitol

DSC - Differential Scanning Calorimetry

DTPA - Diethylenetriaminepentaacetic acid

EDTA - Ethylenediaminetetraacetic acid

Fab – Fragment antigen-binding

Fc - Fragment crystallizable region

FcγR - Fc gamma receptor

FcRn - Neonatal Fc receptor

GSH – reduced glutathion

HC – Heavy chain

HCl - Hydrochloric acid

HIC - Hydrophobic interaction chromatography

His - Histidine

HP - Hydrogen peroxide

HPLC - High-Performance Liquid Chromatography

HMW – Higher molecular weight

HT - High throughput

HTS - High throughput screening

icIEF - Imaged capillary isoelectric focusing

ICH - International Council for Harmonisation

IdeS - Immunoglobulin G-degrading enzyme from *Streptococcus pyogenes*

IgG - Immunoglobulin G

ITFE - Intrinsic tryptophan fluorescence emission

klux - Kilolux (measurement of visible light exposure)

LC – Light Chain

LC-MS - Liquid chromatography-mass spectrometry

LED – Light-emitting diode

LMW – Lower molecular weight

mAb – Monoclonal Antibody

mAU – milli-absorbance units

MES - 2-(N-Morpholino)ethanesulfonic acid

Met - Methionine

MMP - Matrix metalloprotease

MCO - Metal-catalyzed oxidation

MWCO - Molecular weight cut-off

NaCl - Sodium chloride

NIST - National Institute of Standards and Technology

O/N – Over night

PBS - Phosphate buffered saline

PDA – Photodiode array detector

PES – Polyethersulfone

PS – Polystyrene

PS 80 / PS 20 – Polysorbate 80 / Polysorbate 20

QbD - Quality by design

Rel.Area% - relative area percentage

RP - Reversed-Rhase Chromatography

RT – Room temperature

ROS - Reactive oxygen species

SASA - Solvent accessible surface area

SEC - Size Exclusion Chromatography

SIA - Stability indicating attributes

Succ – Succinate

tBHP - tert-Butyl hydroperoxide

TCEP - Tris(2-carboxyethyl)phosphine hydrochloride

TFA - Trifluoroacetic acid

Tris - Tris(hydroxymethyl)aminomethane

Trp – Tryptophan

UF/DF - Ultrafiltration/Diafiltration

UHPLC - Ultra-High-Performance Liquid Chromatography

UV – Ultraviolet

UV-A – Ultraviolet A range (320-400 nm)

UV-VIS - Ultraviolet-visible spectroscopy

WCN - Water coordination number

WFI - Water for injection

I. OXIDATION OF THERAPEUTIC ANTIBODIES & HIGH THROUGHPUT SCREENING APPROACHES

1. Preface: Therapeutic Antibody Products

Biopharmaceuticals, including monoclonal antibody therapeutics, have become essential tools in disease treatment [1,2] . However, their large size and complex structure make them susceptible to physical and chemical degradation, including oxidation, which is the focus of this thesis [3–5] . As advancements in biotechnology and pharmaceutical science continue, the development of novel biotherapeutics broadens the scope of treatment options across a wide array of diseases. This growth brings increasing complexity in formulation development, as new biotherapeutics often possess unique structural and stability challenges. Consequently, ensuring structural integrity throughout production, storage, transport, and administration is critical, necessitating the identification of potential liabilities and an optimal formulation composition as a key part of biologic development.

The following sections will provide a brief introduction to the topic of "oxidation of therapeutic antibody products" and explore the potential for integrating oxidation stress testing within a high-throughput screening setup, along with the associated challenges.

2. Oxidation of therapeutic antibody products

Oxidation is one of the most common degradation pathways and a significant concern in the life cycle of biopharmaceuticals [6–9] . It occurs during manufacturing, transport, storage or patient administration and can result in a number of structural and biological consequences that may negatively affect the product. Hence, identification of oxidation risks, continuous analytical monitoring as well as the establishment of appropriate mitigation strategies is crucial to ensure the safety of a biopharmaceutical product.

2.1. Causes of oxidation, mechanisms and biological consequences

The individual oxidation susceptibility of a therapeutic protein is controlled by its intrinsic structure, mainly the amino acid sequence and the presence and localization of oxidation prone amino acid residues. Certain amino acids are known to be especially susceptible to oxidation, including methionine, tryptophan, cysteine, histidine and tyrosine [7–10] . Depending on their position in the 3D structure, and consequently their accessibility for oxidants, the protein is more or less prone to oxidation. Apart from intrinsic factors, the oxidation potential is influenced by various extrinsic parameters. Those extrinsic factors include the product formulation, but also external triggers such as reactive contaminations, leachables or degradation products derived from the manufacturing process or unsuitable environmental conditions during processing, storage and handling (Figure I-1). However, unlike intrinsic prerequisites, which are identified and eliminated prior to selection of a candidate molecule, external oxidation risks should be detected, monitored, and reduced within later stages of the drug product development process.

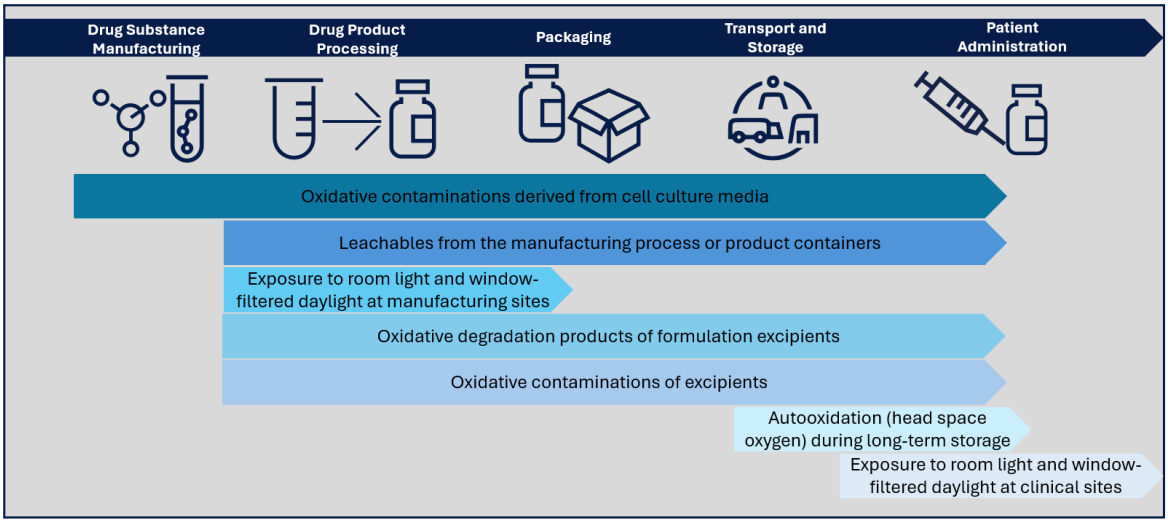

Figure I-1: Environmental oxidation risks in the life cycle of a therapeutic antibody product

Formulation excipients can equally decrease or increase the oxidation risk of therapeutic proteins. The targeted application of formulation components to reduce the oxidation risk will be covered in section 2.4. Conversely, an increased oxidation risk associated with the formulation is often connected to the degradation of excipients themselves. A well-known example in this context are polysorbates, which are frequently used as surfactants in protein formulations [11]. Degradation of polysorbates via oxidation results in H_2O_2 formation, potentially initiating oxidation processes of the protein [12,13]. Impurities of excipients in the protein formulation, for example traces of metal ions, can also initiate oxidation processes in the protein. Besides those specific examples, the overall stability of the product, which is mainly controlled by the formulation, has a great impact on oxidation susceptibility. An inappropriate formulation selection is therefore a major risk factor for chemical modifications like oxidation.

Apart from formulation derived contaminations, potential oxidation triggers are also introduced by the manufacturing process. In this context, one major oxidizing agent is hydrogen peroxide. Traces of hydrogen peroxide left after surface sterilization of the manufacturing equipment can contaminate the product. Hydrogen peroxide derived oxidation is based on a free radical initiated mechanism, starting with the formation of hydroxyl radicals [14]. Those highly reactive radicals further react with oxidation prone amino acid residues in the protein. The most susceptible target of hydrogen peroxide induced oxidation is methionine, which is oxidized to methionine sulfoxide or, under severe stress conditions, to methionine sulfone [10,15]. Oxidation of methionine, especially surface exposed residues located in the Fc fragment, are linked to a variety of biological consequences for therapeutic antibodies such as reduced protein A and FcRn binding, decreased conformational stability and reduced half-life [8,16,17].

Furthermore, traces of metal irons, such as iron or copper, have often been described as an initiator for metal-catalyzed oxidation (MCO) [15,18]. Contamination with metal ions can be caused by leaching from steel tanks in the manufacturing process [19]. Metal catalyzed oxidation is initiated by reduction of the metal ion to its lower oxidation state, often in presence of a reducing agent. The metal ions then react with oxygen, leading to formation of multiple reactive oxygen species (ROS) which in turn oxidize susceptible targets in the protein [7,20]. MCO often results in changes of the protein structure as well as increased aggregation and/or particle formation [8,21].

Oxidation processes can also be caused by exposure to light. Biopharmaceuticals are exposed to light in the visible and UV-A range during multiple stages of their life cycle, such as manufacturing, packaging or use of the product. Light-induced oxidation occurs via two main mechanisms, known as type I and type II oxidation pathway (Figure I-2).

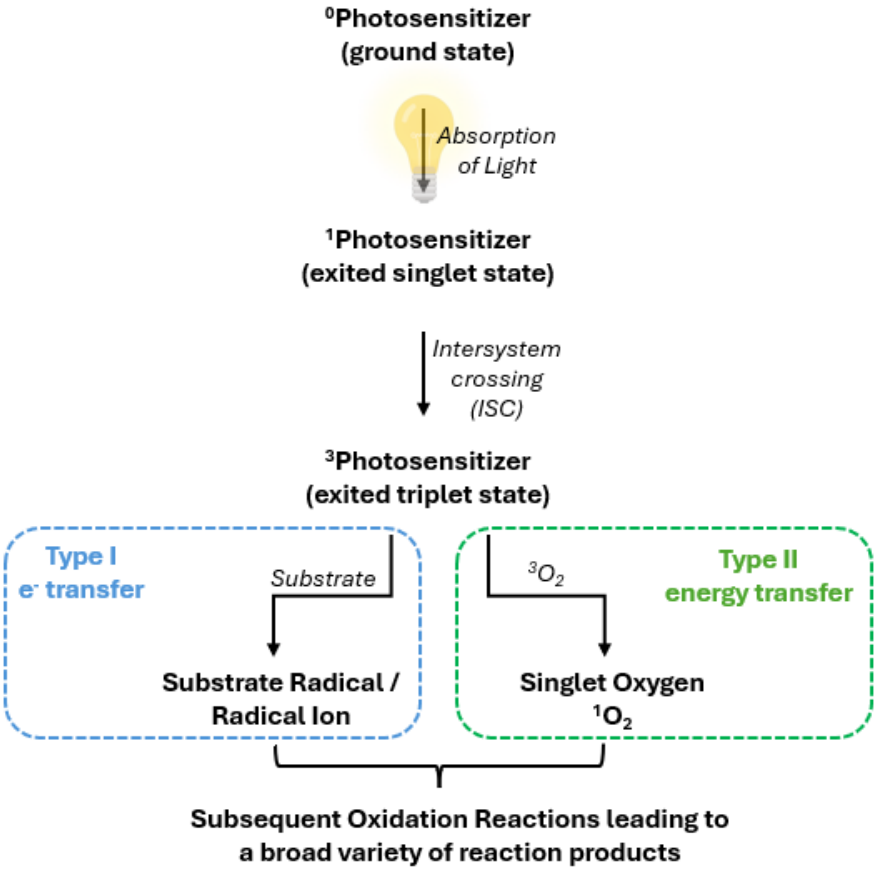

Figure I-2: Photooxidation Pathways: Generation of oxidation products via type I (electron transfer) or type II (energy transfer). Visualization adapted from Hipper et al. [22]

Photo-oxidation is initiated through absorption of light by a photosensitizer, for example aromatic amino acid residues, especially tryptophan, or non-proteinogenic compounds derived from excipients, buffer components or cell culture impurities. While UV radiation can be absorbed by the protein itself due to aromatic amino acid residues, light induced oxidation in the visible range is most likely triggered by an external photosensitizer. The light absorption results in excitation of the photosensitizing compound to its singlet state, followed by conversion to the triplet state. From the triplet state, the photosensitizer returns to ground state by transferring an electron to a suitable substrate (type I – electron transfer) or by energy transfer to an oxygen molecule (type II – energy transfer). Type I oxidation pathway results in formation of free radicals and radical ions, while the energy transfer of

Type II oxidation pathway leads to formation of highly reactive singlet oxygen $^1O_2$. Both mechanisms initiate subsequent reactions promoting the formation of reactive oxygen species (ROS) and therefore result in a cascade of different degradation pathways [22–24]. Photooxidation of therapeutic proteins has been described for multiple light sources, under accelerated as well as more moderate ambient light conditions [25–27]. Furthermore, a recently published study also demonstrated that iron contaminations in combination with exposure to light in the visible range results in a photo-Fenton-reaction, leading to severe damage of the protein [28]. Common consequences are reduced stability and increased formation of aggregates [29,30]. Photooxidation of amino acids in the CDR region can also negatively impact the biological activity of the product [31].

Oxidation attributed solely to oxygen exposure, even under light-protected conditions, has also been reported, particularly during longer storage periods at elevated temperatures [32]. In these situations, the amount of oxygen in the vial's headspace or in the prefilled syringe is a relevant factor that should be considered.

2.2. Forced oxidation studies

Due to its complexity, oxidation remains a degradation pathway which needs to be individually assessed and comprehensively monitored. To ensure stability and therefore safety of the product, oxidation stress testing is an integral part of forced degradation studies and mandatory during early product development stages. The main purpose of these studies is the definition of critical quality attributes (CQAs) by identification of potential degradation pathways as well as the development of suitable analytical techniques to monitor the degradation [33].

In context of oxidation, the individual susceptibility of a molecule is commonly assessed by incubation with different hydrogen peroxide (HP) concentrations over a defined period of time [33,34]. Alternatively, incubations are performed with t-butyl hydroperoxide (tBHP). While both oxidizing agents initiate a similar oxidation mechanism, tBHP mainly oxidizes surface exposed methionine residues [35]. A different strategy to investigate the susceptibility towards free radical induced oxidation is the treatment with 2,2'-Azobis(2-amidinopropane) dihydrochloride (AAPH). The free radical generating compound produces alkoxyl and alkyl peroxyl radicals and is therefore a useful tool to simulate ROS initiated oxidation [36]. In contrast to peroxide-based oxidation treatments like HP or tBHP, the AAPH generated radicals can oxidize methionine as well as tryptophan residues [37,38]. In addition to chemical oxidation assays, the photosensitivity of a molecule is commonly assessed in light stress studies performed according to the *ICH Q1B - Photostability Testing of New Active*

Substances and Medicinal Products [39]. The guideline recommends exposure to 1200 klux*h of visible light and 200 Wh/m² of UV-A light, using either a light source that combines both (Option 1) or two individual light sources consecutively (Option 2). Photosensitivity testing should be conducted to identify potential degradation pathways and support analytical method development, but also to confirm stability under light conditions the product might be exposed to in its life cycle. However, while the ICH guideline Q1B provides a useful protocol for photostability testing of small molecules, those intense light doses will cause severe, non-representative degradation in biopharmaceuticals. Hence, light stress testing under more representative light conditions, suitable to assess the photostability of therapeutic proteins, is becoming more and more a focus of general interest [27,40].

Forced oxidation studies are a useful tool to evaluate the oxidation susceptibility of a candidate molecule and support the determination of potential oxidation mitigation strategies, if necessary. However, especially during early development stages, the drug substance availability is limited and therefore the experimental set up is often reduced to a small number of samples, not including all potential oxidation risks or relevant formulation parameters. Hence, the results from forced oxidation studies alone are not sufficient to generate a comprehensive picture of a protein's oxidation susceptibility.

2.3. Analytical techniques for oxidation detection

The extent of oxidation is conventionally identified and monitored using chromatographic techniques. Size exclusion chromatography (SEC) allows the detection of oxidation induced aggregation or fragmentation [30,41–46]. Other approaches include chromatographic separation techniques based on alterations in the hydrophobicity profile such as hydrophobic interaction chromatography (HIC) or changes in charge distribution detected via ion exchange chromatography or imaged capillary isoelectric focusing (icIEF) [42,43,46,47]. Furthermore, protein A chromatography has been described as an efficient method to identify oxidation of methionine residues in the Fc fragment of the antibody [41,42,48,49].

Apart from chromatographic methods, techniques focusing on structural analysis such as far and near-ultraviolet (UV) circular dichroism (CD) measurements [29,43] and differential scanning calorimetry (DSC) [29,46] or spectroscopic techniques like intrinsic tryptophan emission spectroscopy (ITFE) [29,44,46,50,51] are useful tools to detect oxidation in therapeutic proteins. However, those methods are often limited to the differentiation of intact and oxidized species and do not allow site specific quantification. For more detailed analysis of the protein structure, peptide mapping coupled to LC-MS has been established as the

preferred standard method [15,32,52,53]. The workflow includes proteolytic digest of the target protein into peptides, followed by reversed-phase separation and mass detection using LC/MS analysis. For larger sample sets, middle-out/middle down approaches based on limited proteolysis of antibodies offer a sufficient, less time-consuming alternative [54,55]. In contrast to the complete proteolytic cleavage in the peptide mapping workflow, those methods focus on the analysis of IgG subdomains generated via enzymatic digest followed by disulfide reduction.

For an additional functional characterization, to assess the consequences of oxidative stress, FcRN or receptor binding assays, ADCC assay or cell-based bioactivity assays are performed [17,18,38,43]. In general, for an in-depth assessment of oxidation and its consequences, the combination of multiple analytical techniques is required.

2.4. Mitigation strategies

The continuous monitoring and evaluation of oxidation risks facilitates the establishment of appropriate mitigation strategies, if required. Depending on the source of oxidation, those strategies could include the reduction of light exposure or the introduction of less harmful light sources during the manufacturing process [26,56]. The selection of appropriate storage conditions, such as low temperatures, light-protective environments and suitable packaging that reduces the oxygen exposure and has no or minimal risk for reactive leachables, can further reduce the risk of oxidation [6].

Apart from optimization of manufacturing and storage conditions, the oxidation risk can also be mitigated by formulation adjustments. Common strategies include the addition of antioxidative excipients like methionine or metal chelators like EDTA or DTPA [15,53,57]. Marketed products containing metal chelating agents include Zevalin® (0.4 mg/ml DTPA), Opdivo® (0.008 mg/ml DTPA) or Ajovy™ (0.14 mg/ml EDTA) [57] . Products formulation with methionine as antioxidant are for example Actemra® (4.4 mg/ml), Phesgo™ (1.5 mg/ml) or Stelara™ (0.4 mg/ml) [57].

Other formulation parameters, such as the formulation buffer, pH, or the concentration of the therapeutic antibody product, have occasionally been identified as factors influencing oxidation potential [10,41,51,58]. Consequently, choosing an appropriate formulation should be considered an effective strategy for mitigation.

2.5. Prediction models

In the last years, several prediction tools have been established to support oxidation monitoring and mitigation. The oxidation susceptibility of individual methionine or tryptophan residues can be predicted based on structural accessibility using solvent accessible surface area (SASA) or water coordination number (WCN) models [31,32,59] . Furthermore, machine learning approaches, such as the random forest model, have been successfully applied for oxidation predictions [60,61] . Those models include various factors for accurate prediction, combining intrinsic descriptors such as SASA, secondary structure or neighboring amino acid residues as well as external factors like formulation buffer or pH. However, for efficient AI based prediction, extensive experimental data sets are the essential prerequisite.

3. Formulation development of biologics

The definition of the formulation composition for a therapeutic antibodies is a key element in ensuring stability of the product during processing and shelf life. However, due to increasing complexity of the molecules (e.g. antibody-drug-conjugates or bispecific proteins) and administration forms (e.g. ultra-high concentrated formulations), the collection of sufficient data and subsequent definition of the formulation design space becomes more and more challenging. In this context, high throughput screening approaches are an efficient tool to improve formulation development workflows.

3.1. High throughput screening (HTS)

In the last years, AbbVie has developed a robotized, fully automated high throughput liquid formulation screening (HTS) line (Figure I-3). This automation line enables a quality by design (QbD)-based formulation development approach by evaluating the combination and interaction of multidimensional input variables, such as different stress conditions and formulation excipient parameters, to define the formulation design space [62].

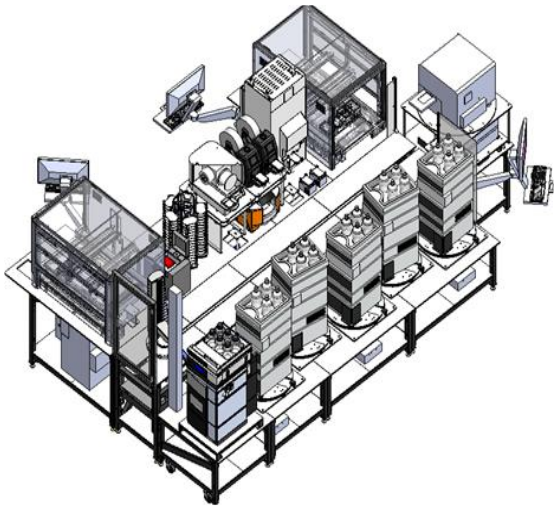

Figure I-3: HTS Screening Line

In a fully automated process, ensuring smooth operation of all components is essential for efficient data generation. Using standardized materials and harmonized workflows for sample processing, analytics, and data handling can significantly reduce error susceptibility. Additionally, employing analytical methods that are applicable to the majority of tested candidate molecules, along with maintaining identical stress conditions in each screening, ensures comparability across different datasets and molecules. Currently, protein stability is assessed in three different stress assays, simulating the “real-life” degradation risk of a

therapeutic protein. Those assays mimic freeze/thaw procedures during storage and transport, mechanical stress during manufacturing processes as well as incubation at storage (5 °C), accelerated and stress conditions (25 and 40 °C) as proposed by the ICH guidelines. The impact of different stress factors is identified and quantified by a variety of standardized HT methods. In addition to standardization, each of those methods is characterized by fast execution and low sample consumption. Suitable methods in the HTS context are mostly chromatography-based or plate reader analytics [63]. A high-level overview of the present HTS workflow applied in formulation development is shown in Figure I-4.

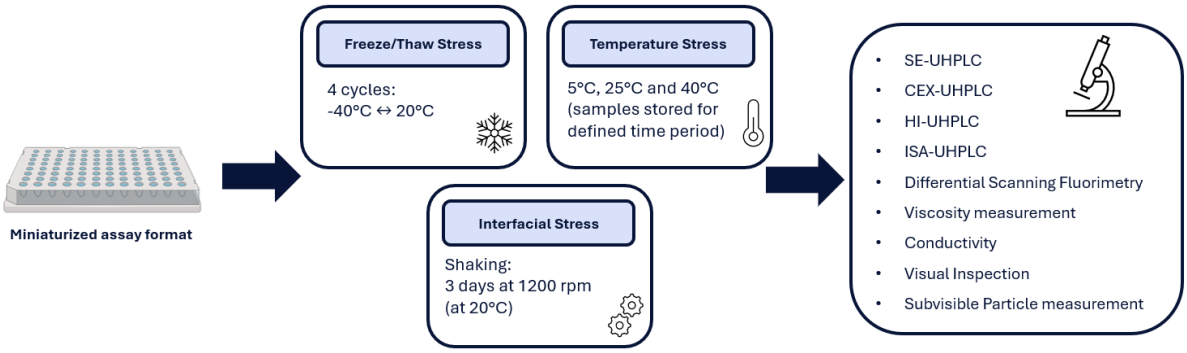

Figure I-4: Overview of the present HTS workflow

As in early development stages the drug substance availability is often limited, the HT-screenings are performed in a miniaturized assay format in multi-well plates. This approach requires only small amounts of the candidate protein per screening, enabling the testing of a broader range of conditions without being restricted by material availability. However, consequently all stress assays and analytical methods included in the screening must be optimized to operate effectively within the constraints of the plate-based format and low sample volume availability.

Furthermore, an efficient data management strategy is required throughout the whole screening process, starting from screening planning and set up, handling of analytical results to data storage. In the last step, evaluation of HT data sets is conducted by visualization and statistical analysis. In addition, a scoring tool has been developed to enable the comparison and ranking of different formulation compositions, supporting formulation recommendations. In a future perspective, those data sets also lay the groundwork for machine learning approaches and in silico formulation development. Compared to a standard manual formulation development approach, which is often limited to a reduced set of formulation compositions, automated HTS formulation development facilitates the generation of larger, multidimensional data sets within a shorter period.

3.2. Integration of oxidation stress testing in HTS: advantages and challenges

While the existing HTS workflow addresses the most common stress conditions, it currently does not include routine screenings for oxidation, potentially leaving liabilities in molecules undiscovered. As detailed in section 2 of this chapter, oxidation of therapeutic antibodies is initiated by various stressors and mechanisms. The HTS approach, which tests multiple stress and formulation conditions simultaneously, is therefore an ideal tool to evaluate the impact of different oxidation assays. Miniaturization and comprehensive analytical assessment allow for thorough evaluation of the oxidation susceptibility of individual candidate molecules. Furthermore, this approach enables the identification of formulation liabilities as well as potential mitigation strategies within a single screening process.

Figure I-5: Assay and method requirements for HTS integration

However, integrating an additional stress arm into the existing workflow presents challenges and requirements due to the complexity of the HTS screening line, as illustrated in Figure I-5. Each stress assay step must be fully automatable to operate within a robotic framework. Furthermore, to generate data efficiently, multiple process steps occur simultaneously, necessitating precise planning of each step—timing and required equipment included—to avoid unnecessary hold times that could adversely affect screening outcomes. Consequently, for any newly integrated oxidation stress assay, incubation times should be minimized to reduce potential interference with other process steps, particularly when

shared equipment, such as the HTS line's liquid handling systems, is involved. Despite the shortened incubation, it is crucial to induce a sufficient level of stress to effectively discriminate between different formulated samples. Another significant challenge is detecting oxidation in an HTS setup. Unfortunately, the existing chromatographic HTS methods alone are not sufficient to detect oxidation in proteins, necessitating the development and integration of additional methods. To meet HTS criteria, each method must be capable of analyzing molecules in a platform approach, feature short run times, and utilize low solvent consumption. Furthermore, as the HTS line has no mass spectrometry setup, the method development is limited to plate reader or UV-based chromatographic analytics. Finally, a data evaluation strategy is needed to assess the effects of oxidation independently, as well as within the context of the entire HTS screening setup.

In summary, integrating oxidation stress testing into the HTS workflow requires careful consideration of automation, analytical methods, and data evaluation to ensure comprehensive and efficient assessment of potential liabilities.

4. References

1. Lu RM, Hwang YC, Liu IJ, et al. Development of therapeutic antibodies for the treatment of diseases. *J Biomed Sci*. 2020;27(1):1.

2. Buss NA, Henderson SJ, McFarlane M, Shenton JM, Haan L de. Monoclonal antibody therapeutics: history and future. *Curr Opin Pharmacol*. 2012;12(5):615-622.

3. Manning MC, Chou DK, Murphy BM, Payne RW, Katayama DS. Stability of Protein Pharmaceuticals: An Update. *Pharm Res*. 2010;27(4):544-575.

4. Manning MC, Holcomb RE, Payne RW, et al. Stability of Protein Pharmaceuticals: Recent Advances. *Pharm Res*. 2024;41(7):1301-1367.

5. Krause ME, Sahin E. Chemical and physical instabilities in manufacturing and storage of therapeutic proteins. *Curr Opin Biotechnol*. 2019;60:159-167.

6. Gabrič A, Hodnik Ž, Pajk S. Oxidation of Drugs during Drug Product Development: Problems and Solutions. *Pharmaceutics*. 2022;14(2):325.

7. Grassi L, Cabrele C. Susceptibility of protein therapeutics to spontaneous chemical modifications by oxidation, cyclization, and elimination reactions. *Amino Acids*. 2019;51(10-12):1409-1431.

8. Torosantucci R, Schöneich C, Jiskoot W. Oxidation of Therapeutic Proteins and Peptides: Structural and Biological Consequences. *Pharm Res*. 2014;31(3):541-553.

9. Gupta S, Jiskoot W, Schöneich C, Rathore AS. Oxidation and Deamidation of Monoclonal Antibody Products: Potential Impact on Stability, Biological Activity, and Efficacy. *J Pharm Sci*. 2021;111(4):903-918.

10. Li S, Schöneich C, Borchardt RT. Chemical instability of protein pharmaceuticals: Mechanisms of oxidation and strategies for stabilization. *Biotechnol Bioeng*. 1995;48(5):490-500.

11. Weber J, Buske J, Mäder K, Garidel P, Diederichs T. Oxidation of polysorbates – An underestimated degradation pathway? *Int J Pharm: X*. 2023;6:100202.

12. Ha E, Wang W, Wang YJ. Peroxide formation in polysorbate 80 and protein stability. *J Pharm Sci*. 2002;91(10):2252-2264.

13. Kerwin BA. Polysorbates 20 and 80 used in the formulation of protein biotherapeutics: Structure and degradation pathways. *J Pharm Sci*. 2008;97(8):2924-2935.

14. Stadtman ER, Levine RL. Free radical-mediated oxidation of free amino acids and amino acid residues in proteins. *Amino Acids*. 2003;25(3-4):207-218.

15. Ji JA, Zhang B, Cheng W, Wang YJ. Methionine, tryptophan, and histidine oxidation in a model protein, PTH: Mechanisms and stabilization. *J Pharm Sci*. 2009;98(12):4485-4500.

16. Pan H, Chen K, Chu L, Kinderman F, Apostol I, Huang G. Methionine oxidation in human IgG2 Fc decreases binding affinities to protein A and FcRn. *Protein Sci*. 2009;18(2):424-433.

17. Wang W, Vlasak J, Li Y, et al. Impact of methionine oxidation in human IgG1 Fc on serum half-life of monoclonal antibodies. *Mol Immunol*. 2011;48(6-7):860-866.

18. Glover ZK, Wecksler A, Aryal B, et al. Physicochemical and biological impact of metal-catalyzed oxidation of IgG1 monoclonal antibodies and antibody-drug conjugates via reactive oxygen species. *mAbs*. 2022;14(1):2122957.

19. Zhou S, Schöneich C, Singh SK. Biologics Formulation Factors Affecting Metal Leachables from Stainless Steel. *AAPS PharmSciTech*. 2011;12(1):411-421.

20. Stadtman ER. Metal ion-catalyzed oxidation of proteins: Biochemical mechanism and biological consequences. *Free Radic Biol Med*. 1990;9(4):315-325.

21. Heinzl GA, Lai L, Rao VA. Differentiating the Effects of Oxidative Stress Tests on Biopharmaceuticals. *Pharm Res*. 2019;36(7):103.

22. Hipper E, Blech M, Hinderberger D, Garidel P, Kaiser W. Photo-Oxidation of Therapeutic Protein Formulations: From Radical Formation to Analytical Techniques. *Pharmaceutics*. 2022;14(1):72.

23. Schöneich C. Photo-Degradation of Therapeutic Proteins: Mechanistic Aspects. *Pharm Res*. 2020;37(3):45.

24. Kerwin BA, Remmele RL. Protect from light: Photodegradation and protein biologics. *J Pharm Sci*. 2007;96(6):1468-1479.

25. Wasylaschuk W, Pierce B, Geng X, et al. Assessing the Impact of Different Light Sources on Product Quality During Pharmaceutical Drug Product Manufacture – Fluorescent Versus Light-Emitting Diode Light. *J Pharm Sci*. 2020;109(11):3360-3369.

26. Du C, Barnett G, Borwankar A, et al. Protection of therapeutic antibodies from visible light induced degradation: Use safe light in manufacturing and storage. *Eur J Pharm Biopharm*. 2018;127:37-43.

27. Sreedhara A, Yin J, Joyce M, et al. Effect of ambient light on IgG1 monoclonal antibodies during drug product processing and development. *Eur J Pharm Biopharm*. 2016;100:38-46.

28. Schöneich C. Advanced Oxidation Processes in Pharmaceutical Formulations : Photo-Fenton Degradation of Peptides and Proteins. *International Journal of Molecular Sciences*. Published online 2022.

29. Shah DD, Zhang J, Maity H, Mallela KMG. Effect of photo-degradation on the structure, stability, aggregation, and function of an IgG1 monoclonal antibody. *Int J Pharm*. 2018;547(1-2):438-449.

30. Hernández-Jiménez J, Salmerón-García A, Cabeza J, Vélez C, Capitán-Vallvey LF, Navas N. The Effects of Light-Accelerated Degradation on the Aggregation of Marketed Therapeutic Monoclonal Antibodies Evaluated by Size-Exclusion Chromatography With Diode Array Detection. *J Pharm Sci*. 2016;105(4):1405-1418.

31. Bommana R, Chai Q, Schöneich C, Weiss WF, Majumdar R. Understanding the Increased Aggregation Propensity of a Light-Exposed IgG1 Monoclonal Antibody Using Hydrogen Exchange Mass Spectrometry, Biophysical Characterization, and Structural Analysis. *J Pharm Sci*. 2018;107(6):1498-1511.

32. Jacobitz AW, Liu Q, Suravajjala S, Agrawal NJ. Tryptophan Oxidation of a Monoclonal Antibody Under Diverse Oxidative Stress Conditions: Distinct Oxidative Pathways Favor Specific Tryptophan Residues. *J Pharm Sci*. 2021;110(2):719-726.

33. Nowak C, Cheung JK, Dellatore SM, et al. Forced degradation of recombinant monoclonal antibodies: A practical guide. *mAbs*. 2017;9(8):1217-1230.

34. Halley J, Chou YR, Cicchino C, et al. An Industry Perspective on Forced Degradation Studies of Biopharmaceuticals: Survey Outcome and Recommendations. *J Pharm Sci*. 2020;109(1):6-21.

35. Keck RG. *The Use of T-Butyl Hydroperoxide as a Probe for Methionine Oxidation in Proteins*.; 1996:56-62.

36. Dion MZ, Wang YJ, Bregante D, et al. The Use of a 2,2'-Azobis (2-Amidinopropane) Dihydrochloride Stress Model as an Indicator of Oxidation Susceptibility for Monoclonal Antibodies. *J Pharm Sci*. 2018;107(2):550-558.

37. Folzer E, diepold K, bomans K, et al. Selective Oxidation of Methionine and Tryptophan Residues in a Therapeutic IgG1 Molecule. *J Pharm Sci*. 2015;104(9):2824-2831.

38. Shah DD, Zhang J, Hsieh M ching, Sundaram S, Maity H, Mallela KMG. Effect of Peroxide- Versus Alkoxyl-Induced Chemical Oxidation on the Structure, Stability, Aggregation, and Function of a Therapeutic Monoclonal Antibody. *J Pharm Sci*. 2018;107(11):2789-2803.

39. Q1B undefined I. ICH Q1B Photostability Testing of New Active Substances and Medicinal Products. Published online 1998:1-9.

40. Luis LM, Hu Y, Zamiri C, Sreedhara A. Determination of the Acceptable Ambient Light Exposure during Drug Product Manufacturing for Long-Term Stability of Monoclonal Antibodies. *PDA J Pharm Sci Technol*. 2018;72(4):393-403.

41. Hipper E, Lehmann F, Kaiser W, et al. Protein photodegradation in the visible range? Insights into protein photooxidation with respect to protein concentration. *Int J Pharm: X*. 2023;5:100155.

42. Kaiser W, Schultz-Fademrecht T, Blech M, Buske J, Garidel P. Investigating photodegradation of antibodies governed by the light dosage. *Int J Pharm*. 2021;604:120723.

43. Qi P, Volkin DB, Zhao H, et al. Characterization of the photodegradation of a human IgG1 monoclonal antibody formulated as a high-concentration liquid dosage form. *J Pharm Sci*. 2009;98(9):3117-3130.

44. Zheng K, Ren D, Wang YJ, et al. Monoclonal Antibody Aggregation Associated with Free Radical Induced Oxidation. *Int J Mol Sci*. 2021;22(8):3952.

45. Fongaro B, Cian V, Gabaldo F, Paoli GD, Miolo G, Laureto PP de. Managing antibody stability: Effects of stressors on Ipilimumab from the commercial formulation to diluted solutions. *Eur J Pharm Biopharm*. 2022;176:54-74.

46. Alam ME, Slaney TR, Wu L, et al. Unique Impacts of Methionine Oxidation, Tryptophan Oxidation, and Asparagine Deamidation on Antibody Stability and Aggregation. *J Pharm Sci*. 2020;109(1):656-669.

47. Yang Y, Zhang F, Gan Y, et al. In-Depth Characterization of Acidic Variants Induced by Metal-Catalyzed Oxidation in a Recombinant Monoclonal Antibody. *Anal Chem*. 2023;95(14):5867-5876.

48. Loew C, Knoblich C, Fichtl J, et al. Analytical protein A chromatography as a quantitative tool for the screening of methionine oxidation in monoclonal antibodies. *J Pharm Sci*. 2012;101(11):4248-4257.

49. Gaza-Bulseco G, Faldu S, Hurkmans K, Chumsae C, Liu H. Effect of methionine oxidation of a recombinant monoclonal antibody on the binding affinity to protein A and protein G. *J Chromatogr B*. 2008;870(1):55-62.

50. Barnett GV, Balakrishnan G, Chennamsetty N, et al. Probing the Tryptophan Environment in Therapeutic Proteins: Implications for Higher Order Structure on Tryptophan Oxidation. *J Pharm Sci*. 2019;108(6):1944-1952.

51. Mason BD, Schöneich C, Kerwin BA. Effect of pH and Light on Aggregation and Conformation of an IgG1 mAb. *Mol Pharm*. 2012;9(4):774-790.

52. Xu C, Khanal S, Pierson NA, et al. Development, validation, and implementation of a robust and quality control-friendly focused peptide mapping method for monitoring oxidation of co-formulated monoclonal antibodies. *Anal Bioanal Chem*. 2022;414(29-30):8317-8330.

53. Thakkar SV, Rodrigues D, Zhai B, et al. Residue-Specific Impact of EDTA and Methionine on Protein Oxidation in Biotherapeutics Formulations Using an Integrated Biotherapeutics Drug Product Development Workflow. *J Pharm Sci*. 2023;112(2):471-481.

54. Zhang B, Jeong J, Burgess B, Jazayri M, Tang Y, Zhang YT. Development of a rapid RP-UHPLC–MS method for analysis of modifications in therapeutic monoclonal antibodies. *J Chromatogr B*. 2016;1032:172-181.

55. An Y, Zhang Y, Mueller HM, Shameem M, Chen X. A new tool for monoclonal antibody analysis. *mAbs*. 2014;6(4):879-893.

56. Allain LR, Pierce BC, Wuelfing WP, Templeton AC, Helmy R. In-Use Photostability Practice and Regulatory Evaluation for Pharmaceutical Products in an Age of Light-Emitting Diode Light Sources. *J Pharm Sci*. 2019;108(3):1172-1176.

57. Strickley RG, Lambert WJ. A review of Formulations of Commercially Available Antibodies. *J Pharm Sci*. 2021;110(7):2590-2608.e56.

58. Bai L, Zhang Y, Zhang C, et al. Investigation of excipients impact on polysorbate 80 degradation in biopharmaceutical formulation buffers. *J Pharm Biomed Anal*. 2023;233:115496.

59. Agrawal NJ, Dykstra A, Yang J, et al. Prediction of the Hydrogen Peroxide–Induced Methionine Oxidation Propensity in Monoclonal Antibodies. *J Pharm Sci*. 2018;107(5):1282-1289.

60. Delmar JA, Buehler E, Chetty AK, et al. Machine learning prediction of methionine and tryptophan photooxidation susceptibility. *Mol Ther Methods Clin Dev*. 2021;21:466-477.

61. Sankar K, Hoi KH, Yin Y, et al. Prediction of methionine oxidation risk in monoclonal antibodies using a machine learning method. *mAbs*. 2018;10(8):1281-1290.

62. Siedler M, Eichling S, Huelsmeyer M, Angstenberger J. Formulation Development for Biologics Utilizing Lab Automation and In Vivo Performance Models. In: Jameel" ["Feroz, Skoug" "John W, Nesbitt"] "Robert R, eds. *Development of Biopharmaceutical Drug-Device Products*. AAPS Advances in the Pharmaceutical Sciences Series, vol 35. Springer; 2020:299-341.

63. Samra HS, He F. Advancements in High Throughput Biophysical Technologies: Applications for Characterization and Screening during Early Formulation Development of Monoclonal Antibodies. *Mol Pharm*. 2012;9(4):696-707.

II. AIM OF THIS THESIS

While the HTS workflow considers the most common stress conditions, it currently does not include routine screenings for oxidation, leaving potential molecule liabilities (and in turn formulation remedies) undiscovered. The objective of this thesis is to develop a high-throughput oxidation screening approach that can be seamlessly integrated into an existing fully automated formulation screening workflow, incorporating representative stress assays in combination with efficient HT analytics, to comprehensively evaluate the oxidation susceptibilities of monoclonal antibody products, while also identifying formulation liabilities and potential mitigation strategies.

In the first part (Chapter III), the repertoire of HTS analytics was expanded by development and optimization of additional analytical workflows (RP-UHPLC subunit analysis and HT Protein A Chromatography) for detection of oxidation stress.

In the fourth chapter, appropriate assay parameters, such as oxidant concentrations and incubation times, within the HTS criteria were identified. An oxidation threshold was defined based on the outcome of an assay variability screening. Additionally, the chapter focuses on the definition of an HTS compatible oxidation quenching strategy to ensure standardization and comparability among different oxidation screenings.

The aim of the fifth chapter was the establishment of an HTS compatible profiling strategy for monoclonal antibody products, considering the most effective oxidation stress assays and HT analytics.

In the last part (Chapter VI), those findings were applied in a formulation screening considering common formulation parameters as well as antioxidative excipients, evaluating the ability of the established workflow to identify formulation impacts.

III. OPTIMIZATION OF ANALYTICAL TECHNIQUES FOR OXIDATION DETECTION IN A HIGH THROUGHPUT WORKFLOW

1. Introduction

To fully assess the extent of oxidation in therapeutic antibodies, the combination of multiple analytical techniques is required. However, as already discussed in the first chapter, due to the existing HTS framework and associated criteria for analytical methods, the selection of analytical techniques is limited to chromatographic methods with UV-A detection and plate reader analytics. While some of the existing methods, such as Size Exclusion Chromatography (SEC) and Cation Exchange Chromatography (CEX), are effective to detect the effects of oxidative damage (aggregation, fragmentation and changes in the charge profile) [1–4] , those methods alone are not sufficient to comprehensively characterize oxidation in mAbs. Hence, additional analytics are required to extend the HTS method portfolio for oxidation stress testing in the future.

Reversed-Phase Chromatography (RP) subunit analysis including UV detection of enzymatically digested antibodies has proven to be an effective alternative to LS-MS peptide mapping, for example if no mass spectrometry equipment is available or if a less-time consuming sample preparation and data evaluation is preferred [5,6] . Antibody subunits are generated by enzymatic cleavage in the hinge region followed by disulfide bond reduction. This generates three fragments: a heavy chain Fc fragment (Fc HC), light chain (LC) and a heavy chain Fd fragment (Fd HC), resulting in three individual peaks after chromatographic separation. As oxidation leads to changes in the hydrophobicity profile, changes can be easily detected and located to the affected fragment. Enzymatic digest is commonly performed using IdeS, an IgG-specific cysteine protease that cleaves IgG1 antibodies at a specific site below the hinge region [5–8] (Figure III-1). While IdeS has shown to be highly efficient, the presence of mutations in the hinge region might reduce or completely impair IdeS cleavage. Intended mutations in the hinge region of monoclonal antibody products, such as the LALA mutation, which involves changing leucine (L) residues at positions 234 and 235 to alanine (A), are often introduced to reduce the binding affinity to Fc gamma receptors (FcγRs) and therefore decrease undesired effector functions of the antibody [9,10] . While there are few marketed enzyme products suitable to

digest hinge-mutated mAbs, their application in a RP-UHPLC subunit analysis approach for oxidation analysis has not been described in literature so far. To meet the platformability criteria of the HTS workflow, it's essential to develop an optimized sample preparation process capable of digesting all potential antibody products in the pipeline, including those with hinge mutations. To achieve this, a variety of enzymes were evaluated to identify the most effective one for inclusion in the HTS RP method workflow.

Furthermore, since the initial signs of oxidation in IgG1 antibodies typically appear in the sensitive methionine residues within the Fc subunit, analytical protein A chromatography has become a well-established technique for detecting this specific Fc methionine oxidation. The method takes advantage of the strong affinity between the Fc region of antibodies and Protein A, which is used as the stationary phase in analytical Protein A chromatography. When the Fc-located methionine residues become oxidized, their affinity for Protein A is reduced [11,12] . As a result, oxidized monoclonal antibodies elute earlier during the chromatography process due to decreased binding capacity. The use of protein A chromatography for identifying oxidation in protein samples was first published by Loew et al. [13] and has since been successfully utilized in numerous other studies [3,4,14] . However, the methods described in literature typically involve longer run times per injection, which do not meet the HTS criteria of ≤ 15 minutes. Consequently, a new approach needs to be developed to make the method compatible with HTS requirements.

In summary, this chapter highlights the development of an HTS RP-UHPLC subunit analysis method, optimizing enzymatic digestion for hinge-mutated antibodies, as well as the adaptation of a published Protein A Chromatography method to create an HTS-compatible version.

2. Materials

Five monoclonal antibodies developed for therapy (referred to as mAb1, 3, 4, 5 & 6) of the isotype IgG1 were used in this study. All five antibodies were manufactured in-house. All antibodies were formulated in water for injection at a protein concentration of 100 mg/ml. Protein concentration was determined by UV-VIS spectroscopy (Stunner, Unchained Labs, Pleasanton, CA, USA). For analytical method development of the RP subunit analysis, mAb4 was selected as an exemplary antibody with hinge mutation (LALA), mAb3 was used as reference without mutation. Protein A chromatography experiments were initially conducted using mAb3, the platformability of the method was subsequently evaluated with mAbs 1, 4, 5 and 6.

Water for injection (WFI) Ampuwa® was purchased from Fresenius Kabi (Bad Homburg vor der Höhe, Germany). Hydrochloric acid (HCl), sodium chloride (NaCl), Tris(hydroxymethyl)-aminomethan (Tris), tert-Butyl hydroperoxide (tBHP), sodium sulfate (Na_2SO_4), sodium phosphate dibasic heptahydrate ($Na_2HPO_4 \cdot 7H_2O$), sodium phosphate dibasic dihydrate ($Na_2HPO_4 \cdot 2H_2O$), and acetonitrile gradient grade for liquid chromatography were purchased from Merck (Darmstadt, Germany). Hydrogen peroxide 30 % (H_2O_2), and 2,2-azo-bis-(2-amidinopropane) dihydrochloride (AAPH) were purchased from Sigma-Aldrich (St. Louis, MO). Dithiothreitol (DTT) was purchased from Fluorochem (Hadfield, UK), trifluoroacetic acid from VWR chemicals (Leuven, Belgium) and L-methionine from J.T. Baker (Radnor, PA, USA). Phosphate buffered saline (PBS 10x), matrix metalloproteases 3 and 12 were purchased from Thermo Fisher Scientific (Waltham, MA, USA). IgG-specific proteases FabRICATOR® (IdeS), FabALACTICA® and FabDELLO™ were obtained from Genovis AB (Lund, Sweden).

3. Methods

3.1. Proteolytic digest

To identify an one-fits-all enzymatic cleavage approach for subunit generation, four different proteases were evaluated, including two marketed products (FabALACTICA® and FabDELLO™, Genovis) as well as two matrix metalloproteases (MMP-3 and MMP-12). In contrast to IdeS (FabRICATOR®), FabALACTICA® and FabDELLO™ cleave in the upper hinge region. The cleavage site of MMP-3 and MMP-12 is located in the lower hinge region, but at a different position than the IdeS cleavage site [15–17] (Figure III-1).

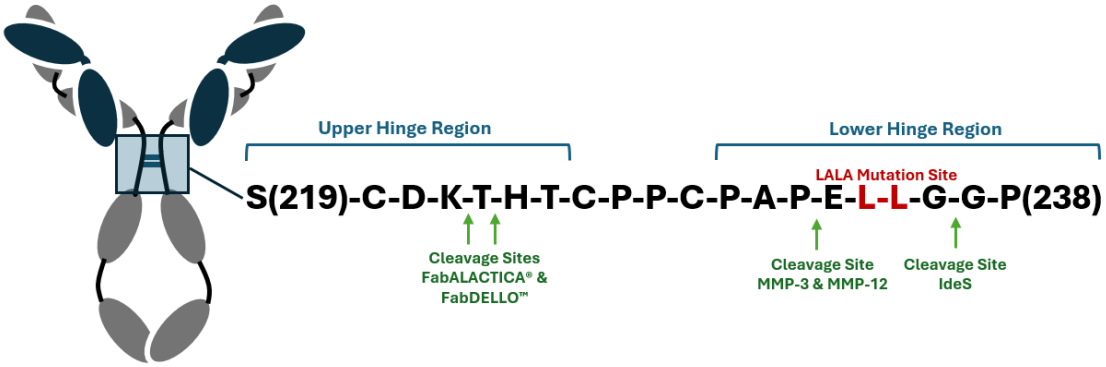

Figure III-1: Cleavage sites of different protases used in this study

The experimental conditions for each individual proteolytic digest performed in this study are summarized in Table III-1.

Table III-1: Experimental conditions for proteolytic cleavage experiments

Enzyme	Protein : Enzyme Ratio	Reconstitution buffer/solution	Digestion Buffer	Incubation	Co-Factor
IdeS (FabRICATOR®)	1 µg : 1 unit	WFI	WFI	0.5 h at 37 °C or 1 h at RT	n/a
FabALACTICA®	1 µg : 1 unit	WFI	Sodium Phosphate pH 7.0	O/N (16-18 h) at 37 °C	n/a
FabDELLO™	1 µg : 1 unit	Digestion buffer	Tris buffered saline (TBS), pH 7.6	2 h at 37 °C	10 mM $CaCl_2$
MMP-3	1 : 100 (v/v)	WFI	Tris buffered saline (TBS), pH 7.6	O/N (16-18 h) at 37 °C	n/a
MMP-12	1 : 100 (v/v)	WFI	Tris buffered saline (TBS), pH 7.6	O/N (16-18 h) at 37 °C	n/a

Selected enzymes were also analyzed using the oxidation quenching buffer (chapter IV) instead of digestion buffer.

3.2. Preparation of oxidized samples

Oxidized samples for RP-UHPLC subunit experiments were generated either by incubation with 0.05 % H_2O_2 or 150 mM AAPH, both for 1.5 h at RT. For Protein A Chromatography experiments samples were incubated with 1% H_2O_2 for 0.5, 1, 2, 3, 4, 5 or 24 h at RT.

3.3. Reversed-Phase Chromatography (RP)

The subunits generated via enzymatic cleavage were analyzed on an Agilent 1290 Infinity System (Agilent Technologies, Santa Clara, CA, USA) equipped with DAD detector using a BioResolve RP mAb Polyphenyl column 2.1 x 50 mm, 2.7 µm, 450 Å (Waters, Milford, MA, USA). Mobile phase A was water with 0.1% TFA, mobile phase B was acetonitrile with 0.1% TFA. 2 µg sample were injected to the column, separation was performed using a linear gradient from 25% - 45% mobile phase B over 4 min at a flow rate of 0.3 ml/min at 80 °C.

3.4. Size Exclusion Chromatography (SEC)

In addition to RP-UHPLC subunit analysis, SEC was performed to monitor the formation of mAb fragments due to enzymatic digest. For SEC analysis, 40 µg digested sample were injected to a Waters ACQUITY UPLC BEH200 SEC column 4.6 x 150 mm; 1.7 µm, 200 Å (Waters, Milford, MA, USA) and separated by isocratic elution using 100 mM Na_2HPO_4 / 200 mM Na_2SO_4, pH 7.0 at a flow rate of 0.4 ml/min for 6 min. The Column temperature was maintained at 25 °C.

3.5. HT Analytical Protein A Chromatography

All Protein A Chromatography experiments were performed on a Waters Aquity H-Class UHPLC system equipped with PDA detector, monitoring the signal at 280 nm. As the Protein A column used by Loew et al.[13] is not available anymore, experiments were conducted using the Thermo Scientific MAbPac Protein A column (4 x 35 mm, 12 µm). The flow rate was set to 0.2 ml/min. For analysis 2 µg was identified as suitable sample load on the column. Mobile phase A consisted of 50 mM sodium phosphate pH 7.5. To determine the ideal HTS conditions for analytical Protein A Chromatography, multiple gradients were tested. Furthermore, the impact of different mobile phase compositions was investigated. The exact experimental conditions are summarized in Table III-2 below. The overall runtime of the methods was 15 min, always including a 2-minute equilibration step

at the beginning to allow the antibody to bind to the column. To determine the lag time between injection and signal acquisition caused by the column delay volume, a method without gradient was included (V01).

Table III-2: Protein A Chromatography method development

Method Version	Mobile Phase A	Mobile Phase B	Gradient
V01	50 mM sodium phosphate + 150 mM NaCl, pH 7.5	50 mM sodium phosphate + 150 mM NaCl, pH 2.5	Time [min] / %B 0 / 0 2 / 0 2.5 / 100 5 / 100 5.5 / 0 10 / 0
V02	50 mM sodium phosphate + 150 mM NaCl, pH 7.5	50 mM sodium phosphate + 150 mM NaCl, pH 2.5	Time [min] / %B 0 / 0 2 / 0 8 / 40 9 / 100 9.5 / 100 10 / 0 15 / 0
V03	50 mM sodium phosphate + 150 mM NaCl, pH 7.5	50 mM sodium phosphate + 150 mM NaCl, pH 2.5	Time [min] / %B 0 / 0 2 / 0 8 / 60 9 / 100 9.5 / 100 10 / 0 15 / 0
V04	50 mM sodium phosphate + 500 mM NaCl, pH 7.5	50 mM sodium phosphate + 500 mM NaCl, pH 2.5	Time [min] / %B 0 / 0 2 / 0 8 / 60 9 / 100 9.5 / 100 10 / 0 15 / 0
V05	50 mM sodium phosphate + 500 mM NaCl, pH 7.5	50 mM sodium phosphate + 500 mM NaCl, pH 2.5	Time [min] / %B 0 / 0 2 / 0 2.01 / 70 2.5 / 70 9 / 100 9.5 / 100 10 / 0 15 / 0
V06	50 mM sodium phosphate + 150 mM NaCl, pH 7.5	50 mM sodium phosphate + 150 mM NaCl, pH 2.5	Time [min] / %B 0 / 0 2 / 0 2.01 / 70 2.5 / 70 9 / 100 9.5 / 100 10 / 0 15 / 0
V07	PBS buffer pH 7.5	PBS buffer pH 1.9	Time [min] / %B 0 / 0 2 / 0 2.01 / 50 2.5 / 50 9 / 100 9.5 / 100 10 / 0 15 / 0

4. Results & Discussion

4.1. Optimization of proteolytic digestion step

Proteolytic digestion was performed using four different enzymes to evaluate their ability to cleave hinge-mutated antibodies and replace IdeS in future RP-UHPLC experiments. Two commercially available proteases marketed for enzymatic digestion of IgG1 and two matrix metalloproteases (MMPs) with cleavage sites in the lower hinge region of mAbs were compared. Results of the proteolytic digest were analyzed using RP-UHPLC chromatography. For both MMPs the digest was insufficient for the hinge-mutated mAb4 as well as for mAb3, the control sample without mutation (Figure III-2).

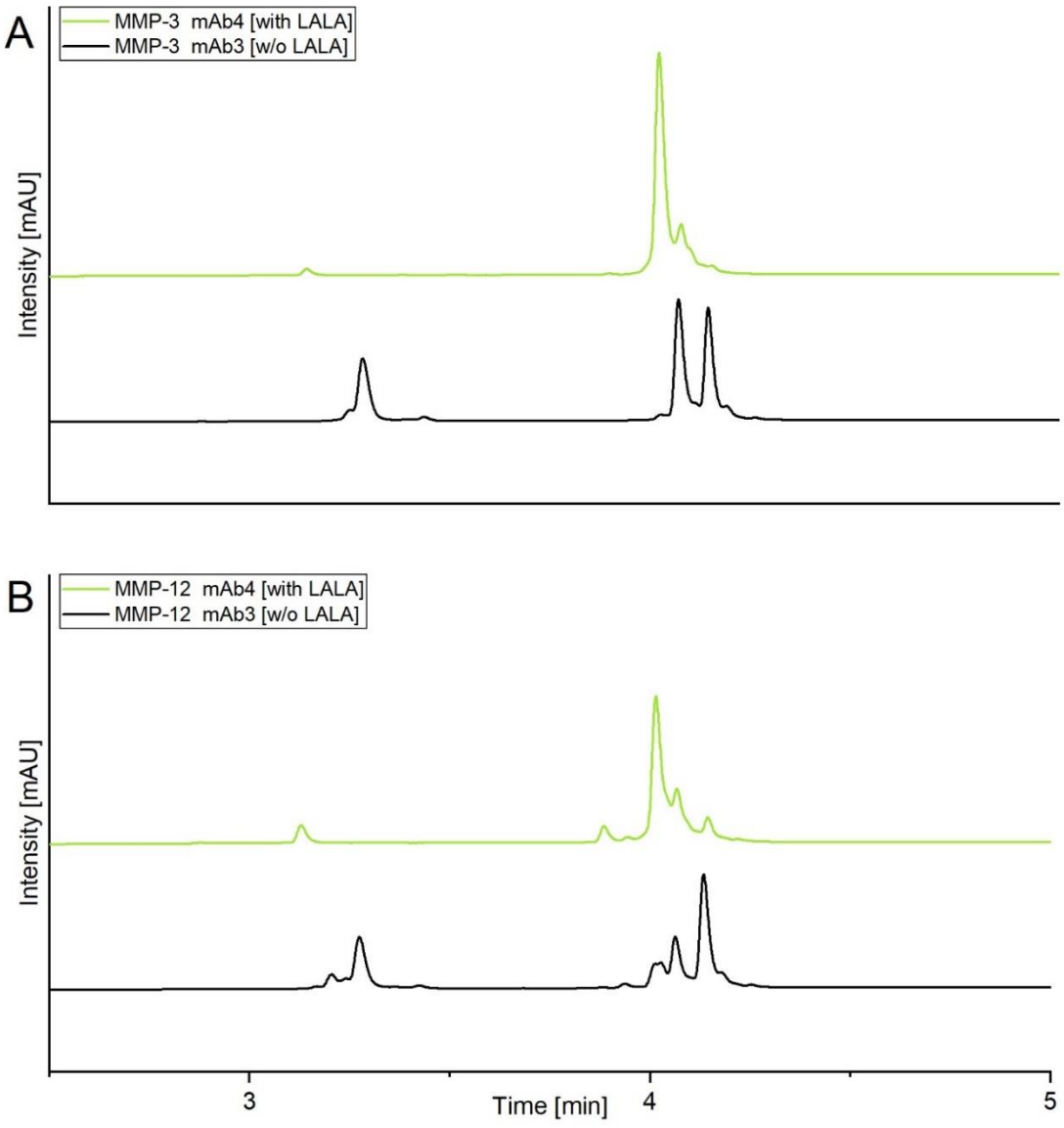

Figure III-2: Proteolytic Digestion of MMP-3 (A) and MMP-12 (B). RP chromatograms of the hinge-mutated mAb4 are displayed in green, while chromatograms of mAb3 are shown in black.

The chromatograms of MMP-3 digested mAbs (Figure III-2A) show a 3-peak-pattern, indicating uncomplete digestion. For the mAb4 (green) this effect is even more pronounced, with the first peak (Fc fragment) being nearly non-existent after digest. In the case of MMP-12 (Figure III-2B) the chromatogram shows additional formation of smaller peaks and peak shoulders. This could be an indicator for additional unspecific cleavage besides the main digestion site, leading to additional fragmentation. In summary, neither of the two MMPs is suitable for proteolytic digestion as a part of RP subunit analysis.

In contrast, both commercial proteases were able to cleave the hinge-mutated mAb4 and non-mutated mAb3 effectively under the conditions recommended by the manufacturer (Figure III-3). As the oxidation workflow required quenching of oxidation reactions (chapter IV) using free methionine, the efficiency of both enzymes in a 200 mM methionine solution was evaluated.

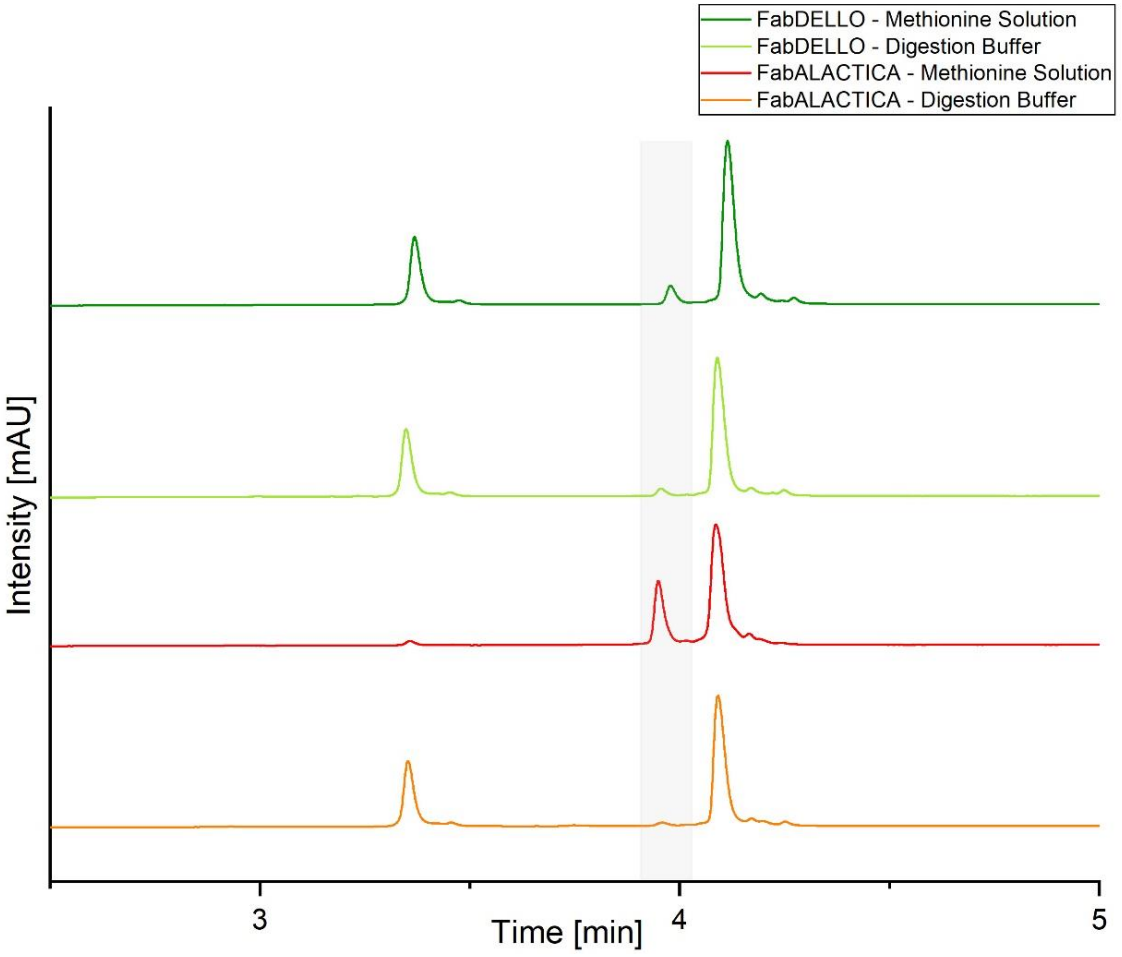

Figure III-3: Proteolytic digestion of FabDELLO™ and FabALACTICA® in the recommended digestion buffer or methionine solution. The light grey shaded area indicates the expected range for peaks originating from incompletely digested samples.

As illustrated in the chromatograms of Figure III-3, the performance of FabDELLO™ in methionine solution is only slightly decreased compared to the recommended digestion buffer, whereas the peak pattern of FabALACTICA® indicates incomplete digestion by an additional peak (red chromatogram). Therefore, as FabDELLO™ shows a preferable performance in the methionine quenching solution, only this protease was further evaluated.

To gain additional insights on the proteolytic cleavage kinetics of FabDELLO™, both antibodies were mixed with the enzyme mix and methionine solution and analyzed via SEC immediately. Figure III-4 illustrates the formation of the two subunits after 1, 2, 3 h and overnight (O/N) incubation at 37 °C sample manger temperature in the system.

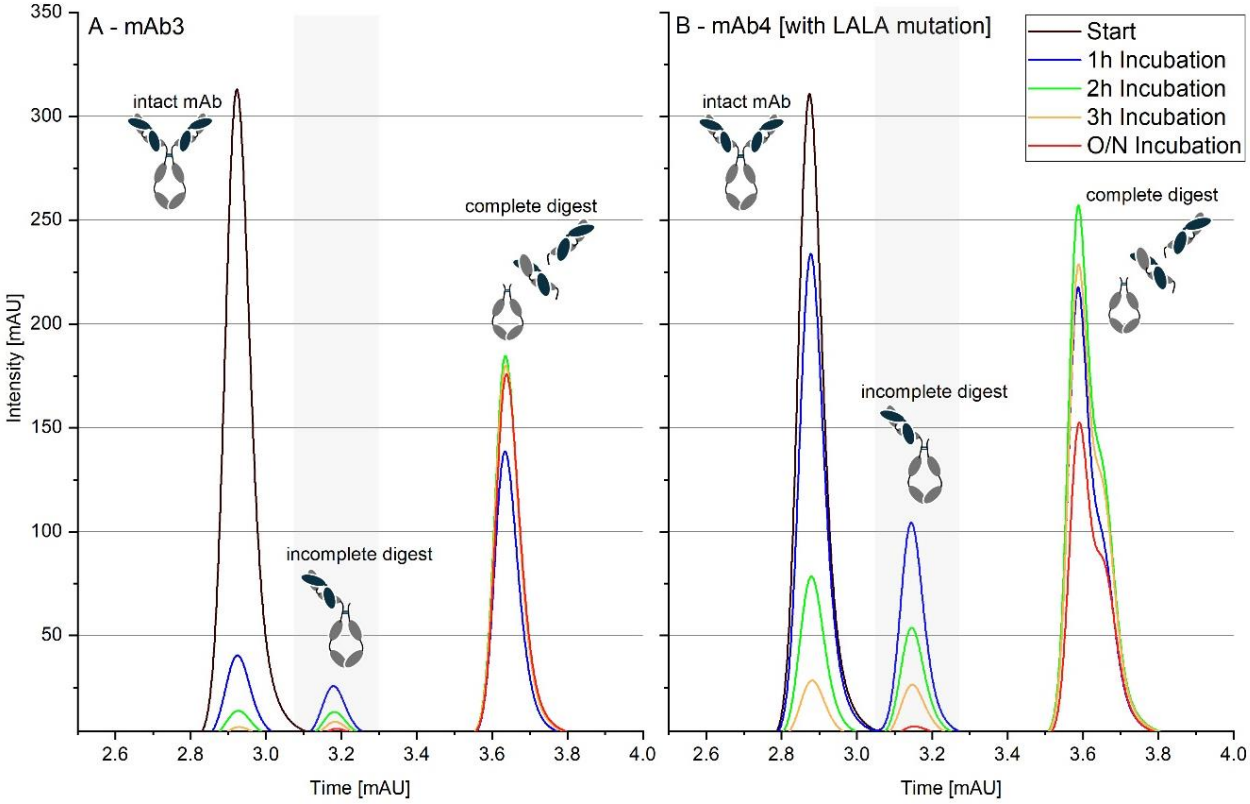

Figure III-4: SEC Analysis of FabDELLO™ cleavage. Results are shown for different incubation times: 1, 2, and 3 h, as well as overnight (O/N). The digest of mAb3 is displayed on the right (A), while mAb4 is presented on the left (B). The light grey shaded area indicates the expected range for peaks originating from incompletely digested samples.

After the recommended two-hour incubation (green chromatograms), both mAbs exhibited incomplete digestion, as indicated by the presence of a middle peak (highlighted in grey). This may result from suboptimal incubation conditions, as the recommended digestion buffer was not utilized. Following the overnight incubation, both mAbs are nearly fully

cleaved into subunits, with only negligible amounts of incompletely digested samples remaining. Interestingly, the overall cleavage process seems to be faster for the non-mutated mAb3. The chromatogram of the O/N digested mAb4 displays a reduced peak height compared to the previous injection. However, this reduction is most likely attributed to insufficient sample injection caused by the low sample volume, rather than being a result of the cleavage kinetics.

In summary, due to the findings of this experiment, an O/N incubation will be preferred. In addition, the methionine used for oxidation will be dissolved in TBS buffer pH 7.6 instead of water to further improve the performance of FabDELLO™.

Due to the different cleavage sites of IdeS (lower hinge region) and FabDELLO™ (upper hinge region), slightly different fragments are generated[18] (Figure III-5).

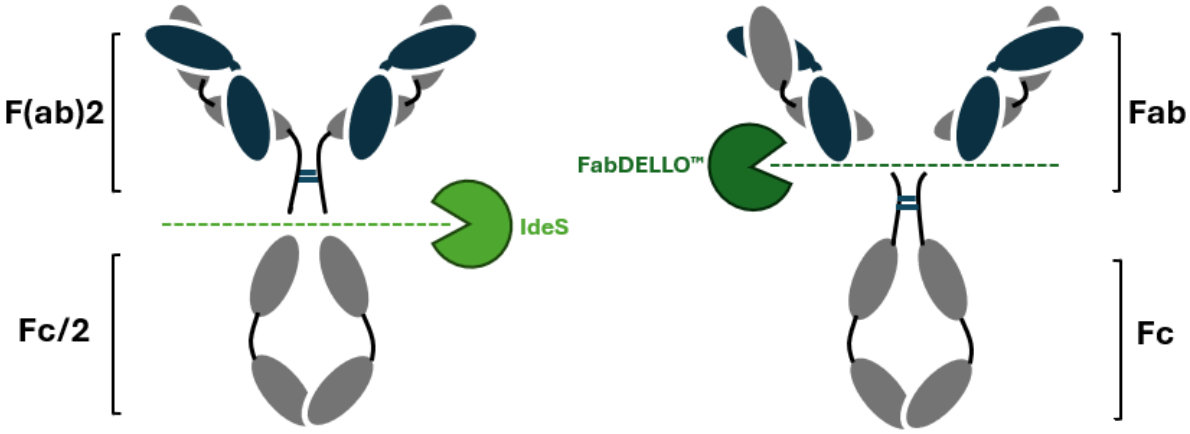

Figure III-5: Enzymatic subunit generation: IdeS vs. FabDELLO™

Consequently, the fragments show varying hydrophobicity profiles, leading to distinct peak patterns following RP separation. While for mAb4 the peak separation after FabDELLO™ digest is acceptable, the retention times of the mAb3 peaks are too close to ensure successful automated Chromeleon integration in the HTS workflow, especially for oxidized samples. This was also observed for other mAbs without hinge mutation (data not shown). Therefore, different gradients and column lengths were tested in order to increase the space between the two peaks and improve peak separation. However, none of the tested approaches was sufficient (data not shown). They either resulted in poorer peak shape or had no impact on the space between both peaks and only changed their overall retention time in the chromatogram. As a result, to achieve optimal separation conditions following proteolytic digestion, it is necessary to use two different enzymes depending on the presence of mutations in the hinge region. Although this approach does not fully meet the HTS platformability criteria, no alternative options are currently available.

To improve the comparison between subunits generated with different enzymes, an additional disulfide bond reduction step was added. Disulfide bond reduction further reduces the size of the fragments and changes their hydrophobicity profile; therefore, a better peak separation can be achieved. Figure III-6 illustrates the final results achieved by using the appropriate enzyme for each mAb, based on the presence of a hinge mutation, followed by a disulfide bond reduction step.

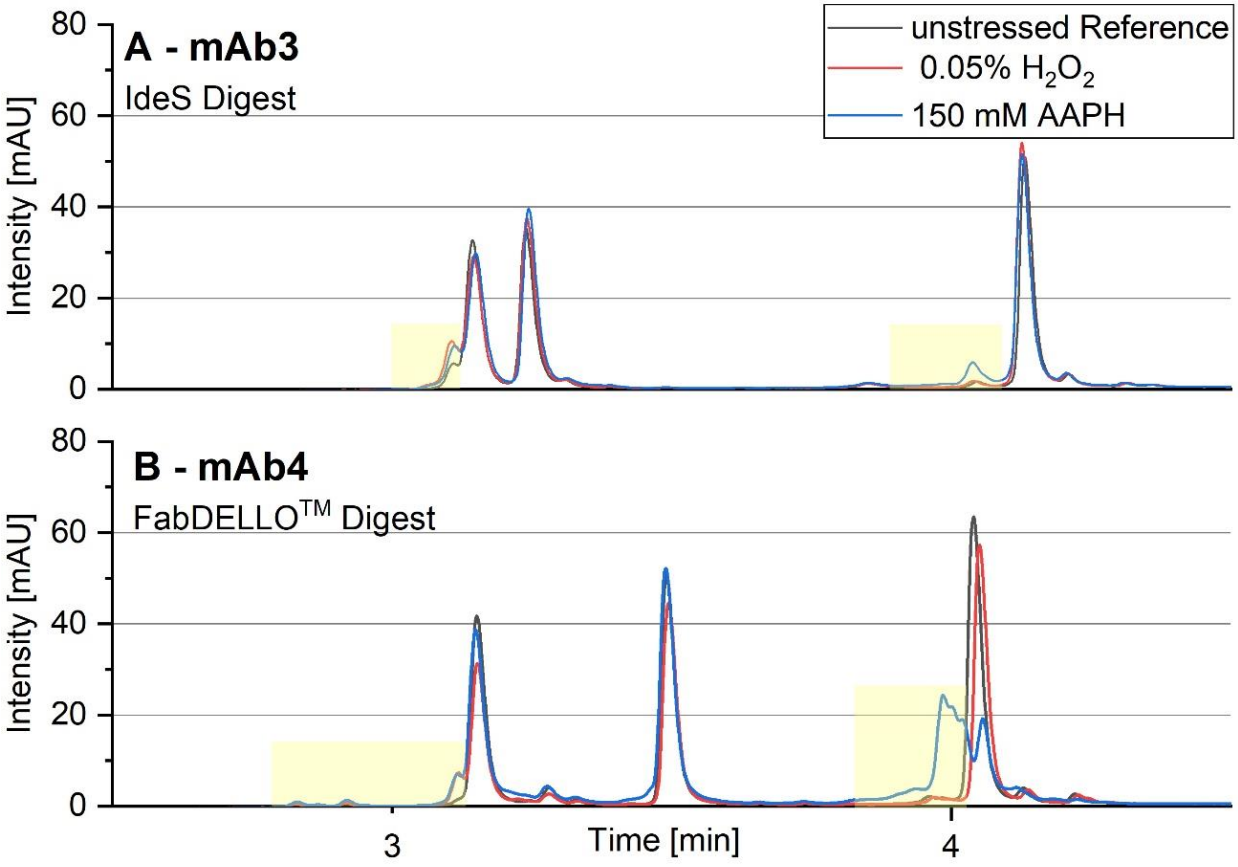

Figure III-6: Enzymatic cleavage followed by disulfide bond reduction. Chromatograms of mAb3 (A) and mAb4 (B) are displayed. Each shows unstressed samples (black), along with oxidized samples treated with 0.05% H2O2 (red) and 150 mM AAPH (blue). The light-yellow shaded area indicates the expected range for additional peaks and peak shoulders generated through oxidation.

Sufficient peak separation for unstressed and oxidized samples (0.05% H_2O_2 or 150 mM AAPH) was detected for both antibodies, allowing the detection of oxidation induced changes in the most relevant areas of the chromatogram, as highlighted in yellow.

4.2. Protein A – HTS conditions

To identify the ideal conditions to perform analytical Protein A Chromatography within the HTS time criteria of max. 15 min analysis time per sample, different methods were tested varying gradients and mobile phase compositions. The results are summarized in Figure III-7 below.

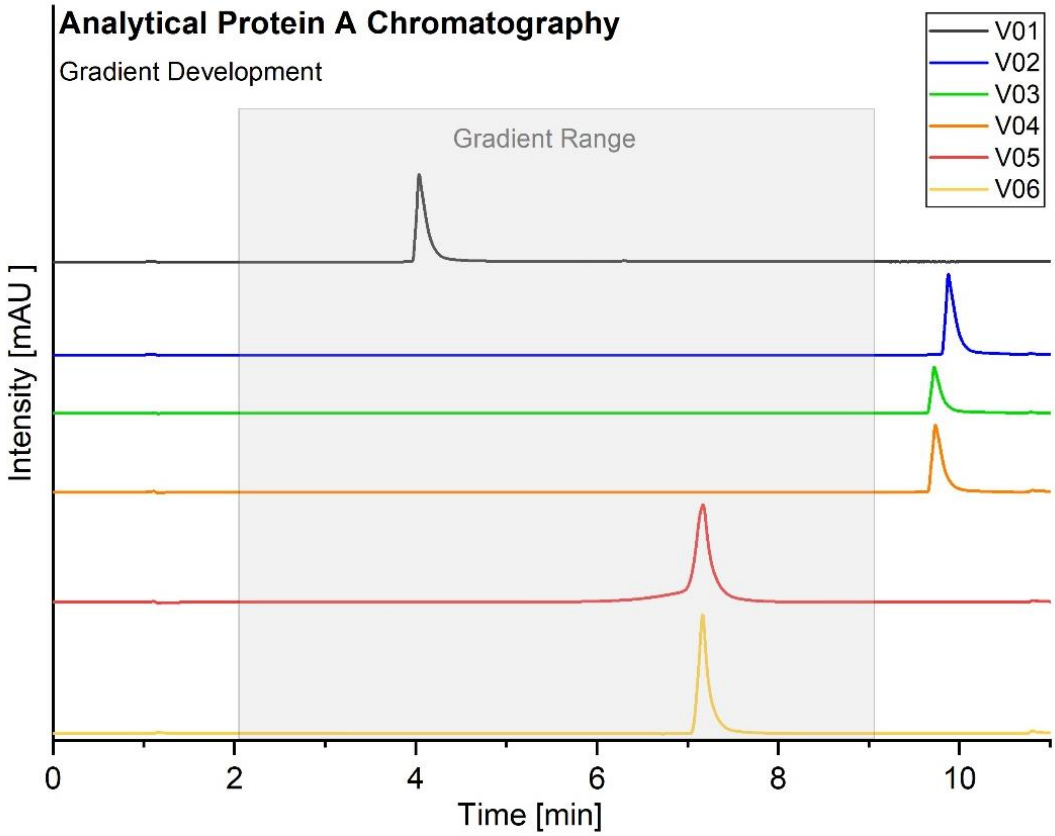

Figure III-7: Development of the Protein A Chromatography method. The figure displays the results from method versions 1 - 6, each represented in different colors.

Prior to gradient optimization experiments, the injection lag time was determined. As shown in Figure III-7, after increasing the mobile phase B to 100%, resulting in loss of binding and consequently elution of the antibody, the elution peak of the mAb was detected approximately 2 min after changing mobile phase composition (V01 – black chromatogram). This delay is the result of the lag time deriving from the extra column volume and the gradient delay volume of the UHPLC system and must be considered in all previous experiments (Table III-2).

In the following approaches, two 6-minute gradients were tested, going from 0-40 % and 0-60% mobile Phase B (V02 & V03). However, no elution occurred within the gradient stage (highlighted in grey); elution only happened after increasing the mobile phase to 100%. This indicates that the pH increase during the gradient stage is still insufficient to

disrupt the mAb's affinity for the column. To ensure proper binding of mAb3 to the column, it is not feasible to shorten the equilibration and re-equilibration steps. Consequently, further increasing the gradient's target %B results in a steeper incline, which in return might reduce peak resolution.

As an alternative approach to reduce the binding between mAb and column, higher salt concentrations in the mobile phase A and B were tested (V04). High salt concentration can impact the protein-column interactions by reducing the electrostatic attraction between the mAb and protein A due to changes in the ionic strength of the environment and consequently the protein's net charge [19].Furthermore, salt ions, which increase in concentration within the gradient, might compete with the antibody for binding sites of the stationary phase and promote elution. Still, as shown in Figure III-7 the increased NaCl concentration did not effectively reduce the affinity of the mAb to the column, as no eluting during gradient stage was observed for V04. Consequently, pH increment seems to be the main modulator to control elution from the Protein A column. To avoid further prolonging of the gradient run time, the initial start concentration of mobile phase B was set to 70% (after column equilibration and mAb binding at low pH), followed by gradual increase to 100% B, similar to the previous methods. This adjustment allows eluting in the high pH range without significantly changing the steepness of the gradient. This method was tested with either higher (V05) or lower (V06) NaCl concentrations in the mobile phases. Both approaches resulted in elution of the mAb during the gradient stage of the method. However, method V06, using higher salt concentrations, resulted in severe peak fronting (red chromatogram). As this might potentially interfere with the detection of oxidation in later experiments, V05 will be preferred.

In the next step oxidized samples were analyzed to evaluate the capacity of the method to detect changes in the elution profile of stressed and unstressed samples, as well as differentiation between different levels of oxidative stress. Samples were spiked with 1% hydrogen peroxide and incubated for 0.5, 1, 2, 3, 4, 5, and 24 h (Figure III-8).

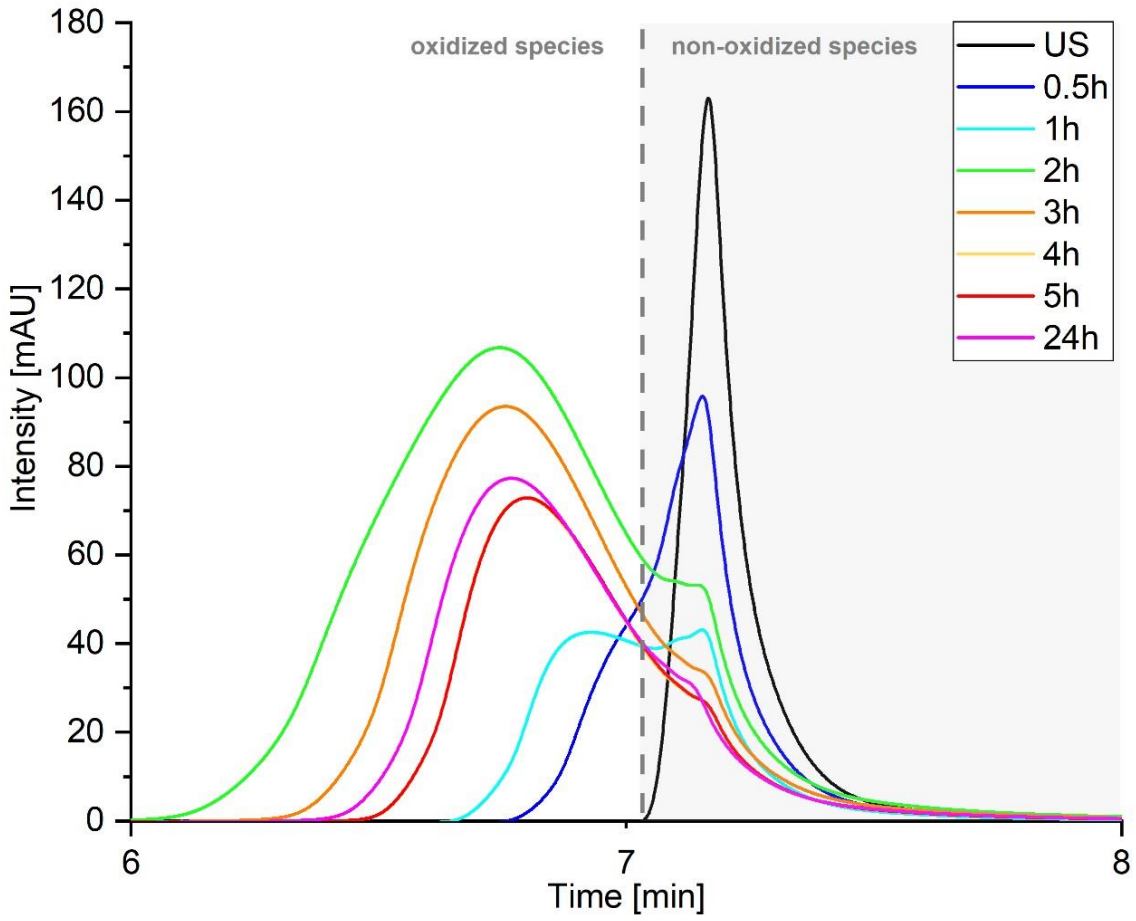

Figure III-8: Protein A chromatograms of an unstressed sample compared to samples incubated with 1% H2O2 for 0.5, 1, 2, 3, 4, 5 and 24 h, displayed in different colors.

The oxidized samples show a gradual loss of the initial unstressed peak shape and shift to earlier elution times. Those observations are in line with findings discussed in literature. Hydrogen peroxide is an effective oxidant for oxidation prone methionine residues located in the Fc fragment [14] . The oxidation levels generated in this experiment caused severe damage, resulting in loss of binding affinity and consequently earlier elution, even under HT chromatographic conditions. Interestingly, the oxidized peaks show high variation in peak area, which was not observed in replicate measurements of unstressed samples (data not shown). As this phenomenon was observed in multiple experiments and is not caused by fluctuations in protein concentration and consequently column load, this might also be a side effect of the severe oxidation. However, as in future screenings only one predefined oxidation level will be used for each oxidant, the method is still considered effective in detecting and differentiating oxidative stress under HT conditions.

To analyze the platformability of the method, four additional mAbs were analyzed. Most of them showed similar elution behavior as mAb3, but no elution peak was observed for mAb5 (data not shown).

As no signs of sample elution was observed throughout the 15-minute run time of the method, the conditions are most likely not sufficient to allow binding of mAb5 to the column at all. Compared to all other mAbs, mAb5 has a lower pI closer to the pH, therefore the ionic environment generated through the salts in the buffer system might be less favorable for electrostatic interactions. Hence, a new mobile phase composition was tested. As the pH of the mobile phase B is lower than in the previous buffer, the gradient conditions were also adapted (Table III-2 – V07). The results demonstrate that changing the mobile phase to PBS buffer also enables binding and thus elution of mAb5. Compared to all other tested mAbs, mab5 shows peak tailing (data not shown). However, as signs of oxidation lead to reduced retention on the column and elution prior to the main peak (Figure III-8), this effect is neglectable. While PBS buffer was suitable for all tested mAbs, the separation of oxidized species was less efficient compared to the buffers used for method V06 (data not shown). Therefore, V06 is selected as final HT Protein A chromatography method, V07 will only be used in specific cases (such as mAb5) that require a lower pH elution step.

5. Conclusion

This part of the thesis successfully optimized the enzymatic digestion step by identifying suitable enzymes for both unmutated and hinge-mutated antibodies. Although no single enzyme fulfilled all HTS platformability criteria, using two different enzymes depending on mutation presence - and incorporating a disulfide bond reduction step - achieved effective separation and analysis of oxidized mAbs.

In the second section, the Protein A chromatography method was successfully adapted to meet the high-throughput screening (HTS) requirements by optimizing the gradient and mobile phase compositions. While methods published in literature did not fit within the ≤ 15-minute criterion, the adjustment of starting pH in the gradient and buffer components enabled sufficient antibody binding and effective elution within the desired timeframe.

6. References

1. Yang Y, Zhang F, Gan Y, et al. In-Depth Characterization of Acidic Variants Induced by Metal-Catalyzed Oxidation in a Recombinant Monoclonal Antibody. *Anal Chem*. 2023;95(14):5867-5876.

2. Alam ME, Slaney TR, Wu L, et al. Unique Impacts of Methionine Oxidation, Tryptophan Oxidation, and Asparagine Deamidation on Antibody Stability and Aggregation. *J Pharm Sci*. 2020;109(1):656-669.

3. Hipper E, Lehmann F, Kaiser W, et al. Protein photodegradation in the visible range? Insights into protein photooxidation with respect to protein concentration. *Int J Pharm: X*. 2023;5:100155.

4. Kaiser W, Schultz-Fademrecht T, Blech M, Buske J, Garidel P. Investigating photodegradation of antibodies governed by the light dosage. *Int J Pharm*. 2021;604:120723.

5. Zhang B, Jeong J, Burgess B, Jazayri M, Tang Y, Zhang YT. Development of a rapid RP-UHPLC–MS method for analysis of modifications in therapeutic monoclonal antibodies. *J Chromatogr B*. 2016;1032:172-181.

6. An Y, Zhang Y, Mueller HM, Shameem M, Chen X. A new tool for monoclonal antibody analysis. *mAbs*. 2014;6(4):879-893.

7. Regl C, Wohlschlager T, Holzmann J, Huber CG. A Generic HPLC Method for Absolute Quantification of Oxidation in Monoclonal Antibodies and Fc-Fusion Proteins Using UV and MS Detection. *Anal Chem*. 2017;89(16):8391-8398.

8. Xu C, Khanal S, Pierson NA, et al. Development, validation, and implementation of a robust and quality control-friendly focused peptide mapping method for monitoring oxidation of co-formulated monoclonal antibodies. *Anal Bioanal Chem*. 2022;414(29-30):8317-8330.

9. Wilkinson I, Anderson S, Fry J, et al. Fc-engineered antibodies with immune effector functions completely abolished. *PLoS ONE*. 2021;16(12):e0260954.

10. Saunders KO. Conceptual Approaches to Modulating Antibody Effector Functions and Circulation Half-Life. *Front Immunol*. 2019;10:1296.

11. Wang W, Vlasak J, Li Y, et al. Impact of methionine oxidation in human IgG1 Fc on serum half-life of monoclonal antibodies. *Mol Immunol*. 2011;48(6-7):860-866.

12. Pan H, Chen K, Chu L, Kinderman F, Apostol I, Huang G. Methionine oxidation in human IgG2 Fc decreases binding affinities to protein A and FcRn. *Protein Sci*. 2009;18(2):424-433.

13. Loew C, Knoblich C, Fichtl J, et al. Analytical protein A chromatography as a quantitative tool for the screening of methionine oxidation in monoclonal antibodies. *J Pharm Sci*. 2012;101(11):4248-4257.

14. Folzer E, diepold K, bomans K, et al. Selective Oxidation of Methionine and Tryptophan Residues in a Therapeutic IgG1 Molecule. *J Pharm Sci*. 2015;104(9):2824-2831.

15. Ryan MH, Petrone D, Nemeth JF, Barnathan E, Björck L, Jordan RE. Proteolysis of purified IgGs by human and bacterial enzymes in vitro and the detection of specific proteolytic fragments of endogenous IgG in rheumatoid synovial fluid. *Mol Immunol*. 2008;45(7):1837-1846.

16. Brezski RJ, Jordan RE. Cleavage of IgGs by proteases associated with invasive diseases. *mAbs*. 2010;2(3):212-220.

17. Deveuve Q, Lajoie L, Barrault B, Thibault G. The Proteolytic Cleavage of Therapeutic Monoclonal Antibody Hinge Region: More Than a Matter of Subclass. *Front Immunol*. 2020;11:168.

18. Mesonzhnik N, Belushenko A, Novikova P, Kukharenko A, Afonin M. Enhanced N-Glycan Profiling of Therapeutic Monoclonal Antibodies through the Application of Upper-Hinge Middle-Up Level LC-HRMS Analysis. *Antibodies*. 2024;13(3):66.

19. Tsumoto K, Ejima D, Senczuk AM, Kita Y, Arakawa T. Effects of salts on protein–surface interactions: applications for column chromatography. *J Pharm Sci*. 2007;96(7):1677-1690.

IV. DETERMINATION OF HIGH THROUGHPUT OXIDATION SCREENING PARAMETERS

1. Introduction

The existing HTS workflow offers the ideal framework to systematically characterize the oxidation susceptibility under relevant conditions, in a time efficient manner and with minimal sample consumption. The screening approach enables the possibility to parallel-test multiple different oxidation stressors, generating a comprehensive picture on potential oxidation liabilities in one screening.

As illustrated in Chapter I, for integration into the existing system, oxidation stress assays must fulfill all relevant criteria for high-throughput (HT) screenings. Each assay should ideally be optimized to produce an appropriate level of stress that can be easily evaluated within an automated workflow in a short timeframe. Additionally, it is crucial to ensure compatibility with multiwell plate formats and automated sample preparation workflows for HTS stress testing. Hence, the aim of this chapter is to identify the optimal parameters for each oxidation condition and develop an experimental workflow suitable for HTS. To facilitate efficient data evaluation in future oxidation screening experiments, an oxidation stress threshold was established to distinguish true oxidation effects from errors introduced by the assay and analytical methods, based on the data collected in this chapter.

Furthermore, to ensure comparability across different data sets, it is essential to stop the oxidation reactions after a predefined period. In forced oxidation studies during biopharmaceutical development, remaining oxidants are typically removed by buffer exchange using spin columns[1] . While this method effectively stops oxidation reactions, it is not feasible within the existing screening environment. As an HTS-compatible alternative, quenching with additional compounds with reducing and/or oxidation scavenging capacities were evaluated.

In summary, the aim of this section is to establish HTS-compatible experimental conditions for oxidation stress assays, by identifying optimal oxidation parameters, ensuring automated sample handling, and evaluating alternative methods to stop oxidation efficiently.

2. Materials

An in-house manufactured therapeutic monoclonal antibody of isotype IgG1 was used in this study (mAb3). The antibody stock solutions were diafiltrated into water for injection and concentrated to 150 mg/ml using Vivaspin 6 spin columns (Sartorius, Göttingen, Germany). Protein concentration was determined by UV-VIS spectroscopy (Stunner, Unchained Labs, Pleasanton, CA, USA). The pH was adjusted to 6.0. All oxidation experiments were performed in 96 well plates (Greiner Bio-One, Kremsmünster, Austria) sealed with transparent adhesive foil (Applied Biosystems, Foster City, CA, USA). All experiments were carried out at the HTS standard protein concentration of 100 mg/ml.

Hydrochloric acid (HCl), sodium chloride (NaCl), Tris(hydroxymethyl)-aminomethan (Tris), tert-Butyl hydroperoxide (tBHP), sodium sulfate (Na_2SO_4), sodium phosphate dibasic heptahydrate ($Na_2HPO_4 \bullet 7H_2O$), sodium phosphate dibasic dihydrate ($Na_2HPO_4 \bullet 2H_2O$), MES monohydrate and acetonitrile gradient grade for liquid chromatography were purchased from Merck (Darmstadt, Germany). Hydrogen peroxide 30% (H_2O_2), iron(II) sulfate heptahydrate, iron(III) sulfate hydrate, reduced glutathione (GSH), sodium sulfite and 2,2-azo-bis-(2-amidinopropane) dihydrochloride (AAPH) were purchased from Sigma-Aldrich (St. Louis, MO). Dithiothreitol (DTT) was purchased from Fluorochem (Hadfield, UK), trifluoroacetic acid from VWR chemicals (Leuven, Belgium) and L-methionine from J.T. Baker (Radnor, PA, USA). IgG-specific protease FabRICATOR® (IdeS) was obtained from Genovis AB (Lund, Swede

3. Methods

3.1. Preparation of oxidized samples

Multiple oxidation stress assays were chosen to generate a comprehensive data set, representing a realistic oxidation risk for a therapeutic protein. To determine the ideal oxidation conditions in an automated HT screening workflow, a broad concentration range was tested for the selected oxidants (Table IV-1).

Table IV-1: Experimental conditions for oxidation stress assays

Assay	Oxidant	Experimental Range	Incubation Time	Incubation Temperature
HP	H_2O_2	0.0, 0.01, 0.05, 0.1, 0.5, 1.0%	1.5 h	25 °C
tBHP	tBHP	0.0, 0.25, 0.5, 0.75, 1.0, 1.25%	1.5 h	25 °C
AAPH	AAPH	0, 50, 100, 150, 200, 250 mM	1.5 h	40 °C
MCO	Fe(II) ($+H_2O_2$)	0, 0.25 (+2.5), 0.4 (+ 4.0) mM	3.0 h	25 °C
VIS	Visible Light	0, 100, 250, 600 klux*h	n/a	25 °C
UV-A	UV-A Radiation	0, 10, 40, 100 Wh/m²	n/a	25 °C

For chemical oxidation assays, antibody samples were either incubated with 0.01 – 1.0% H_2O_2 and 0.25 – 1.25% tBHP at 25 °C for 1.5 h, or with 50-250 mM AAPH at 40 °C for 1.5 h. Metal catalyzed oxidation was simulated by treatment with 0.25 mM Fe(II) + 2.5 mM H_2O_2 or 0.4 mM Fe(II) + 4 mM H_2O_2 (Fenton reaction) at 25 °C for 3 h. Samples without any oxidants were prepared as reference samples. All oxidation assays described above were conducted under light protection in temperature-controlled incubators (Thermo CRS Ltd., Burlington, Canada). Photooxidation experiments were carried out in an ICH compliant photostability chamber (Aralab, Rio de Mouro, Portugal) equipped with a fluorescent cool white light tube and an UV-A light source. Samples were exposed to either 100 - 600 klux*h of visible light or 10 - 100 Wh/m² of UV-A light. The illuminance of the fluorescent light was set to 29 klux, for the UV-A light an irradiance of 30 W/m² was used. Samples were exposed to light until the desired light dose was reached, then stored under light protection. Reference samples in a glass vial wrapped in aluminum foil (dark control) were stored next to the 96 well plates during light exposure for both tested light conditions. To determine the variability of each oxidation assay, the experiment was repeated on three consecutive days.

3.2. Quenching of oxidation reactions

To evaluate different strategies to stop oxidation reactions after a defined period of time, oxidized samples were spiked with an excess of quenchers (1:100 H_2O_2 : quencher, with additional ratios tested during method development for individual quenchers), including free methionine, reduced glutathione (GSH) and sodium sulfite.

Previous experiments demonstrated that especially residual H_2O_2, if not completely removed, caused significant oxidation of the Fab subunit during enzymatic cleavage, resulting in severe peak deformation during RP-UHPLC analysis (Figure IV-1A). Therefore, RP-UHPLC analysis was used to analyze the effectiveness of the different quenchers. For comparison with the spiking approach, a standard oxidation quenching method was also evaluated: an H_2O_2-stressed mAb sample was buffer exchanged into water using Vivaspin 6 spin columns (Sartorius, Göttingen, Germany).

3.3. Reversed-Phase Chromatography Subunit Analysis (RP)

For enzymatic cleavage, the oxidized mAb samples were diluted to 2 mg/ml using water containing 100 units of IdeS (FabRICATOR, Genovis) and incubated for 60 min at 25 °C. Disulfide bond reduction was conducted by addition of 50 mM DTT and incubation for 1 h at 40 °C. This procedure generates three fragments: a heavy chain Fc fragment (Fc HC), light chain (LC) and a heavy chain Fd fragment (Fd HC). The generated subunits were analyzed on an Agilent 1290 Infinity System (Agilent Technologies, Santa Clara, CA, USA) equipped with DAD detector using a BioResolve RP mAb Polyphenyl column 2.1 x 50 mm, 2.7 µm, 450 Å (Waters, Milford, MA, USA). Absorption was monitored at 280 nm. The UHPLC column used in this study was conditioned as recommended by the manufacturer prior to the measurements. Mobile phase A was water with 0.1% TFA, mobile phase B was acetonitrile with 0.1% TFA. 2 µg sample were injected to the column, separation was performed using a linear gradient from 25% - 45% mobile phase B over 4 min at a flow rate of 0.3 ml/min at 80 °C. The temperature in the sample manager of the UPLC system was maintained at 4 °C. Analysis of chromatographic data was conducted using Chromeleon™ chromatography software (Thermo Fisher Scientific Inc., Waltham, MA, USA).

3.4. Size Exclusion Chromatography (SEC)

To monitor the formation of high molecular weight species (HMW) and low molecular weight species (LMW), size exclusion analysis was performed. 40 µg were injected to a Waters ACQUITY UPLC BEH200 SEC column 4.6 x 150 mm; 1.7 µm, 200 Å (Waters, Milford, MA, USA) and separated by isocratic elution using 100 mM Na_2HPO_4 / 200 mM Na_2SO_4, pH 7.0 at a flow rate of 0.4 ml/min for 6 min. Column temperature was maintained at 25 °C.

3.5. Cation Exchange Chromatography (CEX)

Cation exchange chromatography of oxidized mAbs was performed to investigate the formation of charged isoforms. Per sample, 40 µg were injected to a Protein-Pak Hi Res CM column 4.6 x 100 mm, 7 µm (Waters, Milford, MA, USA). Samples were separated by salt gradient elution using 20 mM MES at pH 6.5 as mobile phase A and 20 mM MES + 500 mM NaCl at pH 6.5 as mobile phase B. For mAb 4, the NaCl content of mobile Phase B was decreased to 250 mM. A linear gradient from 0 to 50% in 12.5 min was applied to elute the samples at 40 °C. The flow rate was set to 0.6 ml/min.

3.6. Protein A Chromatography

Methionine oxidation in the Fc fragment was detected using an HTS-optimized version of a previously described analytical Protein A Chromatography method 21. Analysis was performed on a MAbPac Protein A Column 4 x 35 mm (Thermo Scientific, Dreieich, Germany) using 50 mM $Na_2HPO_4 \cdot 2H_2O$ / 150 mM NaCl at pH 7.5 as mobile phase A and at pH 2.5 as mobile phase B. After the injection of 10 µg sample, the column was rinsed with 100% mobile phase A for 2 min to allow binding of the antibody to the stationary phase. Sample elution was performed using a linear gradient from 70% to 100% mobile phase B in 7 min, followed by a re-equilibration step with 100% mobile phase A for 6 min. Protein A analysis was carried out at 30 °C column temperature using a flow rate of 0.2 ml/min.

4. Results & Discussion

4.1. HTS suitable approach for oxidation quenching

Oxidation quenching is necessary to ensure that oxidation processes are uniformly stopped across all samples in a large dataset after a specified incubation or light exposure period. This prevents further oxidation during subsequent processing and storage, thus allowing for accurate comparisons across datasets. Furthermore, any remaining oxidants can significantly disrupt the analysis by causing unwanted secondary oxidation and severe, misleading degradation of samples (Figure IV-1A). To address these challenges, various spiking approaches for effective oxidation quenching were evaluated.

However, aside from methionine, all other compounds resulted in significant degradation of the antibody. GSH and sodium sulfite are reducing agents capable of stopping oxidation reactions by donating electrons to oxidizing agents, thereby reducing them. Therefore, they are both effective antioxidants for a variety of radical oxygen species[2,3] . Although both agents completely stopped further oxidation in the samples, their reducing capacity also leads to the reduction of disulfide bonds in the tested mAb, even at low concentrations and in the presence of an antibody surplus (data not shown).

In contrast, free methionine has no reducing capacity, only acting as oxidation scavenger and is preferably oxidized by reactive oxygen species [4,5] .

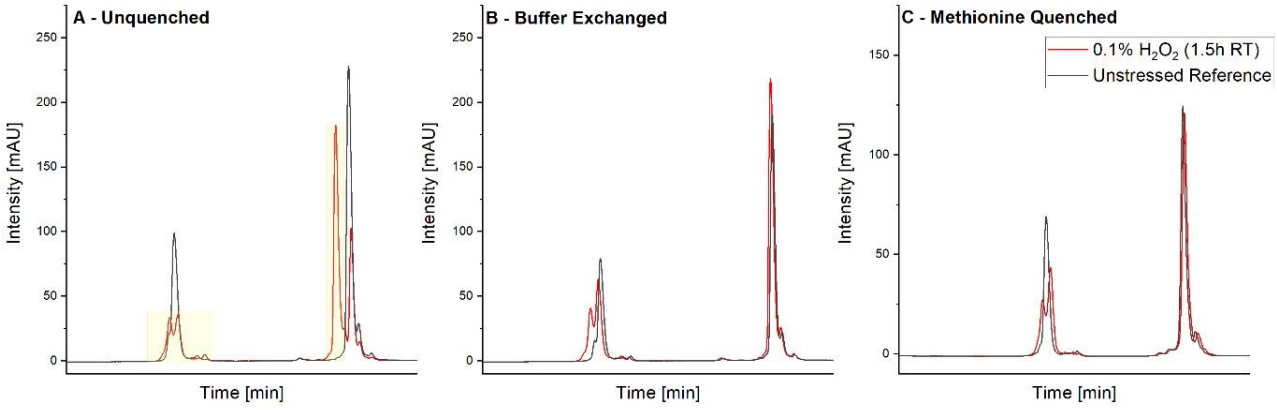

Figure IV-1: Evaluation of a HTS compatible quenching Strategy. This figure compares chromatograms of a sample stressed with 0.1% hydrogen peroxide for 1.5 h at room temperature (red) against an unstressed reference (black). The conditions include no quenching (A), quenching via buffer exchange (B), and methionine quenching (C). The yellow shaded area highlights the additional peaks generated through severe, non-representative oxidation under unquenched conditions.

As demonstrated in Figure IV-1, the addition of free methionine as an oxidation scavenger (Figure IV-1C) is as effective as oxidant removal via buffer exchange (Figure IV-1B). In both scenarios, the RP-UHPLC subunit analysis showed no signs of oxidation in the Fab subunit (second peak), with oxidation occurring solely in the Fc fragment. Compared to buffer exchange, the methionine spiking method can be seamlessly integrated into fully automated liquid handling workflows, eliminating the need for manual steps or additional equipment like centrifuges. Since the methionine concentration in the quenching solution does not negatively impact the analytical workflow or the tested samples, the final concentration was set to 200 mM. However, during the quenching experiments, it was observed that free methionine, even in excess relative to hydrogen peroxide, requires a minimum incubation time of one hour to ensure complete removal of oxidants before conducting further subunit analysis.

4.2. Selection of oxidation levels

The existing HTS concept includes automated data handling to enable a time efficient evaluation of chromatographic results. To establish reproducible oxidation stress assays that fit into the existing workflow, it is crucial to ensure clear differentiation of relevant oxidation signals from random noise, allowing automated peak detection. On the other hand, it is also necessary to avoid too severe damage of the samples, as extremely degraded peak shapes increase the risk of incorrect peak integration drastically.

To comprehensively assess the extent of oxidation, the combination of multiple analytical methods might be necessary. In case of the HTS workflow, the reversed phase subunit analysis provides the highest information content in terms of oxidative degradation. This method not only allows detection of oxidation, but also localization on subunit level. Therefore, RP-UHPLC subunit analysis is considered the most important method for this stress arm. However, as the peak pattern is more complex compared to other established HTS UHPLC methods, showing three peaks including subgroups instead of one main peak, the data evaluation is most likely more error prone. Hence, to ensure optimal performance of the method in detection of oxidation, suitable oxidation conditions were selected based on the data set acquired with the RP-UHPLC subunit analysis.

The effect of oxidation was determined by examining the elution profile for additional peak shoulders and peaks prior to the main peaks, indicating changes in the hydrophobicity of the mAb subunits induced by oxidation. As seen in previous oxidation experiments during analytical method development, oxidation of the Fd HC peak fragment often leads to formation of an additional peak, which can be easily detected (Figure III-6, third peak). In

contrast, due to the short run time of the HT RP UHPLC analysis, what is a prerequisite to be applicable in the HTS environment, oxidation of the Fc HC fragment often only results in formation of a peak shoulder (Figure III-6, first peak). This significantly increases the difficulty of detecting oxidation induced changes of the peak shape and area in a HTS setting. So far, changes of 10-20% in the Fc HC pre peak area have given the best results for automated peak detection in preliminary experiments. Therefore, to identify the best oxidation conditions to generate changes in peak area of 10-20%, a broad range of different oxidation levels was tested for each potential HTS oxidation assay.

4.3. Peroxide-based oxidation stress

Peroxide-based assays, such as treatment with H_2O_2 or tBHP, are common practice to evaluate the oxidation susceptibility in forced oxidation studies [1,6]. However, as often described in literature, high concentrations and/or long incubation times are recommended for both oxidants. To develop assays compliant with the time efficiency aspect of the HTS workflow, in this study the incubation time was limited to only 1.5 h.

As shown in Figure IV-2, none of the peroxide-based assays led to modifications of the Fd HC peak, whereas changes in hydrophobicity of the Fc Hc peak were detected for both oxidants. Especially incubation with higher concentrations of H_2O_2 generated severe changes in the elution profile, as well as deformation of the peak (Figure IV-2B). Treatment with an H_2O_2 concentration of 1.0% resulted in a complete shift of the first peak to earlier retention times in the chromatogram, hence drastically changing the hydrophobicity of the Fc HC fragment. It is also noticeable that with increasing H_2O_2 concentration, the variation of the degradation extent between the individual experiments also increases (Figure IV-2A). Modifications after treatment with tBHP are less pronounced (Figure IV-2 C+D). It is generally assumed, while both oxidants induce similar oxidation mechanisms, that due to its larger size tBHP mainly oxidizes surface exposed amino acid residues whereas H_2O_2 can damage the protein on a deeper level [7]. For H_2O_2 the most promising results were received using a concentration of 0.05%. At this concentration level, detectable modifications of the Fc HC fragment were generated, without leading to peak deformation, which increases the assay variability.

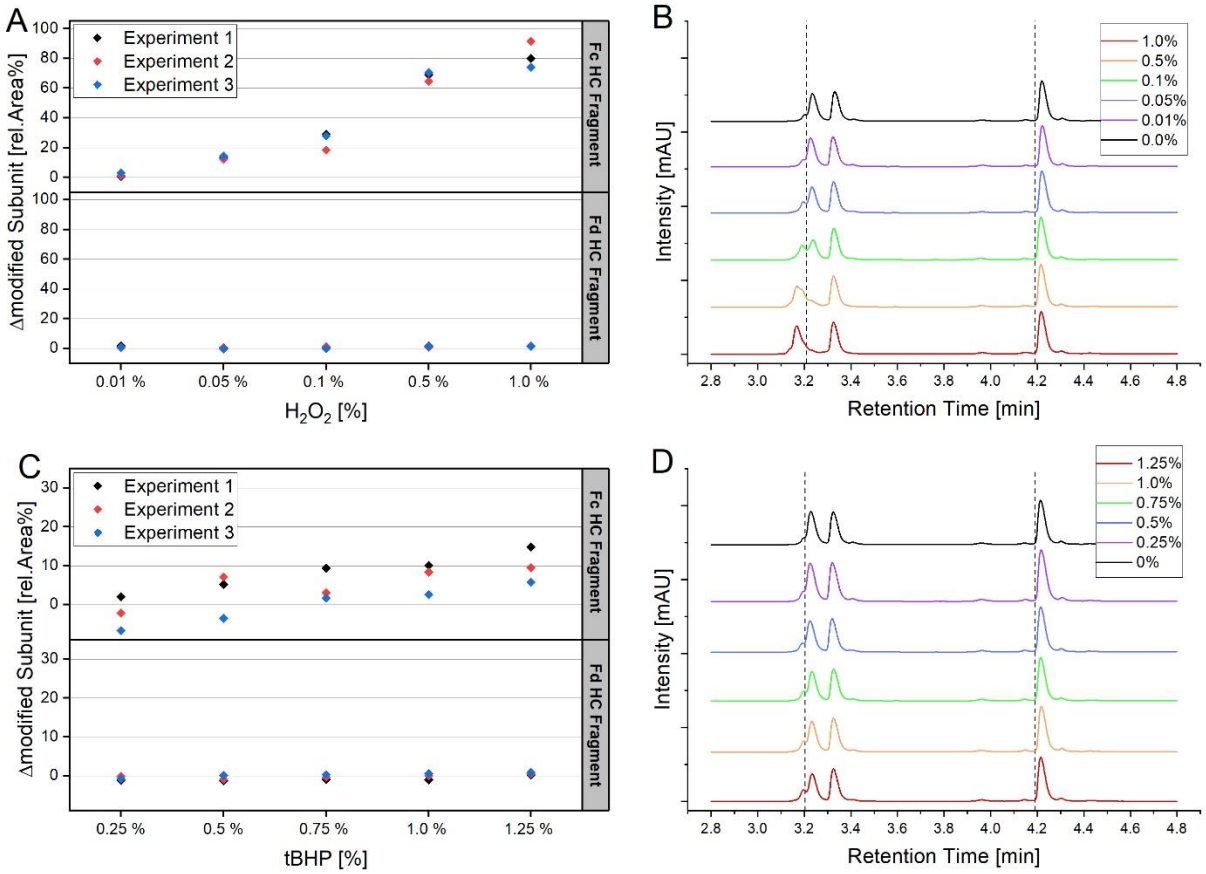

Figure IV-2: Peroxide-based assays. The figure shows the increase in Fc (top) and Fd fragment (bottom) modifications following treatment with H_2O_2 (A) and tBHP (C) across three individual experiments (black, red, and blue). The corresponding chromatograms for H_2O_2 (B) and tBHP (D) treated samples are displayed on the left. Different concentrations of the respective oxidants are represented by different colors.

The tBHP assay results show large variations between individual experiments, even at lower concentration levels (Figure IV-2C). However, unlike the other stress assays, the tBHP data set also shows deviations in the peak shape of the unstressed references and the peak shape of the unstressed samples in experiments 2 and 3 show signs of degradation. As the level of modification is calculated based on the difference in pre peak size detected for the oxidized samples compared to the unstressed reference, hence the data sets generated in experiment 2 and 3 are only of limited information value and not suitable to identify the required tBHP concentration. Still, based on the results of experiment 1 and previous experiments with tBHP oxidation during assay development, a concentration of 0.75% was selected.

4.4. Free radical oxidation assay (AAPH)

Free radical induced oxidation was simulated using the free radical generating compound AAPH [8]. In contrast to peroxide-based oxidation, free radical induced mechanisms are known to generate oxidative stress is both mAb subunits [9]. Also in this study, AAPH treatment induced modifications in both mAb subunits, as shown in Figure IV-3. Interestingly, concentrations higher than 100 mM hardly increased the level of degradation detected for both subunits. Similar trends were observed in SEC, CEX, and Protein A chromatography data for the same samples (data not shown). The lack of additional degradation with higher AAPH concentrations suggests that the AAPH-generated radicals target specific sites on the protein. Once these target sites, which likely serve as the initiation points for oxidative degradation, are fully modified, an excess of radicals does not cause additional damage or trigger new oxidation mechanisms. This indicates a potential saturation of the oxidation process at specific protein targets.

Like incubation with H_2O_2, higher concentrations of AAPH increase the deviation in degradation extent between individual experiments. As the “saturation level” of Fc HC and Fd HC modifications is already reached at 100 mM AAPH and higher concentrations only increase assay variability, 100 mM AAPH treatment is selected as preferred HTS oxidation condition.

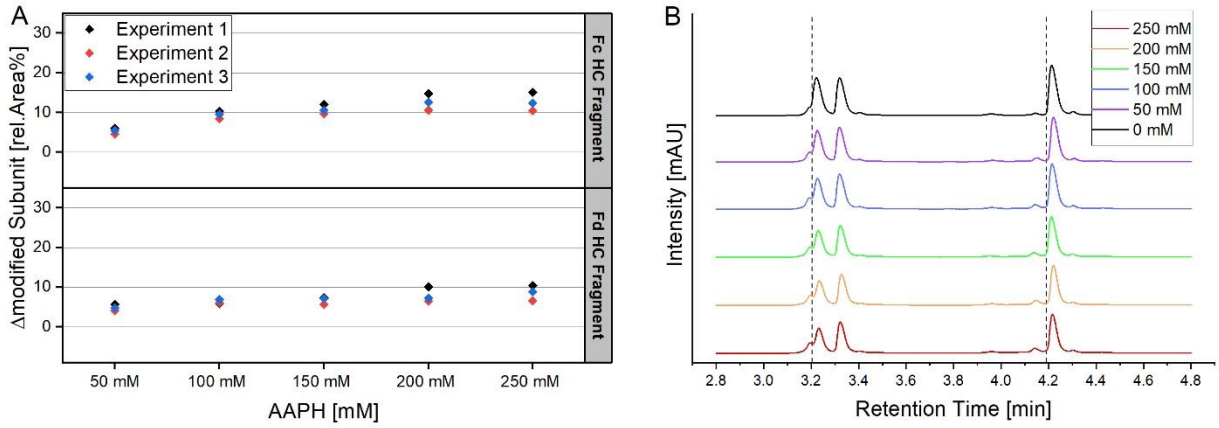

Figure IV-3: AAPH Assay. Part A of the figure shows the increase in Fc (top) and Fd fragment (bottom) modifications following AAPH treatment across three individual experiments (black, red, and blue). The corresponding chromatograms (B) are displayed on the right. Different concentrations of the AAPH are represented by different colors.

4.5. Visible light and UV-A radiation assays

Visible light as well as UV-A radiation are known to induce degradation in mAbs [10–12], hence both light conditions were included in the study. The mAbs were exposed to milder light conditions (100 klux*h and 10 Wh/m²) as well as accelerated stress conditions (250/600 klux*h and 40/100 Wh/m²). As demonstrated in Figure IV-4, none of the tested milder light conditions (100 klux*h and 10 Wh/m²) induced considerable modification of mAb subunits. However, under accelerated conditions, visible light exposure (Figure IV-4 A+B) and UV-A irradiation (Figure IV-4 C+D) led to changes in the hydrophobicity profile of the Fc HC peak. In contrast, no modifications of the Fd HC peak were detected after exposure to 600 klux*h of visible or 100 Wh/m² UV-A light.

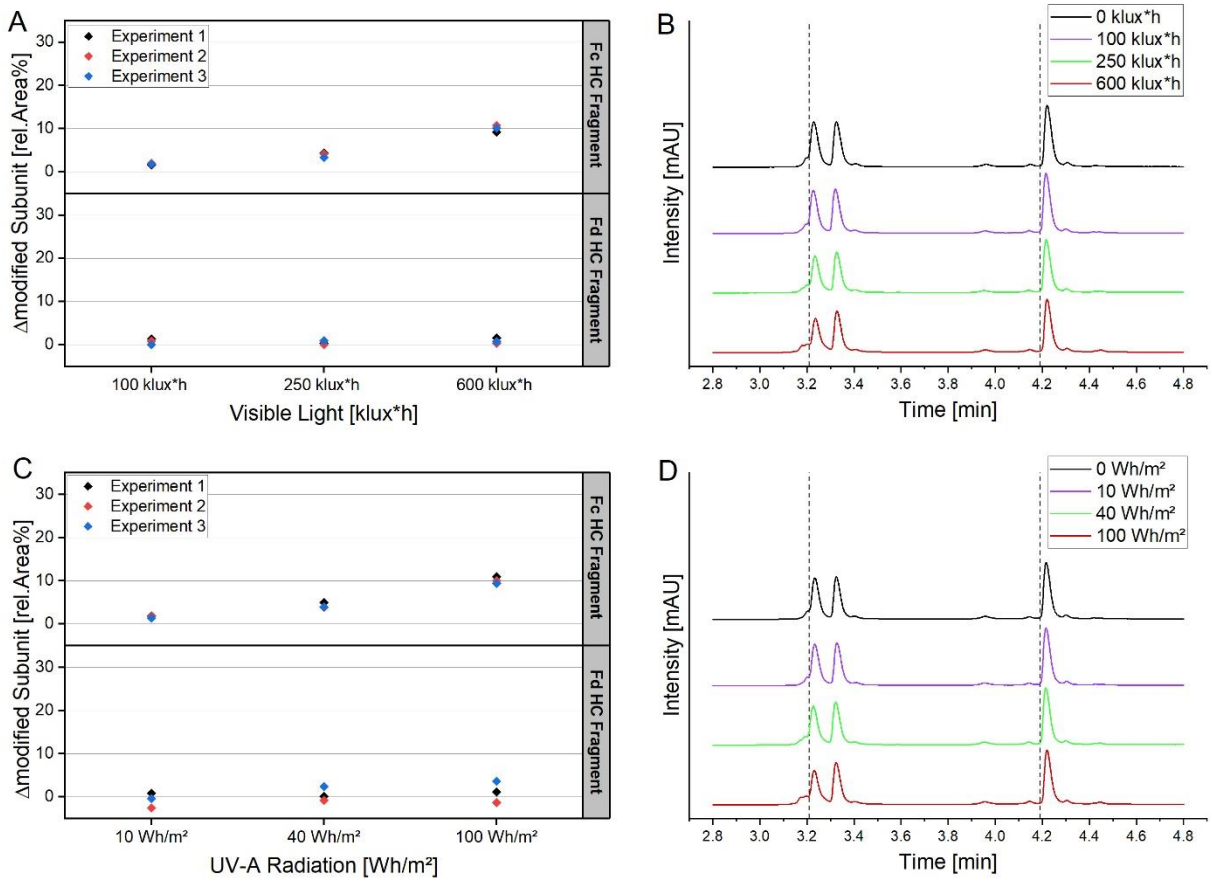

Figure IV-4: Light Stress Assays. The figure shows the increase in Fc (top) and Fd fragment (bottom) modifications following exposure to visible light (A) and UV-A radiation (C) across three individual experiments (black, red, and blue). The corresponding chromatograms for VIS (B) and UV-A (D) exposed samples are displayed on the left. Different light/radiation doses are represented by different colors.

However, exposure to UV-A radiation increases the variability in degradation of the Fc HC peak. This effect was not observed for visible light exposure. While for most chemical assays the incubation time can be significantly reduced by increasing the oxidant concentration, longer exposure times are required to generate a detectable level of light

induced oxidation. As described by Kaiser et al. [13] and also observed in own photostability studies, the extent of photodegradation in mAbs is mainly controlled by the overall light dose the sample is exposed to, not the exposure time or illuminance of the light source used. The HTS workflow requires an adequate level of degradation to ensure sufficient automated peak detection, hence 600 klux*h of visible light and 100 Wh/m² are selected as HTS light stress conditions, even though this results in longer exposure times.

4.6. Metal catalyzed oxidation assay (MCO)

Metal catalyzed oxidation was tested using a Fenton reaction-based assay. While metal catalyzed oxidation effects have also been reported for other transition metals such as cupper [14–16] , iron ions were considered as the most representative metal contamination in the manufacturing process of biotherapeutics and was therefore selected as stress compound. Previous experiments had shown that low Fe(II) concentrations did not induce modifications of mAb subunits in higher concentrated antibody formulations (100 mg/ml). In contrast, concentrations higher than 0.4 mM Fe(II) caused complex formation in higher concentrated mAb samples, hence the sample number for this oxidation assay was reduced to two potential oxidant concentrations. As expected, only the higher concentration level (0.4 mM Fe(II) + 4 mM H_2O_2) could generate Fc HC modifications on a moderate level. In contrast, severe degradation of the Fd HC peak was observed for both tested oxidant concentrations (Figure IV-5). However, it is assumed that in this specific case, the degradation was generated by an undesired secondary oxidation reaction during the disulfide bond reduction. The remaining iron ions in the sample further react with DTT [17] , leading to severe oxidation events of the Fd HC fragment. Contrary to the intact mAb, the enzymatically generated Fd HC fragment is more prone to oxidation, as the accessibility of potential oxidation targets is most likely increased due to the proteolytic cleavage. Interestingly, this effect was only observed for the Fd HC fragment, but not for the Fc subunit. To avoid undesired secondary reactions in future studies, no reduction step should be performed in samples containing iron ions, even though this might reduce the resolution of the RP UHPLC separation. In future studies, a concentration of 0.4 mM Fe(II) and 4 mM H_2O_2 will be used to simulate metal catalyzed oxidation.

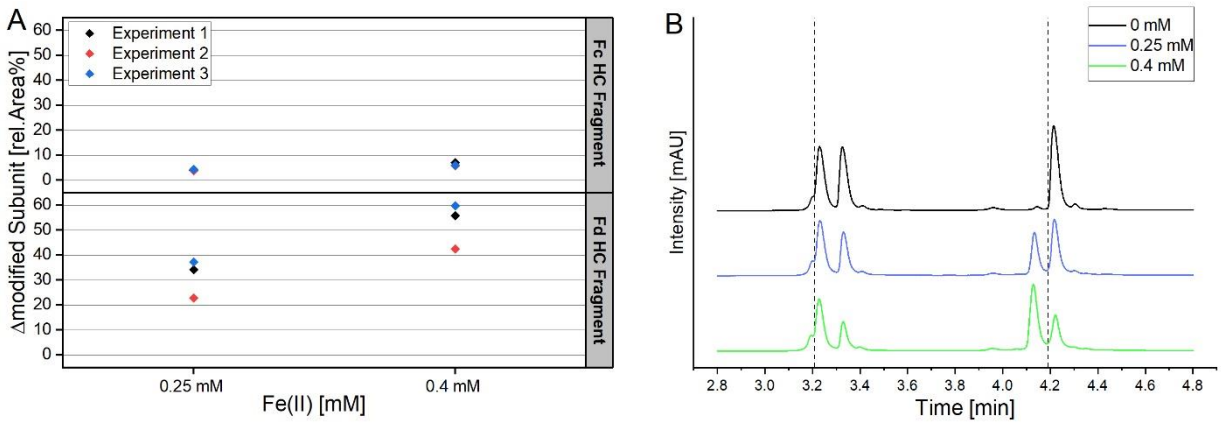

Figure IV-5: MCO Assay. Part A of the figure shows the increase in Fc (top) and Fd fragment (bottom) modifications following MCO treatment across three individual experiments (black, red, and blue). The corresponding chromatograms (B) are displayed on the right. Different concentrations of Fe(II) + H_2O_2 are represented by different colors.

In conclusion, under the selected conditions changes in Fc HC and Fd HC pre peak area of approx. 6 -14% were determined, allowing reliable detection in the HTS workflow. All stress assays were able to induce modification of the Fc HC fragment. In most cases, this resulted in formation of a more pronounced peak shoulder prior to the “main” Fc HC peak. In more severely oxidized samples, the peak was completely shifted. However, this simultaneously increased the deviation in oxidation extent in individual samples. Modification of the Fd HC fragment was only initiated by AAPH treatment and led to formation of an additional peak, separate from the Fd HC fragment.

4.7. Assay variability

To generate a comprehensive picture of oxidation susceptibility, multiple stress assays, as well as analytical techniques are required. Depending on the assay type, the experimental procedures include multiple steps, such as preparation of working- and stock solutions, addition of oxidants, quenching with dilution buffer or enzymatic cleavage. Each part of the protocol increases the risk of inaccuracies. In terms of analytical techniques, contrary to analytical quantitation methods, where method error and detection limits can be determined by performing appropriate validation experiments, the HTS evaluation of chromatographic data relies on changes in relative peak areas compared to an unstressed control, making the definition of method error ranges more difficult.

Furthermore, as the existing HTS workflow, due to the large sample sets, does often not allow replicates in the test set up, it is necessary to generate reliable results with a minimum of samples. On the one hand, this is possible by choosing accelerated oxidation conditions that will generate a detectable level of stress, considerably higher than the baseline noise. On the other hand, it must be carefully differentiated between changes generated through actual oxidation processes and data variability caused by the assay procedure itself.

To investigate the variability of each assay-method combination that might be potentially used in the future oxidation profiling workflow and determine the “worst-case” variation, the oxidation experiments were repeated three times on individual days, then analyzed using RP-UHPLC subunit analysis, SE-UHPLC, CEX-UHPLC and protein A chromatography. The impact of oxidation, such as increased oxidation or modifications of the Fc and Fab subunits, was evaluated by calculating the difference (Δ) between oxidized samples (using the stress conditions determined in the previous section) and an unstressed reference. Subsequently, the variability range of these deltas for each assay-method combination was defined and depicted in Figure IV-6. This section focuses solely on evaluating the variability of the method in combination with different stress assays, while their effectiveness in detecting oxidation will be discussed in the next chapter.

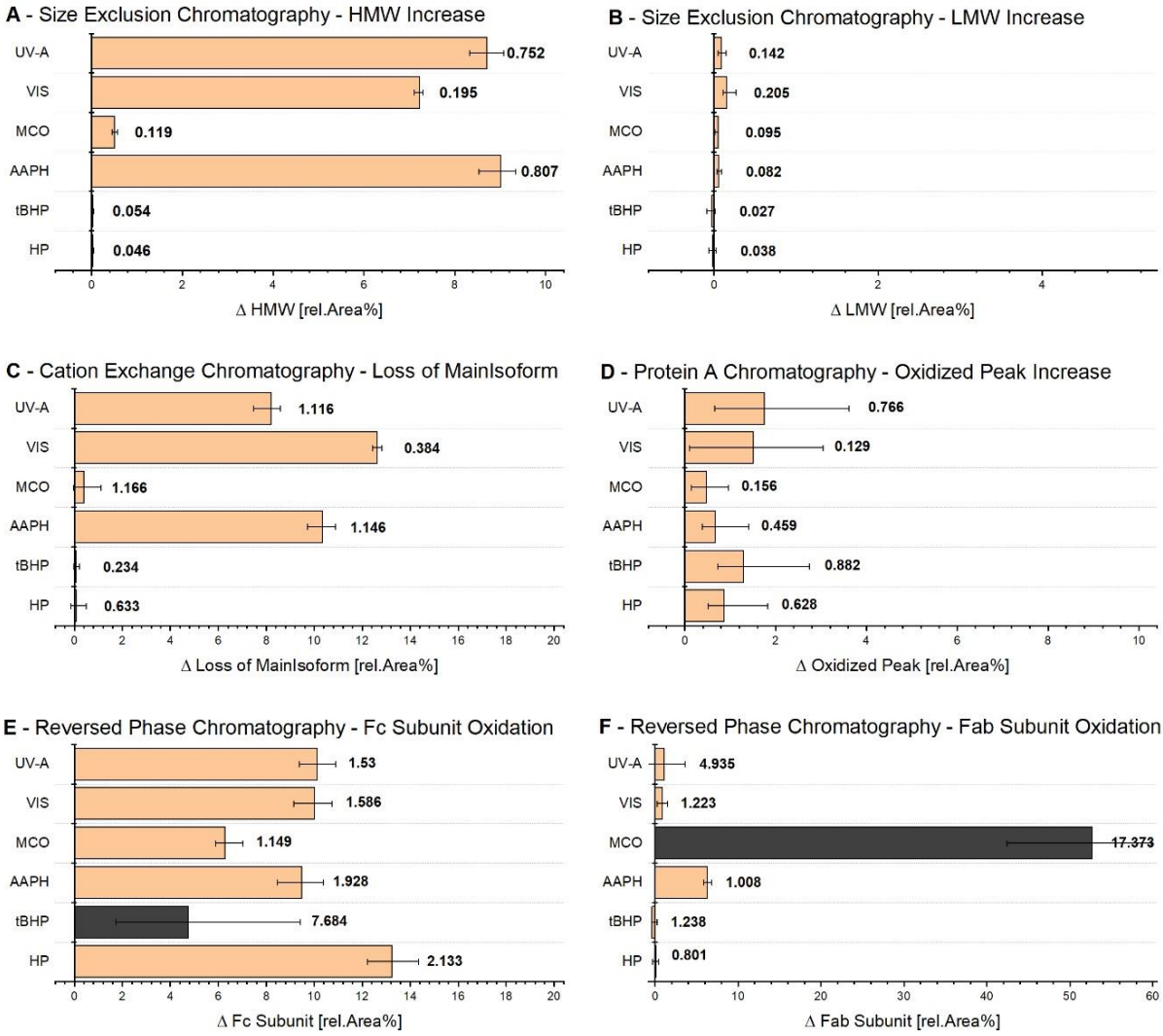

Figure IV-6: Assay-Method Variability. This figure illustrates the variability ranges of the assay-method combinations used to establish an oxidation threshold for future experiments, based on data sets generated over three consecutive days. The bars represent the effect of oxidation, calculated as the delta between stressed samples and an unstressed reference. The error bars indicate the variability range [rel.Area%], with the exact range also noted beside each bar. Bars colored in grey were excluded from threshold determination.

As discussed in the previous section of this chapter, due to secondary oxidation reactions of MCO treated samples after disulfide bond reduction, non-representative degradation was found for the Fab subunit (Figure IV-6F), therefore this variability range was not considered for threshold determination. Additionally, also discussed above, the tBHP samples showing signs of oxidation in the unstressed references, leading to high deviations, were also excluded.

For the majority of the remaining assay-method combinations the variability range is between 0.1-1.9 rel.Area%. Based on this outcome, a threshold of 2% will be applied in future data sets. Only if the difference between the unstressed reference and the oxidized

sample exceeds the 2% limit, will the change be categorized as oxidation induced modification.

Exceptions include the Fab subunit modifications observed in UV-A light-exposed samples (Figure IV-6F) and the Fc subunit modifications in samples treated with hydrogen peroxide (Figure IV-6E). In these cases, the RP-UHPLC subunit analysis showed higher variability, exceeding 2%. As this method is still in the exploratory phase, its robustness and effectiveness within the HTS framework must be carefully monitored and optimized as needed. However, since an oxidation threshold is necessary for evaluating all future experiments in this study and determining which assay and/or method will be selected for high-throughput oxidation screening in the future, the 2% threshold will also be used for the RP-UHPLC method, despite its variability exceeding the limit in these two instances.

5. Conclusion

This chapter focused on identifying the optimal experimental parameters for HTS oxidation stress assays. Based on the findings, the ideal conditions were established as follows: incubation with 0.05% hydrogen peroxide (HP), 0.75% tert-butyl hydroperoxide (tBHP), and 100 mM AAPH for 1.5 h at room temperature achieved the best results. For a HTS-compatible metal-catalyzed oxidation (MCO) assay, incubation with 0.4 mM Fe(II) and 4 mM H_2O_2 was selected. Light stress conditions were set at 600 klux*h of visible light and 100 Wh/m² of UV exposure. Additionally, an oxidation stress threshold of 2% was established to distinguish true oxidation effects from assay variation, ensuring consistent and accurate data evaluation across multiple experiments.

Furthermore, this chapter also highlighted the importance of quenching oxidation reactions uniformly across all samples to maintain data integrity and comparability. Spiking with an excess amount of free methionine was identified to be equally effective as traditional buffer exchange approaches.

6. References

1. Halley J, Chou YR, Cicchino C, et al. An Industry Perspective on Forced Degradation Studies of Biopharmaceuticals: Survey Outcome and Recommendations. *J Pharm Sci*. 2020;109(1):6-21.

2. Swadesh JK, Thannhauser TW, Scheraga HA. Sodium sulfite as an antioxidant in the acid hydrolysis of bovine pancreatic ribonuclease A. *Anal Biochem*. 1984;141(2):397-401.

3. Forman HJ, Zhang H, Rinna A. Glutathione: Overview of its protective roles, measurement, and biosynthesis. *Mol Asp Med*. 2009;30(1-2):1-12.

4. Folzer E, diepold K, bomans K, et al. Selective Oxidation of Methionine and Tryptophan Residues in a Therapeutic IgG1 Molecule. *J Pharm Sci*. 2015;104(9):2824-2831.

5. Ji JA, Zhang B, Cheng W, Wang YJ. Methionine, tryptophan, and histidine oxidation in a model protein, PTH: Mechanisms and stabilization. *J Pharm Sci*. 2009;98(12):4485-4500.

6. Nowak C, Cheung JK, Dellatore SM, et al. Forced degradation of recombinant monoclonal antibodies: A practical guide. *mAbs*. 2017;9(8):1217-1230.

7. Keck RG. *The Use of T-Butyl Hydroperoxide as a Probe for Methionine Oxidation in Proteins*.; 1996:56-62.

8. Werber J, Wang YJ, Milligan M, Li X, Ji JA. Analysis of 2,2'-Azobis (2-Amidinopropane) Dihydrochloride Degradation and Hydrolysis in Aqueous Solutions. *J Pharm Sci*. 2011;100(8):3307-3315.

9. Shah DD, Zhang J, Hsieh M ching, Sundaram S, Maity H, Mallela KMG. Effect of Peroxide- Versus Alkoxyl-Induced Chemical Oxidation on the Structure, Stability, Aggregation, and Function of a Therapeutic Monoclonal Antibody. *J Pharm Sci*. 2018;107(11):2789-2803.

10. Schöneich C. Photo-Degradation of Therapeutic Proteins: Mechanistic Aspects. *Pharm Res*. 2020;37(3):45.

11. Shah DD, Zhang J, Maity H, Mallela KMG. Effect of photo-degradation on the structure, stability, aggregation, and function of an IgG1 monoclonal antibody. *Int J Pharm*. 2018;547(1-2):438-449.

12. Du C, Barnett G, Borwankar A, et al. Protection of therapeutic antibodies from visible light induced degradation: Use safe light in manufacturing and storage. *Eur J Pharm Biopharm*. 2018;127:37-43.

13. Kaiser W, Schultz-Fademrecht T, Blech M, Buske J, Garidel P. Investigating photodegradation of antibodies governed by the light dosage. *Int J Pharm*. 2021;604:120723.

14. Heinzl GA, Lai L, Rao VA. Differentiating the Effects of Oxidative Stress Tests on Biopharmaceuticals. *Pharm Res*. 2019;36(7):103.

15. Stadtman ER. Metal ion-catalyzed oxidation of proteins: Biochemical mechanism and biological consequences. *Free Radic Biol Med*. 1990;9(4):315-325.

16. Glover ZK, Wecksler A, Aryal B, et al. Physicochemical and biological impact of metal-catalyzed oxidation of IgG1 monoclonal antibodies and antibody-drug conjugates via reactive oxygen species. *mAbs*. 2022;14(1):2122957.

17. Netto LES, Stadtman ER. *The Iron-Catalyzed Oxidation of Dithiothreitol Is a Biphasic Process: Hydrogen Peroxide Is Involved in the Initiation of a Free Radical Chain of Reactions Nyl (RSO •), Sulfonyl Peroxyl (RSO 2 OO •), and Sulfora*.; 1996:233-242.

V. DEVELOPMENT OF A HIGH-THROUGHPUT OXIDATION PROFILING STRATEGY FOR MONOCLONAL ANTIBODY PRODUCTS

The following chapter was published in European Journal of Pharmaceutics and Biopharmaceutics (doi:10.1016/j.ejpb.2024.114301).

Abstract

Oxidation is one of the most common degradation pathways of biopharmaceutics, potentially leading to altered product stability, pharmacokinetics, reduced biological activity and/or an increased immunogenicity. However, it is often insufficiently assessed in early development stages, leaving potential molecule liabilities undiscovered. The aim of the present work is the development of a high throughput oxidation profiling strategy, applicable throughout various stages of biopharmaceutical development. The study demonstrates that the combination of multiple stress assays, including peroxide-based, visible light, and metal-catalyzed oxidation (MCO), enables a comprehensive understanding of a mAb's oxidation susceptibility. The most effective parameters to evaluate oxidation in a high-throughput screening workflow are aggregation, tryptophan oxidation and changes in the hydrophobicity profile of the Fc and Fab subunit measured via Size Exclusion Chromatography, Intrinsic Tryptophan Fluorescence Spectroscopy and Reversed-Phase Chromatography subunit analysis, respectively. This oxidation profiling approach is a valuable tool to systematically characterize the oxidation susceptibility under relevant conditions, time effective and with minimal sample consumption.

1. Introduction

Biopharmaceuticals, including monoclonal antibody therapeutics, have become an important tool in the treatment of various diseases [1–3]. However, due to their size and complex structure, biotherapeutics are prone to chemical and physical degradation [4,5]. To ensure structural integrity throughout production, storage, transport and patient administration, identifying the ideal formulation composition is a crucial part of the biologic development process, which requires a comprehensive understanding of the candidate molecule. This task becomes more and more challenging since the continuous growth in this pharmaceutical area consequently increases the complexity of formulation development.

In the last years, AbbVie has developed a robotized, fully automated high throughput liquid formulation screening (HTS) line. This automation line enables a quality by design (QbD)-based approach by parallel testing of multiple stress conditions in combination with formulation excipient parameters [6]. As in early development stages the drug substance availability is often limited, the HT-screenings are performed in a miniaturized assay format in multi-well plates, thus only small amounts of the candidate protein are required. To evaluate the protein stability, various stress assays are performed, simulating the “real-life” degradation risk of a therapeutic protein, such as freeze/thaw, interfacial and temperature stress. They mimic freeze/thaw procedures during storage and transport, mechanical stress during manufacturing processes as well as incubation at storage (5 °C), accelerated and stress conditions (25 and 40 °C) as proposed by the ICH guidelines. To identify and quantify the impact of different stress factors, the standardized workflow includes a set of analytical methods, compatible with HT applications and multi-well formats. Each method is characterized by fast execution, universal applicability for all candidate molecules and low sample consumption. Suitable methods are chromatography-based or plate reader analytics [7]. Compared to a standard manual formulation development approach, HTS formulation development facilitates the generation of large data sets that allow comprehensive characterization of the candidate molecule, the identification of critical formulation parameters, and hence the definition of the corresponding design space. Furthermore, due to standardization of the screening process, data comparison across multiple development projects is possible, creating opportunities for data science and prediction models in the future.

While the existing HTS workflow already considers the most common stress conditions, it currently does not include routine screenings for oxidation, leaving potential molecule liabilities undiscovered. Oxidation, one of the most common chemical degradation pathways of therapeutic proteins, can be induced by a large variety of mechanisms.

Examples are oxidative contaminations during the manufacturing process or oxidants derived from excipients, such as hydrogen peroxide [8,9]. Further causes of oxidation are the presence of transition metals [10,11], leading to metal-catalyzed oxidation (MCO) or exposure to visible and UV light (photooxidation) [12–14]. Each of the examples described above, promotes the generation of reactive oxygen species (ROS) and/or free radicals. Depending on the extent and location, oxidation of amino acid residues can lead to modifications of the protein structure and thus changes in the protein's physicochemical properties. As a consequence, the oxidized product might have altered pharmacokinetics, a reduced biological activity and an increased immunogenicity compared to the native form [15]. The different oxidation mechanisms and their consequences have already been extensively reviewed in literature [16,17]. To ensure quality and safety of the product, oxidation susceptibility of candidate molecules is routinely assessed in forced degradation studies, using chemical oxidants such as H_2O_2 or tBHP. Other strategies are treatment with the free radical generating compound 2,2-azo-bis(2-amidinopropane)dihydrochloride (AAPH) or photostability studies according the 1QB ICH guideline [18,19]. These studies, as part of the early-stage development, aim to identify potential degradation pathways of the molecule, hence harsh stress conditions are used. However, these conditions do not necessarily reflect practical oxidation risks. Additionally, oxidation experiments are often conducted using a limited set of oxidants or non-representatively low protein concentrations. Consequently, the oxidation susceptibility assessed in early stage forced oxidation studies cannot be applied for predicting molecule liabilities during formulation development.

The aim of the present study was the development of an HT oxidation screening strategy which allows comprehensive characterization of the oxidation susceptibility under relevant conditions within a short period of time and with minimal sample consumption. To allow integration in the already existing automated HTS workflow, it was necessary to define effective assay conditions considering representative oxidation risks of therapeutic proteins using the established equipment in the HTS line. To identify universally applicable HTS oxidation assays, in this present study we exposed five different monoclonal antibodies at an HTS standard protein concentration of 100 mg/ml to H_2O_2, tBHP, AAPH, MCO (Fenton reaction) visible and UV-A light. Additionally, the suitability of HTS analytics to detect the impact of oxidation on the proteins under representative stress conditions was evaluated. Therefore, the outcome of the oxidation experiments was characterized by using Size Exclusion Chromatography, Cation Exchange Chromatography, Protein A Chromatography, Intrinsic Tryptophan Fluorescence Spectroscopy and Reversed-Phase Chromatography of antibody subunits. Based on the data set obtained in this study, we established a universally applicable oxidation HT screening strategy for monoclonal antibodies.

2. Materials

Four monoclonal antibodies developed for therapy (referred to as mAb1-4) of the isotype IgG1 as well as the NIST mAb [20], which serve as an external reference, were used in this study. All five antibodies were manufactured in-house. The antibody stock solutions were diafiltrated into water for injection and concentrated to 150 mg/ml using Vivaspin 6 spin columns with a 30,000 MWCO PES membrane or the Ambr UF/DF device equipped with Sartocon® 50 kD PES cassettes (Sartorius, Göttingen, Germany). Protein concentration was determined by UV-VIS spectroscopy (Stunner, Unchained Labs, Pleasanton, CA, USA). All oxidation experiments were performed in clear, non-binding PS 96 well plates with F-bottom (Greiner Bio-One, Kremsmünster, Austria) and sealed with transparent adhesive foil (Applied Biosystems, Foster City, CA, USA).

Hydrochloric acid (HCl), sodium chloride (NaCl), Tris(hydroxymethyl)-aminomethan (Tris), tert-Butyl hydroperoxide (tBHP), sodium sulfate (Na_2SO_4), sodium phosphate dibasic heptahydrate ($Na_2HPO_4 \cdot 7H_2O$), sodium phosphate dibasic dihydrate ($Na_2HPO_4 \cdot 2H_2O$), MES monohydrate and acetonitrile gradient grade for liquid chromatography were purchased from Merck (Darmstadt, Germany). Hydrogen peroxide 30% (H_2O_2), iron(II) sulfate heptahydrate, iron(III) sulfate hydrate and 2,2-azo-bis-(2-amidinopropane) dihydrochloride (AAPH) were purchased from Sigma-Aldrich (St. Louis, MO). Dithiothreitol (DTT) was purchased from Fluorochem (Hadfield, UK), trifluoroacetic acid from VWR chemicals (Leuven, Belgium) and L-methionine from J.T. Baker (Radnor, PA, USA). IgG-specific proteases FabRICATOR® (IdeS) and Fabdello™ were obtained from Genovis AB (Lund, Sweden).

3. Methods

3.1. Preparation of oxidized samples

To generate a comprehensive data set, different stress assays were chosen, including oxidants representing the realistic oxidation risk in the life cycle of a therapeutic protein, such as peroxide, light exposure or contamination with metal ions. Furthermore, often used model compounds such as AAPH and tBHP were included in the screening. All experiments were carried out at the HTS standard protein concentration of 100 mg/ml.

Table V-1: Experimental parameters for oxidation stress screening

Oxidation Conditions				
Oxidant	**Assay Name**	**Concentration/ Light Dose**	**Incubation Time**	**Incubation Temperature**
H_2O_2	HP	0.05%	1.5 h	25 °C
tBHP	tBHP	0.75%	1.5 h	25 °C
AAPH	AAPH	100 mM	1.5 h	40 °C
Fe(II) / H_2O_2	MCO	0.4 / 40 mM	3.0 h	25 °C
Visible Light	VIS	600 klux*h	n/a	25 °C
UV-A Light	UV-A	100 Wh/m²	n/a	25 °C
Visible Light / Fe(III)	PhotoFenton	600 klux*h /10 µM	n/a	25 °C

Stress conditions suitable for a HT screening setting should generate a detectable level of degradation in a limited period of time yet allowing the differentiation of oxidation susceptibility within a large data set. The test conditions applied in the current study were identified in extensive optimization experiments and fulfil the mentioned criteria.

For chemical oxidation assays, mAbs were incubated with 0.05% H_2O_2, 0.75% tBHP or 100 mM AAPH. Metal catalyzed oxidation was simulated by treatment with 0.4 mM Fe(II) + 4 mM H_2O_2 (Fenton reaction). Samples without any oxidants were prepared as reference samples. All chemical oxidation assays were conducted under light protection in temperature-controlled incubators (Thermo CRS Ltd., Burlington, Canada).

Light stress experiments were carried out in an ICH compliant photostability chamber (Aralab, Rio de Mouro, Portugal) equipped with a fluorescent cool white light tube and a UV-A light source. Samples were exposed to either 600 klux*h of visible light or 100 Wh/m² of UV-A light, both representing 50% of the ICH Q1B recommended light dose for photostability testing. The illuminance of the fluorescent light was set to 29 klux, for the UV-A light an irradiance of 30 W/m² was used. Samples were exposed to light until the desired light dose was reached, then stored under light protection. In addition, samples containing 10 µM Fe(III) were exposed to 600 klux*h of visible light to investigate the effects of Photo-Fenton stress. For each light condition, a reference sample in a glass vial wrapped in aluminum foil (dark control) was stored next to the 96 well plate during light exposure. The oxidation conditions are summarized in table 1 below. To stop oxidation reactions after the defined incubation or light exposure time, samples were diluted with TBS buffer (50 mM Tris-HCl, 150 mM NaCl) pH 7.6 supplemented with 200 mM L-Methionine to 10 mg/ml protein content. Irrespective of the assay type, this TBS-Met buffer completely quenches all oxidative processes, to avoid continuation of oxidation during storage.

3.2. High throughput analytical methods

Unless otherwise noted, all chromatographic measurements were performed on an Acquity UPLC H-Class Bio System (Waters, Milford, MA, USA) equipped with a PDA detector to monitor UV absorption at 280 nm. The temperature in the sample manager of the UPLC system was maintained at 4 °C. All UHPLC columns used in this study were conditioned as recommended by the manufacturer prior to the measurements. If no additional sample preparation steps are mentioned in the sections below, all analytical measurements were performed using the quenched sample at 10 mg/ml without any further dilution. Analysis of chromatographic data was conducted using Chromeleon™ chromatography software (Thermo Fisher Scientific Inc., Waltham, MA, USA). The overall workflow of the sample preparation and analytical measurements is summarized below (Figure V-1).

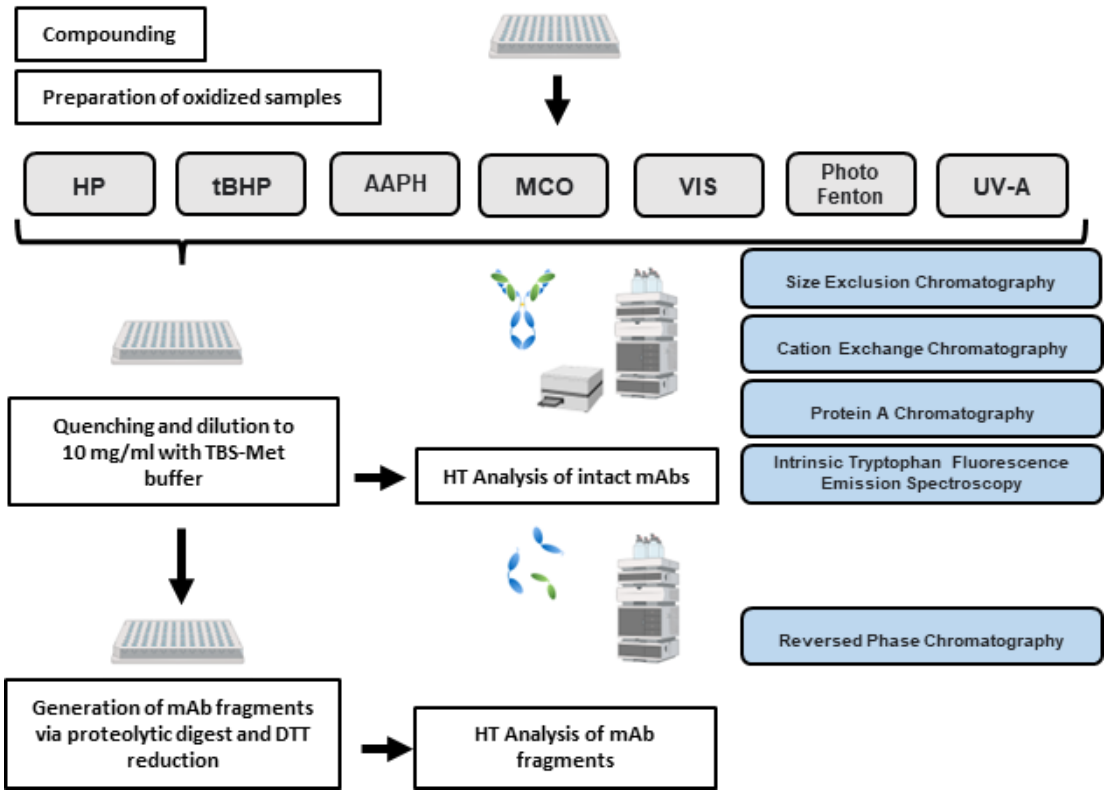

Figure V-1: Schematic workflow of sample preparation and analysis. Samples were oxidized with H_2O_2 (HP), tBHP, AAPH, Fe(II)+ H_2O_2 (MCO), visible light exposure alone (VIS) and in presence of iron ions (PhotoFenton) or UV-A radiation (UV-A).

3.2.1. Size Exclusion Chromatography (SEC)

To monitor the formation of high molecular weight species (HMW) and low molecular weight species (LMW), size exclusion analysis was performed. 40 µg were injected to a Waters ACQUITY UPLC BEH200 SEC column 4.6 x 150 mm; 1.7 µm, 200 Å (Waters, Milford, MA, USA) and separated by isocratic elution using 100 mM Na_2HPO_4 / 200 mM Na_2SO_4, pH 7.0 at a flow rate of 0.4 ml/min for 6 min. Column temperature was maintained at 25 °C.

3.2.2. Cation Exchange Chromatography (CEX)

Cation exchange chromatography of oxidized mAbs was performed to investigate the formation of charged isoforms. Per sample, 40 µg were injected to a Protein-Pak Hi Res CM column 4.6 x 100 mm, 7 µm (Waters, Milford, MA, USA). Samples were separated by salt gradient elution using 20 mM MES at pH 6.5 as mobile phase A and 20 mM MES + 500 mM NaCl at pH 6.5 as mobile phase B. For mAb4, the NaCl content of mobile Phase

B was decreased to 250 mM. A linear gradient from 0 to 50% in 12.5 min was applied to elute the samples at 40°C. The flow rate was set to 0.6 ml/min.

3.2.3. Protein A Chromatography

Methionine oxidation in the Fc fragment was detected using an HTS-optimized version of a previously described analytical protein A chromatography method [21]. Analysis was performed at 30 °C on a MAbPac Protein A Column 4 x 35 mm (Thermo Scientific, Dreieich, Germany) using 50 mM Na_2HPO_4 • $2H_2O$ / 150 mM NaCl at pH 7.5 as mobile phase A and at pH 2.5 as mobile phase B. After the injection of 10 µg sample, the column was rinsed with 100% mobile phase A for 2 min to allow binding of the antibody to the stationary phase. Sample elution was performed using a linear gradient from 70% to 100% mobile phase B in 7 min, followed by a re-equilibration step with 100 % mobile phase A for 6 min. Protein A analysis was carried out at 30 °C column temperature using a flow rate of 0.2 ml/min.

3.2.4. Reversed-Phase Chromatography Subunit Analysis (RP)

Subunit analysis was performed using Reversed Phase Chromatography. Antibody subunits were generated enzymatically by introducing cleavage in the hinge region: mAb 1-3 were diluted to 2 mg/ml using TBS-Met buffer containing 100 units of IdeS, an IgG-specific cysteine protease (FabRICATOR, Genovis), and incubated for 60 min at 25 °C. As the presence of mutations in the hinge region impair cleavage by IdeS, digestion of mAb4 was performed using a protease, which cleaves human IgG1 above the hinge region (FabDELLO, Genovis). After dilution to 2 mg/ml with TBS-Met buffer containing 100 units of FabDELLO and 10 mM $CaCl_2$, samples were incubated over night at 40 °C. Following the enzymatic cleavage, disulfide bonds were reduced by addition of 50 mM DTT to the samples and incubation for 1 h at 40 °C. This generated three fragments: a heavy chain Fc fragment (Fc HC), light chain (LC) and a heavy chain Fd fragment (Fd HC), which resulted in three individual peaks after chromatographic separation (Figure V-2). The additional reduction step improved the resolution of the chromatographic peaks by further reducing the size of the fragments. As each protease cleaves at a different site of the hinge region, the generated fragments also show small differences.

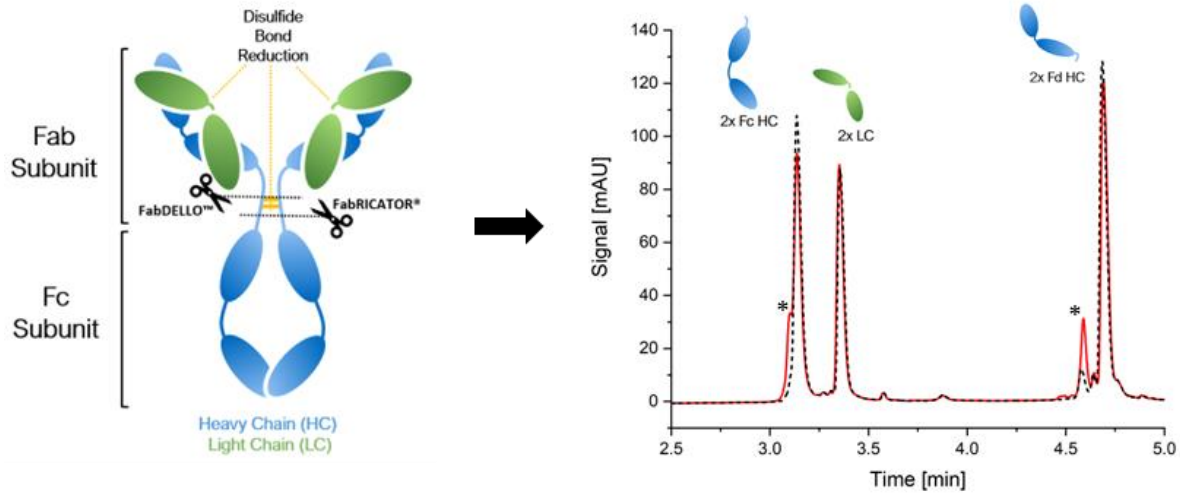

Figure V-2: Schematic representation of a mAb and localization of the enzymatic cleavage sites (left). This proteolysis and disulfide bond reduction procedure results in three fragments Fc HC, LC and Fd HC that can be identified in three individual peaks in the RP-UHPLC (right). The chromatogram shows the unstressed reference elution profile (black) superimposed with an oxidized mAb in red. Oxidation shoulders/peaks are marked with asterisk.

The generated subunits were analyzed on an Agilent 1290 Infinity System (Agilent Technologies, Santa Clara, CA, USA) equipped with DAD detector using a BioResolve RP mAb Polyphenyl column 2.1 x 50 mm, 2.7 µm, 450 Å (Waters, Milford, MA, USA). Mobile phase A was water with 0.1% TFA, mobile phase B was acetonitrile with 0.1% TFA. 2 µg sample was injected into the column, separation was performed using a linear gradient from 25% - 45% mobile phase B over 4 min at a flow rate of 0.3 ml/min at 80 °C.

3.2.5. Intrinsic Tryptophan Fluorescence Emission (ITFE)

Decrease in fluorescence intensity was determined by ITFE measurements using the Infinite® M1000 PRO microplate reader (Tecan Group AG, Männedorf, Switzerland). For ITFE measurements 250 µl per sample were transferred into black µclear®, non-binding PS 96 well plates with F-bottom (Greiner Bio-One, Kremsmünster, Austria). Samples were analyzed in five measuring cycles with an excitation wavelength of 295 nm (bandwidth 5 nm) and an emission wavelength of 330 nm (bandwidth 5 nm). Optimal gain and z-position were calculated by the device. Mean intensity values from all five cycles were calculated and blank corrected by subtracting the signal measured from the dilution buffer.

4. Results

The principal goal of the study was to identify the most effective oxidative stress assays to detect oxidation liabilities in a screening format. Therefore, a set of analytical methods was applied to monitor and evaluate the impact of multiple oxidation stresses. Each technique was already established in the fully automated workflow and was characterized by short analysis times ≤ 15 min (excluding sample preparation), low sample consumption and universal applicability, hence suitable for high throughput applications.

In the context of the new HTS assays, it was necessary to ensure clear differentiation of relevant oxidation signals from random noise. In preceding optimization experiments, reproducibility screenings were performed to determine the individual variability of each possible combination of oxidation assay and analytical method (data not shown). This variability arose from the different sample preparation steps required for the individual oxidation assays, including the preparation of working solutions, oxidant spiking and sample incubation as well as the method error of the respective analytical techniques applied. Based on the range of changes in relative peak area or fluorescent signal compared to an unstressed reference sample observed in the reproducibility screenings, a uniform 2% assay variability was defined, representing the worst-case method error to be expected from an assay and method combination. To simplify the data evaluation in large data sets and fulfill the requirements of the existing HTS workflow, this 2% threshold will be applied for all methods used in this study. As data points in this screening workflow were acquired as single measurements, only differences exceeding the 2% worst-case method error were classified as relevant oxidation. Any change smaller than this threshold was classified as assay variability and not considered for detailed evaluation.

4.1. Aggregation and fragmentation

Aggregation and fragmentation were monitored using SEC. Incubation with H_2O_2 or tBHP did not result in formation of HMWs, whereas treatment with AAPH and light exposure induced aggregation in all tested mAbs (Figure V-3A). The extent of aggregation under light exposure varies strongly between the individual mAbs, with mAb4 and NIST mAb showing the highest and mAb2 the lowest susceptibility. Compared to visible light alone, the addition of Fe(III) had negligible effects on HMW formation in light exposed samples, except for mAb3, where the fraction of aggregates was drastically increased in the presence of iron ions. After AAPH treatment, the highest levels of HMW increase were observed in mAb2 and NIST mAb samples, while the lowest levels were detected in mAb3 samples. Samples incubated with Fe(II)+H_2O_2 only showed minor changes in HMW

formation in all tested mAbs, with exception of mAb2, which just exceeded the oxidation threshold of 2%.

None of the tested oxidation conditions resulted in noteworthy fragmentation (Figure V-3B). LMW formation was below 2% for all samples, however, all samples containing Fe(III) showed a weak signal increase in LMWs after light exposure. This effect was not observed in the dark control samples containing iron; therefore the fragmentation was triggered by the combination of MCO and light exposure.

4.2. Charge isoforms

CEX analysis was performed to identify oxidation-induced charge heterogeneities by monitoring the loss of main isoform after oxidation treatment (Figure V-3C). Treatment with H_2O_2 or tBHP did not change the net charge of the tested mAbs, with exception of mAb4. In contrast, all tested mAbs showed a decrease in their main isoform content after treatment with AAPH. Light exposure also resulted in a loss of main isoform, however, the extent strongly varied between different antibodies. While mAb2 did show almost no change, the effect was drastically more pronounced in mAb1, 3 and 4. The presence of Fe(III) ions in light exposed mAb3 samples further promoted the loss of main isoform, whereas this effect was not noticeable for all other mAbs. Similar to the SEC results, treatment with Fe(II)+ H_2O_2 had nearly no impact on the net charge of the tested mAbs, with exception of mAb4. CEX analysis was not performed for the NIST mAb.

4.3. Oxidation of methionine and tryptophan residues

Following SEC and CEX analysis, modifications of oxidation prone amino acid residues after oxidation treatment were identified. As no LC MS workflow is established in the existing HTS line, two alternative approaches were used, focusing on two common oxidation targets in therapeutic antibodies, tryptophan and methionine residues [15,22].

Since first signs of oxidation in IgG1 antibodies are commonly detected in sensitive Met residues in the Fc subunit [23–25], analytical protein A chromatography is a well-established tool to detect such oxidation events. The application of protein A chromatography to detect oxidation in protein samples was first published by Loew et al.[21]. In this study, oxidized species generated under forced oxidation conditions using H_2O_2 and tBHP were successfully separated from non-oxidized species. An HTS adapted version of the method was used in this study. However, detectable changes above the 2% threshold were only

found in a few samples with no visible trend towards specific oxidation conditions or mAbs (data not shown).

Oxidation of tryptophan residues was detected using intrinsic tryptophan fluorescence spectroscopy (Figure V-3D). Due to its indole chromophore, tryptophan emits a highly specific fluorescence signal, which can be selectively detected after excitation at 295 nm. Tryptophan residues are mainly oxidized by free radical-based oxidation mechanisms [17,26]. A decrease in fluorescence intensity after light exposure has been successfully detected in previous oxidation studies [27,28].

In this oxidation screening, treatment with H_2O_2 did not result in ITFE signal loss. In contrast, even though both compounds triggered similar oxidation pathways, tBHP treatment slightly reduced the detected ITFE signal in mAb2, mAb3 and the NIST mAb. Incubation with AAPH resulted in a signal decrease for all tested mAbs, with the NIST mAb being the most susceptible. Exposure to visible or UV-A light did not lead to signal loss, with exception of mAb4. However, the presence of iron in light exposed samples reduced the signal intensity in mAb2, mAb3, mAb4 and the NIST mAb, with none of the corresponding dark controls showing a similar trend. Therefore, photooxidation of tryptophan seems to be slightly enhanced in the presence of iron. Similar to AAPH stress, treatment with Fe(II) + H_2O_2 also resulted in tryptophan oxidation, as all tested mAbs show a considerable loss of signal in oxidized samples compared to unstressed controls.

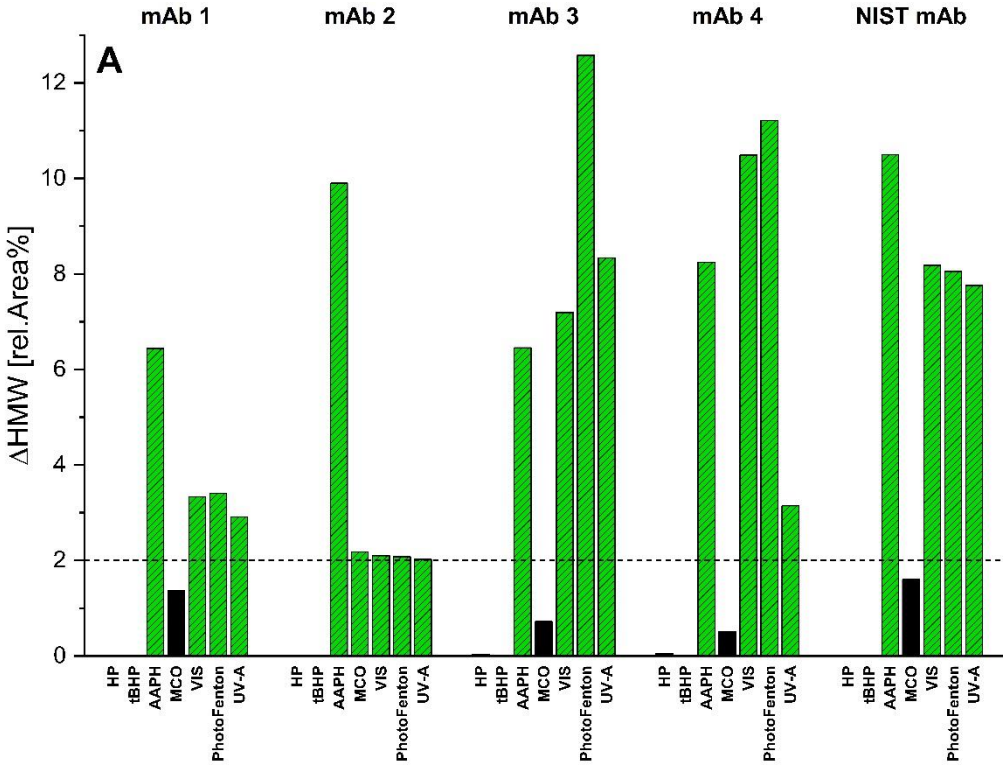

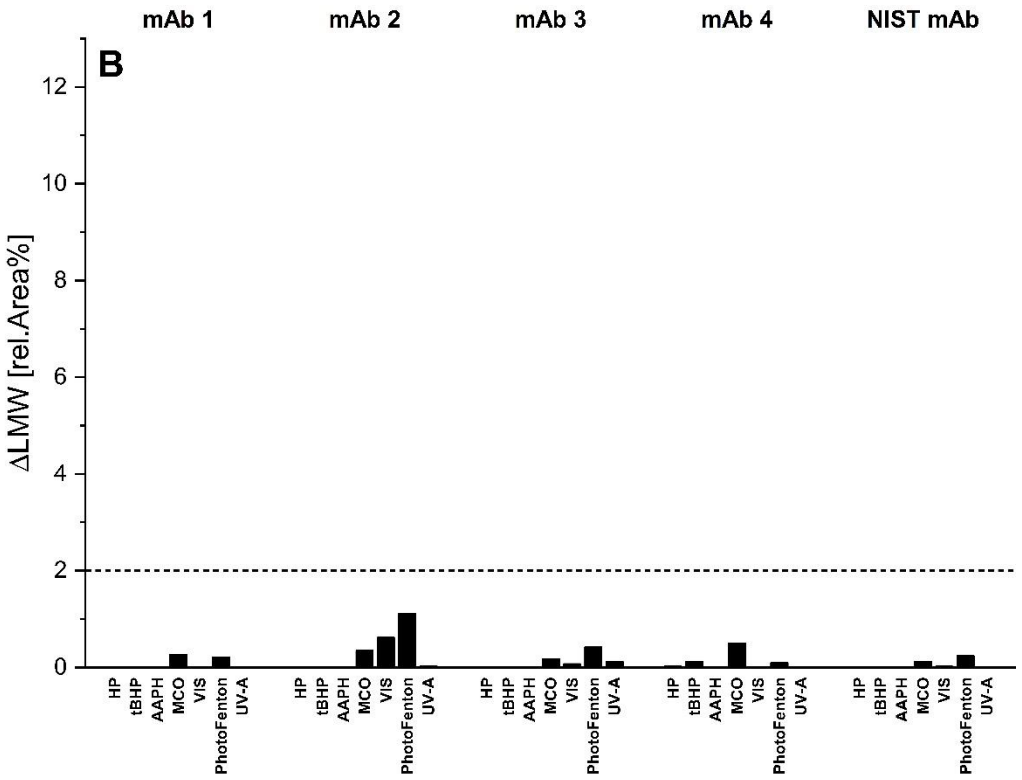
mAb 1
mAb 2
mAb 3
mAb 4
NIST mAb
B
ΔLMW [rel.Area%]
0
2
4
6
8
10
12
HP
tBHP
AAPH
MCO
VIS
PhotoFenton
UV-A

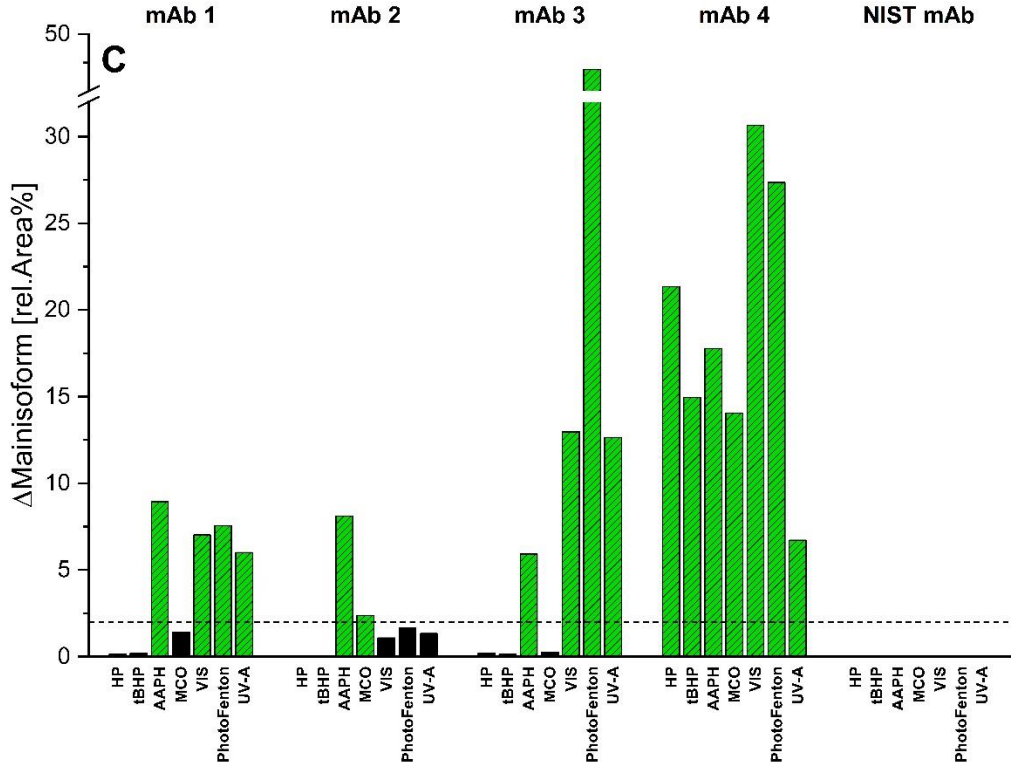
mAb 1
mAb 2
mAb 3
mAb 4
NIST mAb
C
ΔMainisoform [rel.Area%]
0
5
10
15
20
25
30
50
HP
tBHP
AAPH
MCO
VIS
PhotoFenton
UV-A

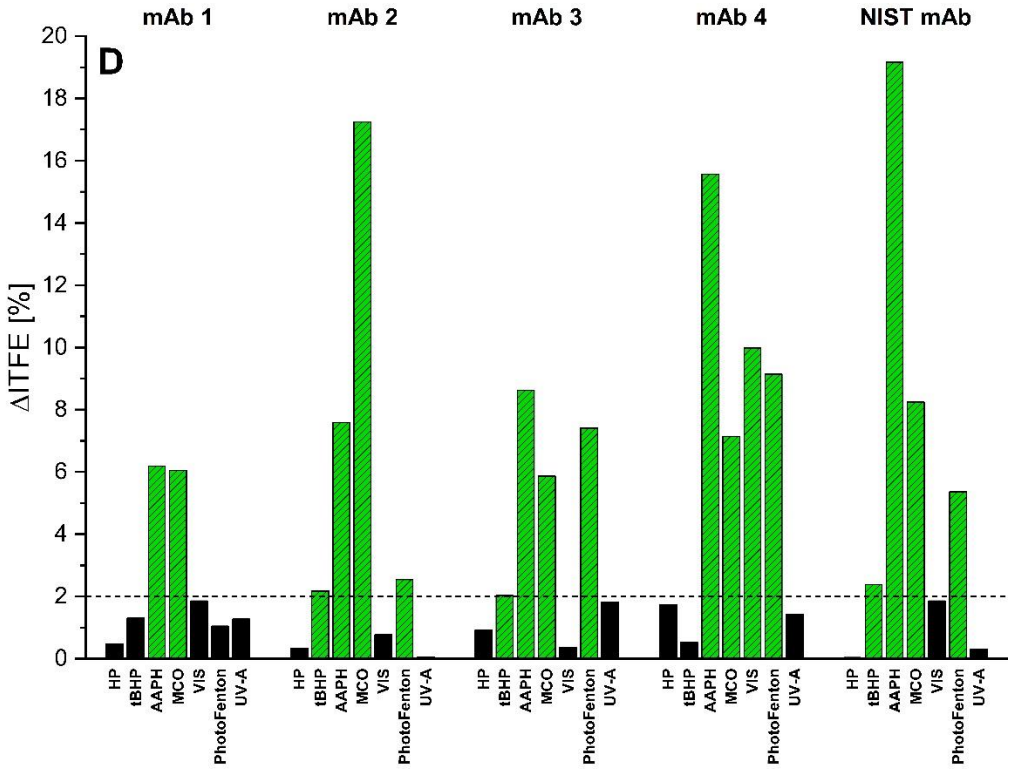

Figure V-3: Change in signal (Δ%) after oxidation stress treatments compared to an unstressed reference. Samples were oxidized with H_2O_2 (HP), tBHP, AAPH, Fe(II)+ H_2O_2 (MCO), visible light exposure alone (VIS) and in presence of iron ions (PhotoFenton) or UV-A radiation (UV-A). Formation of HMW (A) and LMW (B) species were detected using SEC, loss of Mainisoform (C) was monitored via CEX and the loss of intrinsic tryptophan signal (D) was measured using IFTE spectroscopy. Data points were acquired as single measurements. All differences shown in green exceed the largest measurement error of 2% derived from 1200 previous data points (data not shown). Loss of Mainisoform (C) was not determined for the NIST mAb.

4.4. Modification of Fc and Fab subunits

For detection and localization of modifications in the Fc and Fab subunits, RP-UHPLC subunit analysis was performed. To avoid undesired secondary oxidation reactions between DTT and the traces of metal ions left in the samples after quenching and dilution, no reduction step was conducted for samples containing iron. The effect of oxidation was evaluated by examining the elution profile for additional peak shoulders and individual peaks prior to the main Fc HC and Fd HC peak (Figure V-2), indicating changes in the hydrophobicity of the mAb subunits induced by oxidation. Every chosen stress condition promoted the formation of an additional peak shoulder of the Fc HC peak, demonstrating that each oxidant is able to induce modifications of amino acid residues in the Fc subunit (Figure V-4A). For all mAbs, the highest level of degradation was observed in the sample treated with H_2O_2. In contrast, the extent of oxidation observed after Fe(II)+ H_2O_2 treatment or light exposure varies considerably for individual mAbs. RP-MS of selected samples from this data set confirmed that the detected changes in hydrophobicity are the result of oxidation in Fc located methionine residues (data not shown).

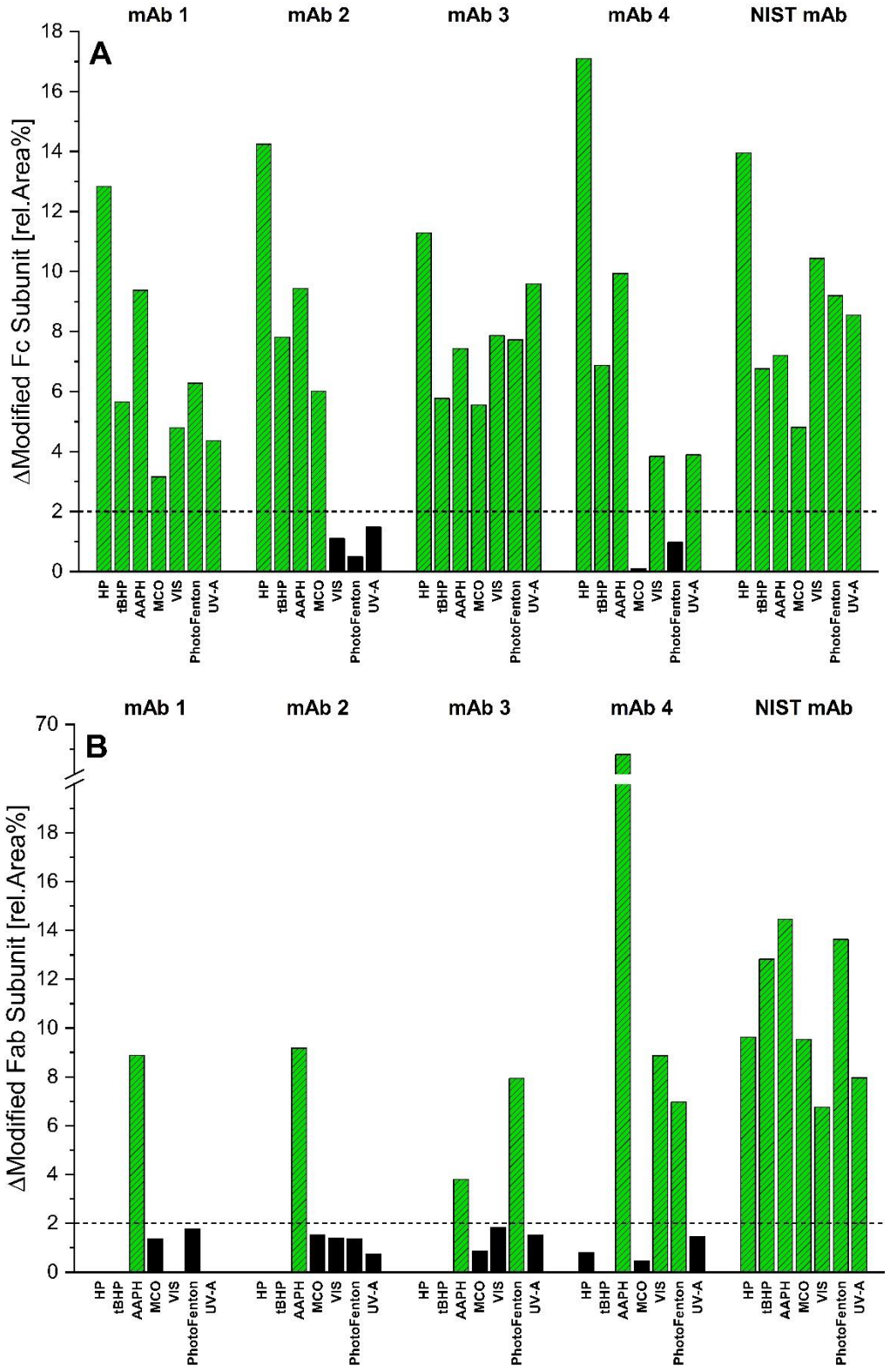

Figure V-4: Change in signal (Δ%) after oxidation stress treatments compared to an unstressed reference. Samples were oxidized with H_2O_2 (HP), tBHP, AAPH, Fe(II)+ H_2O_2 (MCO), visible light exposure alone (VIS) and in presence of iron ions (PhotoFenton) or UV-A radiation (UV-A). Changes in the hydrophobicity of the Fc HC fragment (A) and Fd HC fragment (B), indicating oxidative modifications of the subunits were assessed using RP-UHPLC. Data points were acquired as single measurements. All differences shown in green exceed the largest measurement error of 2% derived from among 1200 previous data points (data not shown).

Modification of the Fab subunit was less pronounced (Figure V-4B). Only the NIST mAb showed an increase of approximately 10% in Fd HC peak shoulder formation after peroxide-based oxidation treatment. This change in hydrophobicity of peroxide stressed NIST samples is caused by oxidation of an Fd located methionine residue, as identified by additional RP-MS analysis (data not shown). In contrast, incubation with AAPH resulted in modification of the Fab subunit in all tested mAbs, with mAb4 being particularly susceptible. Light-induced changes of the Fd HC fragment elution profile were only observed for mAb 4 and NIST mAb. However, the presence of iron during light exposure also promoted Fab subunit modifications in mAb3. Effects of Fe(II)+ H_2O_2 treatment were only detected for the NIST mAb.

5. Discussion

5.1. Selection of HT screening methods

Therapeutic proteins are exposed to various oxidative stressors during product development and manufacturing (e.g. peroxides, light, metal ions). The array of chosen oxidation stress assays used in this work aims to cover as completely as possible all conceivable sources of oxidation in order to reveal any molecular oxidation sensitivity. Since not every oxidation stress leads to a detectable signal in every analytical method, it was necessary to identify these methods with the greatest information content, in the given context of a high throughput screening line and at relevant, moderate oxidative stress conditions. Stability indicating attributes (SIA) that help with this selection are aggregation, fragmentation, charge heterogeneity or polarity changes as the consequence of oxidation events that either lead to local chemical modification of protein side chains and possibly also induce larger structural changes in the protein including aggregation [27,29,30].

Aggregation was observed after multiple oxidation stress treatments (Figure V-3A). Fragmentation, however, was not provoked under the chosen conditions (Figure V-3B), although this type of degradation has been reported for example as a consequence of metal catalyzed oxidation [10,31,32]. Changes in the charge profile of the mAbs were detected using CEX (Figure V-3C). Depending on stress assay and tested mAb, loss of the main isoform was observed. Notably, changes in net charge were only found in samples, which also showed formation of HMWs (Figure V-3A+C). Since aggregation, as a result of structural changes, may also influence the elution behavior in CEX, it is not possible to distinguish if the real origin of the changes was caused by individual modifications of amino acids or by overall structural changes in the protein. While both screening methods are suitable for HT applications, the CEX data evaluation in large sample sets is more error-prone compared to SEC, due to the complex peak pattern and higher variability of charge isoform formation under different stress conditions. Hence CEX analytics was deprioritized.

Apart from stability indicating attributes, localization of oxidation sites by monitoring modifications of individual oxidation prone amino acid residues is common practice and often examined using LC-MS peptide mapping [33–36]. However, while LC-MS analytics are highly efficient in detecting individual modification sites, this technique is not available in our HTS framework. A well-established alternative is Reversed-Phase UHPLC analysis coupled with enzymatic digestion to generate antibody subunits. As shown by Zhang et al.[37], the results of a rapid IdeS-UHPLC method using UV detection demonstrated high correlation to time consuming LC-MS analysis. Additionally, An et al. reported a reliable

detection of peroxide and light induced oxidation of non-conserved methionine residues in the Fc/2 and Fd fragments [38]. This high throughput compatible approach was also used in our study to successfully locate modifications of mAb fragments after oxidation treatment (Figure V-4). In addition to the established IdeS digest step, the protocol was further expanded to also enable the digestion of antibodies containing mutations in the hinge region. The detail level of this approach is sufficiently high for formulation development purposes and to generate comprehensive product understanding.

Identification of oxidation in Fc located methionine residues has been successfully performed via analytical protein A chromatography in multiple oxidation studies [21,23,39,40]. However, adaption of the method to high throughput conditions reduced its sensitivity and consequently efficacy. While heavily oxidized samples were still detected, the method is not suitable as a screening tool for samples stressed under moderate oxidation conditions as described in this study. Nevertheless, from a mechanistical point of view, the method confirms that peroxides target methionine residues in the Fc binding region of the utilized mAbs as expected. As this oxidation screening approach will be integrated in an already existing automated workflow, potential interferences with existing process steps should be minimized by keeping the incubation times for each oxidation assay as short as possible. Even though an increased incubation time of oxidized samples might have improved the conduciveness of the protein A chromatography method, the RP-UHPLC analysis of the Fc HC fragment described above is better suited for HT application due to its higher sensitivity. Another crucial aspect to consider in context of HT screenings is the lifetime of the UHPLC columns. Despite the high temperature required for the analysis, the selected RP column shows higher robustness, allowing >1000 injections per column before showing first signs of performance loss, and is therefore superior to the Protein A column in terms of sustainability.

ITFE was confirmed as an efficient method to detect tryptophan oxidation under the chosen oxidation conditions. ITFE does not need tedious sample preparation, is universally applicable for all antibodies, does not consume any sample and is thus an ideal screening method, capable of examining large sample sets using a plate reader.

Altogether, the combination of aggregation measured via SEC, detection of tryptophan oxidation using ITFE and the assessment of Fc and Fab modification in RP-UHPLC subunit analysis are the most effective parameters to identify oxidation under different stress conditions in the HTS workflow. Fragmentation, albeit often observed under more accelerated conditions, was not observed in this study and is therefore not a suitable SIA in the HTS context. Charge heterogeneity is a similarly sensitive stability parameter as aggregation, however, due to its complexity, it is categorized as a less meaningful SIA

compared to aggregation. Reliable detection of methionine oxidation via HT analytical protein A chromatography was not achieved under the tested oxidation conditions.

5.2. Impact of oxidation

As oxidation can damage a protein via multiple pathways depending on the type of oxidative stress and molecular liabilities of the antibody, different oxidation assays were conducted to evaluate their suitability and necessity for HTS oxidation workflows. The intention of this screening workflow was to develop a high throughput suitable tool for oxidation profiling with broad applicability in various product development stages. As the data evaluation and final conclusion is highly dependent on the initial question the screening is applied for, it is not possible to provide a universal evaluation strategy. Therefore, in this study, all oxidation stress assays were treated equally during data handling, even though they are not equally important in the life cycle of a therapeutic antibody and the interpretation will depend on the development context. The experimental findings for all tested stress assays and their impact on each HTS compatible SIA is visualized in the stress plots. To reduce the complexity of the study, the IgG class was intentionally restricted to IgG1 as it represents the most common molecular format among mAb biotherapeutics (71%) [41]. However, we are convinced that the findings can be transferred to other IgG classes.

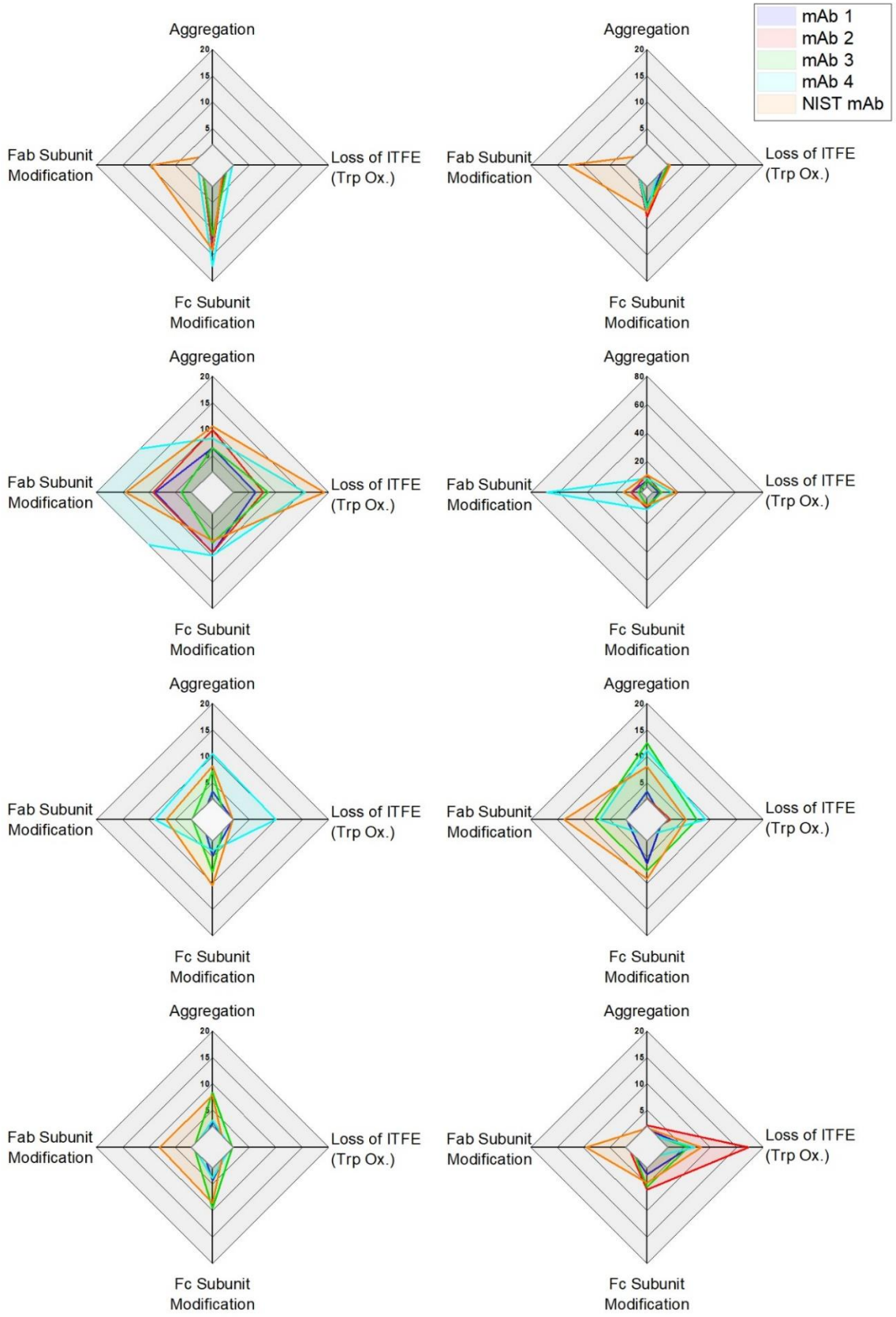

Figure V-5: Oxidation stress profiles after treatment with H_2O_2 (A), tBHP (B), AAPH (C + D), visible light (E), photo-Fenton stress (F), UV-A light (G) and MCO (H). The plots show the change in signal (%) compared to an unstressed reference sample. Apart from figure D the axes of all subfigures are on the same scale. For better visibility the AAPH stress assay is shown at two scales.

Peroxide based oxidative stress induced by incubation with H_2O_2, or alternatively tBHP, is one of the most common strategies used in forced degradation studies to evaluate the oxidation susceptibility of a candidate molecule[18]. Under the selected conditions in this study, H_2O_2 (0.05%) and tBHP (0.75%) mainly targeted the Fc fragment, as detected via RP UHPLC subunit analysis (Figure V-5A+B). The degradation observed was at a comparable level for all tested mAbs, indicating that in all cases the same oxidation-prone amino acid residues in the Fc subunit were affected by hydrogen peroxide and tBHP treatment. Interestingly, even though the Fc fragments of the tested mAbs are almost completely identical and the same amino acid residues are targeted by the peroxide induced oxidation, they still show small variations in Fc oxidation extent. The starting material has been processed to different extents and/or stored for shorter or longer periods, presumably resulting in minute structural perturbations and variable overall stability of the mAb material. Most likely, the pre-processing of the used drug substance influences the oxidation tendency of the Fc fragments. In contrast to the therapeutic mAbs, treatment of the NIST mAb with H_2O_2 and tBHP additionally resulted in modification of the Fab HC fragment, indicating further oxidation liabilities in the Fab subunit. However, neither of the two oxidants induced aggregation or oxidation of tryptophan residues. While both SIAs, aggregation and tryptophan oxidation, are not common consequences of peroxide-based oxidation processes, they are often observed as a result of other representative oxidative stresses, such as light exposure. Hence, forced oxidation studies with H_2O_2 or tBHP alone are not ideal to evaluate the overall oxidation susceptibility of a mAb.

In contrast, treatment with AAPH generated a more diverse stress pattern, including modifications of the Fc HC and Fab HC fragment, tryptophan oxidation and aggregation (Figure V-5C+D). All tested mAbs are affected by AAPH treatment, but the extent of damage detected for each SIA varied based on the individual susceptibility of the mAb. The free radical mediated oxidation initiated by AAPH hydrolysis can trigger different mechanisms and therefore target multiple sites in the antibody [30,36], making AAPH an effective compound for forced oxidation studies. While AAPH does not directly represent a realistic oxidant of biopharmaceutics, oxidation pathways including free radical cascades are also common mechanisms described for photooxidation processes [13,14]. In comparison to photostability studies, a chemical oxidation assay using AAPH is more convenient and time efficient, hence favorable for high throughput applications. However, it has been shown in previous studies that AAPH induced oxidation does not necessarily simulate the oxidation processes generated by more representative stress conditions such as light exposure or metal catalyzed oxidation, even though they both involve free radical based pathways [36,42]. Similar results were obtained in this study using more moderate oxidation conditions, AAPH, MCO and light exposure create different stress patterns.

After exposure to visible and UV-A light, in contrast to the chemical oxidants evaluated, the extent of degradation observed for the individual SIAs shows large variations throughout all antibodies (Figure V-5E+G). Interestingly, the majority of the results indicate a higher susceptibility towards the tested visible light dose compared to UV-A radiation. UV-A light can be directly absorbed by tryptophan residues in the molecule and trigger multiple degradation pathways, while photooxidation under visible light is most likely initiated by photosensitizing contaminations [12] . In its life cycle, a biologic is exposed to light in the visible range during multiple occasions, for example to fluorescent or LED room light in the manufacturing and packaging process or window-filtered daylight during administration [43,44]. Exposure to accelerated UV-A doses up to 200 Wh/m², as proposed in the ICH Q1B guideline, is less common under indoor light conditions. Hence, to evaluate the risk of photooxidation under more representative conditions, an assay using light in the visible range should be preferred. Another aspect investigated in this study was the effect of metal iron contamination on the photodegradation of monoclonal antibodies. A recently published study showed an increased risk of fragmentation in light exposed mAbs formulated in buffers containing additional metal irons [31]. While no increase in LMW formation above the 2% threshold was detected in our experiments, aggregation, tryptophan oxidation and Fab HC modifications were enhanced in mAb 3 samples in the presence of iron (Figure V-5F). Changes in the buffer systems during formulation development of biologics carries the risk of additional metal ion contaminations and might alter the photostability, which was initially determined in early stage forced oxidation studies. The addition of a Photo-Fenton assay to the stress panel can expand the photosensitivity evaluation and minimize the risk of new light liabilities after formulation development. The effect of metal catalyzed oxidation has been demonstrated in many studies, reporting a wide range of degradation, depending on the type of metal ion used and individual susceptibility of the tested protein [10,17,42,45]. Using a Fe(II)+ H_2O_2 assay, we induced tryptophan oxidation in all tested mAbs, leading to a loss of ITFE signal (Figure V-5H). Further, changes in the polarity profile of the Fc HC fragment were identified via reversed phase chromatography for all mAbs except mAb4, indicating oxidation of Fc located methionine residues. In contrast to other free radical based oxidation assays such as AAPH or light stress exposure, the MCO treatment did not result in aggregation. However, those findings are in line with the results of a study published by Glover et al., where the detected levels of HMW formation were significantly lower in samples treated with Fe(II)+ H_2O_2 compared to a Cu(II) + Ascorbate-mediated stress [10]. It should be noted that the extent of degradation observed in our study is less pronounced than the effects of MCO described in literature. It was hypothesized that the high protein concentration used may be prohibitive for the reaction. While literature studies used 1 – 10 mg/ml, our study used the HTS standard protein concentration of 100 mg/ml. Nevertheless,

the oxidation conditions used for the HTS MCO assay were sufficient to induce a detectable level of stress that allows to evaluate the susceptibility towards iron ion mediated oxidation.

6. Conclusion

Oxidation is one of the most common degradation pathways of biopharmaceutics, but often insufficiently assessed due to limited material availability in early development stages. In this study, we aimed to identify an HT compatible oxidation screening strategy, including representative oxidation stress assays and efficient HT analytics.

Based on our findings, aggregation, tryptophan oxidation and changes in the hydrophobicity profile of the Fc and Fab subunit were identified as the most effective parameters to evaluate oxidation in a HT screening workflow. Using these attributes to characterize the impact of different oxidation assays, we were able to identify a unique stress pattern for each tested antibody, depending on the oxidation mechanism of the oxidant and the individual oxidation susceptibility of the mAb. While peroxide-based assays, as the most common forced oxidation treatment, were a reliable tool to generate local modifications in all mAbs, they did not provide a complete picture of all potential oxidation liabilities. In contrast, as demonstrated in the present results, using assays based on different reactive oxygen species, such as AAPH, MCO or light exposure, may be a more efficient strategy. In conclusion, to mitigate the oxidation risk of monoclonal antibodies as effectively as possible, the combination of multiple stress assays is highly suggested.

However, in order to meet the requirements of the HTS framework, the number of oxidation assays should be kept as small as possible, only including the stress assays generating the most comprehensive picture. Therefore, the combination of a peroxide-based, visible light and MCO assay, all representing a realistic degradation risk in the life cycle of a protein, were selected as the most effective tools to evaluate oxidation susceptibility.

In conclusion, the present oxidation screening approach enables time efficient profiling of oxidation liabilities in a high throughput format. The concept is applicable throughout various stages of biopharmaceutical development, such as candidate molecule selection or formulation development.

7. References

1. Lu RM, Hwang YC, Liu IJ, et al. Development of therapeutic antibodies for the treatment of diseases. *J Biomed Sci*. 2020;27(1):1-30. doi:10.1186/s12929-019-0592-z

2. Ecker DM, Jones SD, Levine HL. The therapeutic monoclonal antibody market. *MAbs*. 2015;7(1):9-14. doi:10.4161/19420862.2015.989042

3. Buss NAPS, Henderson SJ, McFarlane M, Shenton JM, De Haan L. Monoclonal antibody therapeutics: History and future. *Curr Opin Pharmacol*. 2012;12(5):615-622. doi:10.1016/j.coph.2012.08.001

4. Krause ME, Sahin E. Chemical and physical instabilities in manufacturing and storage of therapeutic proteins. *Curr Opin Biotechnol*. 2019;60:159-167. doi:10.1016/j.copbio.2019.01.014

5. Manning MC, Chou DK, Murphy BM, Payne RW, Katayama DS. Stability of protein pharmaceuticals: An update. *Pharm Res*. 2010;27(4):544-575. doi:10.1007/s11095-009-0045-6

6. Siedler M, Eichling S, Huelsmeyer M, Angstenberger J. Formulation Development for Biologics Utilizing Lab Automation and In Vivo Performance Models. In: Jameel F, Skoug JW, Nesbitt RR, eds. *Development of Biopharmaceutical Drug-Device Products*. AAPS Advances in the Pharmaceutical Sciences Series, vol 35. Springer; 2020:299-341. https://doi.org/10.1007/978-3-030-31415-6_13

7. Samra HS, He F. Advancements in high throughput biophysical technologies: Applications for characterization and screening during early formulation development of monoclonal antibodies. *Mol Pharm*. 2012;9(4):696-707. doi:10.1021/mp200404c

8. Kerwin BA. Polysorbates 20 and 80 used in the formulation of protein biotherapeutics: structure and degradation pathways. *J Pharm Sci*. 2008;97(8):2924-2935. doi:10.1002/jps.21190

9. Ha E, Wang W, Wang YJ. Peroxide formation in polysorbate 80 and protein stability. *J Pharm Sci*. 2002;91(10):2252-2264. doi:10.1002/jps.10216

10. Glover ZK, Wecksler A, Aryal B, et al. Physicochemical and biological impact of metal-catalyzed oxidation of IgG1 monoclonal antibodies and antibody-drug conjugates via reactive oxygen species. *MAbs*. 2022;14(1):2122957. doi:10.1080/19420862.2022.2122957

11. Stadtman ER. Metal ion-catalyzed oxidation of proteins: Biochemical mechanism and biological consequences. *Free Radic Biol Med*. 1990;9(4):315-325. doi:10.1016/0891-5849(90)90006-5

12. Schöneich C. Photo-Degradation of Therapeutic Proteins: Mechanistic Aspects. *Pharm Res*. 2020;37(3). doi:10.1007/s11095-020-2763-8

13. Pattison DI, Rahmanto AS, Davies MJ. Photo-oxidation of proteins. *Photochem Photobiol Sci*. 2012;11(1):38-53. doi:10.1039/c1pp05164d

14. Kerwin BA, Remmele RLJ. Protect from light: photodegradation and protein biologics. *J Pharm Sci*. 2007;96(6):1468-1479. doi:10.1002/jps.20815

15. Torosantucci R, Schöneich C, Jiskoot W. Oxidation of therapeutic proteins and peptides: Structural and biological consequences. *Pharm Res*. 2014;31(3):541-553. doi:10.1007/s11095-013-1199-9

16. Gupta S, Jiskoot W, Schöneich C, Rathore AS. Oxidation and Deamidation of Monoclonal Antibody Products: Potential Impact on Stability, Biological Activity, and Efficacy. *J Pharm Sci*. 2021;000. doi:10.1016/j.xphs.2021.11.024

17. Ji JA, Zhang B, Cheng W, Wang YJ. Methionine, tryptophan, and histidine oxidation in a model protein, PTH: Mechanisms and stabilization. *J Pharm Sci*. 2009;98(12):4485-4500. doi:10.1002/jps.21746

18. Halley J, Chou YR, Cicchino C, et al. An Industry Perspective on Forced Degradation Studies of Biopharmaceuticals: Survey Outcome and Recommendations. *J Pharm Sci*. 2020;109(1):6-21. doi:10.1016/j.xphs.2019.09.018

19. ICH Q1B. ICH Q1B Photostability Testing of New Active Substances and Medicinal Products. *Eur Med Agency*. 1998;(January):1-9. http://www.ema.europa.eu/docs/en_GB/document_library/Scientific_guideline/2009/09/WC500002647.pdf

20. National Institute of Standards and Technology. NIST Monoclonal Antibody Reference Material 8671. Accessed November 29, 2023. https://www.nist.gov/programs-projects/nist-monoclonal-antibody-reference-material-8671

21. Loew C, Knoblich C, Fichtl J, et al. Analytical protein a chromatography as a quantitative tool for the screening of methionine oxidation in monoclonal antibodies. *J Pharm Sci*. 2012;101(11):4248-4257. doi:10.1002/jps.23286

22. Li S, Schöneich C, Borchardt RT. Chemical instability of protein pharmaceuticals: Mechanisms of oxidation and strategies for stabilization. *Biotechnol Bioeng*. 1995;48(5):490-500. doi:10.1002/bit.260480511

23. Folzer E, Diepold K, Bomans K, et al. Selective Oxidation of Methionine and Tryptophan Residues in a Therapeutic IgG1 Molecule. *J Pharm Sci*. 2015;104(9):2824-2831. doi:10.1002/jps.24509

24. Stracke J, Emrich T, Rueger P, et al. A novel approach to investigate the effect of methionine oxidation on pharmacokinetic properties of therapeutic antibodies. *MAbs*. 2014;6(5):1229-1242. doi:10.4161/mabs.29601

25. Pan H, Chen K, Chu L, Kinderman F, Apostol I, Huang G. Methionine oxidation in human IgG2 Fc decreases binding affinities to protein A and FcRn. *Protein Sci*. 2009;18(2):424-433. doi:10.1002/pro.45

26. Ehrenshaft M, Deterding LJ, Mason RP. Tripping up Trp: Modification of protein tryptophan residues by reactive oxygen species, modes of detection, and biological consequences. *Free Radic Biol Med*. 2015;89:220-228. doi:10.1016/j.freeradbiomed.2015.08.003

27. Zheng K, Ren D, Wang YJ, et al. Monoclonal antibody aggregation associated with free radical induced oxidation. *Int J Mol Sci*. 2021;22(8). doi:10.3390/ijms22083952

28. Barnett G V., Balakrishnan G, Chennamsetty N, et al. Probing the Tryptophan Environment in Therapeutic Proteins: Implications for Higher Order Structure on

Tryptophan Oxidation. *J Pharm Sci*. 2019;108(6):1944-1952. doi:10.1016/j.xphs.2018.12.027

29. Alam ME, Slaney TR, Wu L, et al. Unique Impacts of Methionine Oxidation, Tryptophan Oxidation, and Asparagine Deamidation on Antibody Stability and Aggregation. *J Pharm Sci*. 2020;109(1):656-669. doi:10.1016/j.xphs.2019.10.051

30. Shah DD, Zhang J, Hsieh M ching, Sundaram S, Maity H, Mallela KMG. Effect of Peroxide- Versus Alkoxyl-Induced Chemical Oxidation on the Structure, Stability, Aggregation, and Function of a Therapeutic Monoclonal Antibody. *J Pharm Sci*. 2018;107(11):2789-2803. doi:10.1016/j.xphs.2018.07.024

31. Zhang Y, Schöneich C. Visible Light Induces Site-Specific Oxidative Heavy Chain Fragmentation of a Monoclonal Antibody (IgG1) Mediated by an Iron(III)-Containing Histidine Buffer. *Mol Pharm*. 2023;20(1):650-662. doi:10.1021/acs.molpharmaceut.2c00840

32. Liu Y, Li H, Yan Z, Zhang L, Sun P. Discovery and reduction of tryptophan oxidation-induced IgG1 fragmentation in a polysorbate 80-dependent manner. *Eur J Pharm Biopharm*. 2022;173:45-53. doi:10.1016/j.ejpb.2022.02.015

33. Li X, Xu W, Wang Y, et al. High throughput peptide mapping method for analysis of site specific monoclonal antibody oxidation. *J Chromatogr A*. 2016;1460:51-60. doi:10.1016/j.chroma.2016.06.085

34. Thakkar S V., Rodrigues D, Zhai B, et al. Residue-Specific Impact of EDTA and Methionine on Protein Oxidation in Biotherapeutics Formulations Using an Integrated Biotherapeutics Drug Product Development Workflow. *J Pharm Sci*. 2023;112(2):471-481. doi:10.1016/j.xphs.2022.09.011

35. Jacobitz AW, Liu Q, Suravajjala S, Agrawal NJ. Tryptophan Oxidation of a Monoclonal Antibody Under Diverse Oxidative Stress Conditions: Distinct Oxidative Pathways Favor Specific Tryptophan Residues. *J Pharm Sci*. 2021;110(2):719-726. doi:10.1016/j.xphs.2020.10.039

36. Dion MZ, Wang YJ, Bregante D, et al. The Use of a 2,2'-Azobis (2-Amidinopropane) Dihydrochloride Stress Model as an Indicator of Oxidation Susceptibility for Monoclonal Antibodies. *J Pharm Sci*. 2018;107(2):550-558. doi:10.1016/j.xphs.2017.09.022

37. Zhang B, Jeong J, Burgess B, Jazayri M, Tang Y, Taylor Zhang Y. Development of a rapid RP-UHPLC–MS method for analysis of modifications in therapeutic monoclonal antibodies. *J Chromatogr B Anal Technol Biomed Life Sci*. 2016;1032:172-181. doi:10.1016/j.jchromb.2016.05.017

38. An Y, Zhang Y, Mueller HM, Shameem M, Chen X. A new tool for monoclonal antibody analysis Application of IdeS proteolysis in IgG domain-specific characterization. *MAbs*. 2014;6(4):879-893. doi:10.4161/mabs.28762

39. Kaiser W, Schultz-Fademrecht T, Blech M, Buske J, Garidel P. Investigating photodegradation of antibodies governed by the light dosage. *Int J Pharm*. 2021;604(January):120723. doi:10.1016/j.ijpharm.2021.120723

40. Gaza-Bulseco G, Faldu S, Hurkmans K, Chumsae C, Liu H. Effect of methionine oxidation of a recombinant monoclonal antibody on the binding affinity to protein A and protein G. *J Chromatogr B Anal Technol Biomed Life Sci*. 2008;870(1):55-62. doi:10.1016/j.jchromb.2008.05.045

41. Ahmed L, Gupta P, Martin KP, Scheer JM, Nixon AE, Kumar S. Intrinsic physicochemical profile of marketed antibody-based biotherapeutics. *Biophys Comput Biol*. 2021;118(37). doi:https://doi.org/10.1073/pnas.2020577118

42. Heinzl GA, Lai L, Rao VA. Differentiating the Effects of Oxidative Stress Tests on Biopharmaceuticals. *Pharm Res*. 2019;36(7). doi:10.1007/s11095-019-2627-2

43. Wasylaschuk W, Pierce B, Geng X, et al. Assessing the Impact of Different Light Sources on Product Quality During Pharmaceutical Drug Product Manufacture – Fluorescent Versus Light-Emitting Diode Light. *J Pharm Sci*. 2020;109(11):3360-3369. doi:10.1016/j.xphs.2020.07.020

44. Baertschi SW, Clapham D, Foti C, et al. Implications of in-use photostability: Proposed guidance for photostability testing and labeling to support the administration of photosensitive pharmaceutical products, part 1: Drug products administered by injection. *J Pharm Sci*. 2013;102(11):3888-3899. doi:10.1002/jps.23717

45. Yang Y, Zhang F, Gan Y, et al. In-Depth Characterization of Acidic Variants Induced by Metal-Catalyzed Oxidation in a Recombinant Monoclonal Antibody. *Anal Chem*. 2023;95(14):5867-5876. doi:10.1021/acs.analchem.2c04414

VI. ANTIBODY OXIDATION AND IMPACT OF FORMULATION: A HIGH THROUGHPUT SCREENING APPROACH

The following chapter was published in European Journal of Pharmaceutics and Biopharmaceutics (doi.org/10.1016/j.ejps.2025.107113).

Abstract

Oxidation is a complex degradation pathway in biopharmaceutical products that necessitates comprehensive assessment to ensure product stability and safety. This study focuses on implementing an oxidative profiling workflow within a high-throughput (HT) formulation screening process to identify and mitigate potential oxidation liabilities. To assess the feasibility of integrating oxidative stress testing into HT formulation development, we analyzed the oxidation susceptibility of three monoclonal antibodies by varying several formulation parameters including protein concentration, buffer system and pH, surfactant type and concentration as well as presence of antioxidative excipients. Oxidative stress was induced using visible light, hydrogen peroxide, and metal-catalyzed oxidation. HT analytical methods such as Size Exclusion Chromatography and Reversed-Phase Chromatography subunit analysis were employed to assess aggregation and modification of Fc and Fab subunits. An oxidation scoring tool was developed to simplify the evaluation of large datasets. The results demonstrated that formulation composition can significantly influence oxidation susceptibility. However, the outcomes varied greatly among the different antibodies, highlighting the need for a comprehensive profiling approach. The study confirms that the oxidation profiling workflow is an effective method for routine HT formulation screenings, providing a thorough evaluation of the oxidative stability of biopharmaceutical formulations.

1. Introduction

Oxidation is a common chemical degradation pathway for biopharmaceuticals that might impair the quality and safety of the product and can be triggered by a variety of factors. The underlying reaction mechanisms and resulting consequences have already been extensively studied and reviewed in literature [1–4]. Still, due to the diversity of influencing factors and the complexity of degradation pathways and their interdependencies, a universal anti-oxidation approach that is always successful does not exist. Like many other formulation parameters, oxidation remains a quality attribute which needs to be individually assessed and monitored throughout the manufacturing process.

Apart from intrinsic factors, external parameters such as formulation excipients have been identified to affect the oxidation susceptibility of proteins[1–4]. Excipients with antioxidative capacities, such as free methionine as well as metal chelators like DTPA or EDTA are regularly used in commercial biopharmaceutical products to mitigate the oxidation risk [5–7]. In contrast, degradation products of commonly used surfactants such as polysorbate have been shown to promote oxidation of therapeutic proteins [8–12]. Furthermore, metal contaminations in formulation buffers have been identified as initiator for metal catalyzed oxidation, leading to fragmentation of monoclonal antibodies [13].

To fully understand the impact of a given formulation composition on the oxidation susceptibility of a product, comprehensive knowledge of the molecule's liabilities and potential formulation interactions is required. In this context, automated high throughput (HT) screening approaches, such as the HT screening line established in the AbbVie formulation development workflow, enabling parallel testing of multiple formulation excipient parameters under different stress conditions [14]. The miniaturized assay format, performed in multi-well plates, requires only small amounts of the candidate molecule. In combination with high throughput analytical methods, this screening strategy offers a time efficient solution to comprehensively assess the stability impact of a large number of formulations compositions under different stress conditions.

In our recent work we presented an oxidation profiling strategy for high throughput applications, compatible with our existing screening line [15]. The results demonstrated that the combination of representative oxidation stresses, such as visible light, hydrogen peroxide spiking or metal catalyzed oxidation followed by fast HT analytics, is an effective tool to characterize oxidation susceptibility of individual mAbs.

As a follow-up study, the objective of this work was to implement the outlined oxidation profiling workflow within a representative high-throughput formulation screening for

therapeutic antibodies. The goal was to confirm its effectiveness in detecting mAb-specific oxidation liabilities under representative stress conditions, as well as the identification of potential formulation-derived oxidation risks and formulation-based mitigation strategies, all within one time-efficient screening approach.

In this case study, we investigated the impact of multiple formulation parameters on three monoclonal antibodies, including protein concentration, buffer system and pH, surfactant type and concentration as well as presence of antioxidative excipients on the oxidation susceptibility. After stress treatment, the extent of aggregation as well as Fc and Fab subunit modification was assessed using Size Exclusion Chromatography and Reversed-Phase Chromatography subunit analysis. Collectively, our results are in agreement with reported findings in literature; however, the expression of specific properties depends strongly on the individual behavior of the mAb underlining the need for a screening approach. Furthermore, an oxidation scoring tool was established to simplify evaluation of large data sets. Taken together, the results of the present study demonstrate that the oxidation profiling workflow is fit for purpose to be used in routine high-throughput screening campaigns.

2. Materials

Two therapeutic monoclonal antibodies (referred to as mAb1 and mAb2) of the isotype IgG1 and the NIST mAb, which serves as an external reference, were used in this study. All three antibodies were manufactured in-house.

Hydrochloric acid (HCl), sodium chloride (NaCl), Tris(hydroxymethyl)-aminomethan (Tris), sodium sulfate (Na_2SO_4), sodium phosphate dibasic heptahydrate ($Na_2HPO_4 \cdot 7H_2O$), sodium phosphate dibasic dihydrate ($Na_2HPO_4 \cdot 2H_2O$), sodium dihydrogen phosphate dihydrate ($NaH_2PO_4 \cdot 2H_2O$), citric acid monohydrate, succinic acid, Tris(2-carboxyethyl)phosphine hydrochloride (TCEP), L-tryptophan, ethylenediaminetetraacetic acid (EDTA), diethylenetriaminepentaacetic acid (DTPA), formic acid (FA), ammonium formate for LC-MS and acetonitrile gradient grade for liquid chromatography were purchased from Merck (Darmstadt, Germany). Water for LC-MS, Methanol and isopropyl alcohol, all LC-MS grade, as well as formic acid, were bought from Honeywell (Wien, Austria). L-arginine was obtained from Applichem (Darmstadt, Germany) and trehalose dihydrate from Pfanstiehl (Waukegan, IL, USA). Hydrogen peroxide 30% (H_2O_2), dithiothreitol (DTT), 8M Guanidine HCl, iodoacetic acid sodium salt, iron (II) sulfate heptahydrate and Tris-HCl buffer pH 7.5 were purchased from Sigma-Aldrich (St. Louis, MO, USA), trifluoroacetic acid (TFA) and Urea (≥99.5%) from VWR chemicals (Leuven, Belgium), L-methionine, L-histidine and polysorbate 80 (PS 80) from J.T. Baker (Radnor, PA, USA) and polysorbate 20 (PS 20) were bought from Croda International (Snaith, UK). IgG-specific protease FabRICATOR® (IdeS) was obtained from Genovis AB (Lund, Sweden) and the Trypsin/Lys-C mix from Promega (Walldorf, Germany).

3. Methods

3.1. Experimental design

To evaluate the effect of formulation on the oxidation susceptibility, multiple formulation parameters were varied in this study. The experimental layout covers a selection of the most commonly used formulation excipients in commercially available biopharmaceutics such as histidine, citrate, succinate and polysorbates 20 and 80 [5]. In addition, a subset of samples was also formulated with well-known antioxidants and chelators to investigate their capacity to reduce the oxidation susceptibility under different stress conditions. As a protective effect of arginine on the photostability was reported [16], it was also incorporated into the screening.

Trehalose was used as the basic formulation stabilizer in all compositions, always at the same concentration. The selected formulation parameters that were varied in this screening are summarized in Table VI-1. A more detailed experimental layout and compounding scheme is attached as supplementary data (Tables S1 + S2).

Table VI-1: Formulation Parameters

Parameter	Conditions
mAbs	2 x therapeutic mAbs NIST mAb
Protein Concentration	50, 100, 150 mg/ml
Buffer System	Citrate Phosphate buffer (CP) Histidine buffer (His) Succinate buffer (Succ)
pH	5, 6, 7
Surfactant	Polysorbate 80 (PS 80) Polysorbate 20 (PS 20)
Surfactant Concentration	0, 0.1, 0.5 mg/ml PS 80 0.5 mg/ml PS 20
Additional Excipients (NIST mAb only)	0.8 mM EDTA 0.8 mM DTPA 1.5 mg/ml Methionine 1.5 mg/ml Tryptophan 10 mg/ml Arginine

3.2. Preparation of drug substance and excipient stock solutions

For each antibody three high concentrated stock solutions in water at pH 5, 6 and 7 were prepared. Therefore, the mAb solutions were concentrated to protein concentrations > 220 mg/ml using the Sartorius Ambr UF/DF device equipped with Sartocon® 50 kD PES cassettes (Sartorius, Göttingen, Germany). The pH of each individual stock solution was adjusted afterwards. Protein concentration was determined by UV-VIS spectroscopy (Stunner, Unchained Labs, Pleasanton, CA, USA).

All excipients stock solutions were prepared with deionized water. The respective target concentrations and pH values are attached as supplementary data (Table S3). All excipient solutions were filtered with 0.22 µm PES filters (Sartorius, Göttingen, Germany).

3.3. Formulation compounding

Initially, all prepared antibody and excipient stock solutions were loaded into a HamiltonSTAR™ liquid handling platform (Hamilton Bonaduz AG, Bonaduz, Switzerland). The target formulations were then compounded in a 2 ml deep well plate (Eppendorf, Hamburg, Germany) following the corresponding compounding scheme (supplementary Table S2). The samples were homogenized directly in the deep well plate by pipetting. Post-compounding, the formulated samples were aliquoted into clear, non-binding polystyrene (PS) 96-well plates with a F-bottom (Greiner Bio-One, Kremsmünster, Austria). Each well plate was then sealed with transparent adhesive foil (Applied Biosystems, Foster City, CA, USA) to prevent contamination and evaporation. One plate was stored at 4 °C as unstressed control, all other plates were exposed to oxidative stress as described below.

3.4. Oxidation stress

In our previous work the combination of a peroxide-based (HP), visible light (VIS) and metal catalyzed oxidation (MCO) assay, using the assay conditions described below, was identified as the most effective strategy to evaluate oxidation susceptibility in a high throughput workflow [15]. Those experimental parameters generate a detectable level of oxidative degradation in mAbs in a short period of time that can be reliably detected with HT analytical methods. Light stress experiments were carried out in an ICH compliant photostability chamber (Aralab, Rio de Mouro, Portugal). Samples were exposed to 600 klux*h of a fluorescent cool white light. The illuminance of the fluorescent light source was set to 29 klux. Metal catalyzed oxidation was simulated by incubation with 0.4 mM Fe^{2+} + 4 mM H_2O_2 (Fenton reaction) over a duration of 3 h at room temperature (RT). To generate peroxide induced oxidation, samples were incubated with 0.05% hydrogen peroxide for 1.5 h at RT. As spiking the samples with hydrogen peroxide and iron solution changes the volume and consequently the sample compositions, 10 µl water were added to each sample of the plate exposed to light and unstressed control plate to ensure comparability throughout the whole data set. To stop oxidation reactions after the defined incubation or light exposure time, samples were diluted 1:10 with Tris-buffered saline (TBS) buffer (50 mM Tris-HCl, 150 mM NaCl) pH 7.6 supplemented with 200 mM L-Methionine. The unstressed control plate was also diluted with TBS buffer to ensure similar treatment and comparability to the stress plates. Irrespective of the assay type, the TBS-Met buffer completely quenches all oxidative processes, to avoid the continuation of oxidation during storage.

3.5. Size Exclusion Chromatography (SEC)

To monitor the formation of high molecular weight species (HMW), size exclusion analysis was performed. The SEC was conducted on an Acquity UPLC H-Class Bio System (Waters, Milford, MA, USA) equipped with a PDA detector to monitor UV absorption at 280 nm. After quenching with TBS-Met buffer, 40 µg sample were injected to a Waters ACQUITY UPLC BEH200 SEC column 4.6 x 150 mm; 1.7 µm, 200 Å (Waters, Milford, MA, USA) and separated by isocratic elution using 100 mM Na_2HPO_4 / 200 mM Na_2SO_4, pH 7.0 at a flow rate of 0.4 ml/min for 6 min. Column temperature was maintained at 25 °C. The temperature in the sample manager of the UPLC system was maintained at 4 °C. Analysis of chromatographic data was conducted using Chromeleon™ chromatography software (Thermo Fisher Scientific Inc., Waltham, MA, USA).

3.6. Reversed-Phase Chromatography Subunit Analysis (RP)

Subunit analysis was performed using Reversed Phase Chromatography (RP). Prior analysis, the oxidized mAb samples were subjected to enzymatic cleavage by dilution to 1 mg/ml with TBS-Met buffer containing 100 units of IdeS (FabRICATOR, Genovis) and incubation at 25 °C for 60 min. IdeS cleaves the monoclonal antibody at a specific site below the hinge region, resulting in F(ab')2 and Fc/2 fragments**.** Afterwards, the samples were spiked with 10 mM TCEP for disulfide bond reduction and incubated for 60 min at 25 °C**.** This procedure generates three fragments: a heavy chain Fc fragment (Fc HC), light chain (LC) and a heavy chain Fd fragment (Fd HC). The generated subunits were analyzed on an Agilent 1290 Infinity I System (Agilent Technologies, Santa Clara, CA, USA) equipped with DAD detector using a BioResolve RP mAb Polyphenyl column 2.1 x 50 mm, 2.7 µm, 450 Å (Waters, Milford, MA, USA). Absorption was monitored at 280 nm. Mobile phase A was water with 0.1% TFA, mobile phase B was acetonitrile with 0.1% TFA. Per run, 2 µg sample were injected to the column, separation was performed using a linear gradient from 25% - 45% mobile phase B over 4 min at a flow rate of 0.3 ml/min at 80 °C. The temperature in the sample manager of the UHPLC system was maintained at 4 °C. Analysis of chromatographic data was conducted using Chromeleon™ chromatography software (Thermo Fisher Scientific Inc., Waltham, MA, USA).

3.7. Polysorbate Quantitation by AEX/RP mixed mode HPLC with charged aerosol detection (CAD)

Determination of Polysorbate 80 or 20 content in protein-containing samples was performed by AEX/RP mixed mode HPLC on an Agilent 1290 Infinity I System (Agilent Technologies, Santa Clara, CA, USA) equipped with Corona Veo RS CAD (Thermo Fisher) for charged aerosol detection (CAD). Mobile phase A consisted of 35 mM ammonium formate pH 3.8 + 20% isopropyl alcohol, 100% isopropyl alcohol was used as mobile phase B.

Polysorbate was separated from protein and other formulation components using an OasisMAX mixed mode HPLC column 2.1x20 mm, 30 µm (Waters, Milford, MA, USA). Proteinaceous matrix and other excipients were removed during a 5 min isocratic hold step of 100% mobile phase A. In a 6 min gradient to 100% mobile phase B followed by a 3 min hold step, polysorbate was eluted in one single peak and detected by charged aerosol detection. Afterwards the column was re-equilibrated for 2 min with 100% mobile phase A. Analysis was performed at a flow rate of 1 ml/min, the column temperature was set to 30 °C. The gas nitrogen inlet pressure for the CAD was 75 psi, the evaporation temperature was set to 70 °C.

Data analysis was carried out using Chromeleon™ chromatography software (Thermo Fisher Scientific Inc., Waltham, MA, USA). The polysorbate content of the samples was determined using a quadratic regression fit based on a calibration curve between 0.01 and 0.07 mg/ml polysorbate 80 or 20. As low polysorbate concentrations were expected due to the 1:10 dilution for oxidation quenching, the maximum volume of 20 µl was injected to the column. Samples containing only 0.01 mg/ml polysorbate 80 after oxidation quenching are at the lower quantitation limit of this method and were therefore not analysed.

3.8. LC/MS peptide Mapping

To support data interpretation and evaluation, additional in-depth information was generated by analyzing selected samples of the data set via LC/MS peptide mapping. For tryptic digestion, 125 µg of NIST mAb samples were mixed with denaturing buffer (8 M Guanidine HCl, 400 mM Tris, 20 mM L-Methionine, pH 8.0) to top up the sample to 215 µL resulting in a final guanidine concentration higher than 6 M. After 10 µL of 0.5 M DTT was added, samples were then incubated for 1 h at room temperature (RT). Afterwards, 10 µL of 1 M Iodoacetic acid sodium salt was added to the mixture, followed by an additional incubation for 1 h at RT. The alkylation reaction was quenched by a further addition of 15

µL of 0.5 M DTT. For desalting, samples were loaded on a PhyTip® column (Biotage, Uppsala, Sweden) pre-equilibrated with digestion buffer (50 mM Tris-HCl, pH 7.5) and eluted with 200 µL digestion buffer. Trypsin/Lys-C Mix was added to a final enzyme to protein ratio of 1:20 and incubated for 2 h at RT. The digestion reaction was quenched by adding FA to a final concentration of 0.3%.

Samples were analyzed using a Vanquish Flex UHPLC system coupled to an Exploris 240 mass spectrometer (Thermo Fisher Scientific Inc., Waltham, MA, USA). Peptides were separated on a Waters ACQUITY UPLC Peptide BEH C18 reverse-phase column (2.1 mm × 150 mm, 1.7 µm, 300 Å) heated to 55 °C at a flow rate of 0.55 ml/min. Mobile phase A (LC-MS grade water with 0.08% FA, 0.02% TFA) and mobile phase B (LC-MS grade ACN with 0.08 % FA, 0.02% TFA) were used as elution solvents. Peptides were eluted on a 26 min linear gradient (17 min 8-30% B, 6 min 30-60% B, 3 min 60-90% B). MS1 scans were acquired from *m/z* 200 – 2000 (resolution 90k at *m/z* 200). Automatic Gain Control (AGC) was set to 3e6 with a maximum Injection Time (IT) of 50 ms. MS/MS scans were collected in data-dependent mode (resolution 22.5k at *m/z* 200) using the top 5 most intense peptides in the MS1 scan. A dynamic exclusion of 2 s, an isolation width of *m/z* 2, and a maximum IT of 150 ms was applied. Peptides were fragmented using higher-energy collisional dissociation (HCD) with a normalized collision energy of 28%. Raw data were analyzed using Protein Metrics v5.5 (Dotmatics, Boston, MA, USA).

3.9. Data evaluation, oxidation scoring and formulation ranking

To identify the formulation parameters that demonstrate a relevant change during the study, a statistical data evaluation was performed using Minitab. For this purpose, the data set was divided into smaller, equally distributed subsets. For each response variable a linear regression model with interaction through second order and quadratic terms was applied. If the factor is significant according to the statistical analysis, but still within the method variation, changes for this factor will be considered as irrelevant.

To simplify the data handling in the formulation screening workflow, an individual oxidation score, represented by a single number, is determined for each tested sample. This strategy allows a time efficient site-by-site comparison of different formulation approaches in context of oxidation susceptibility and facilitates the comparison of complex data sets across different molecules, while still considering multiple potential liabilities simultaneously. In this study, three stability indicating attributes (SIA) were selected to evaluate the impact of oxidative stress on the tested mAbs: Formation of oxidation induced aggregates analyzed

via SEC (ΔHMW), as well as modifications of Fc and Fab subunits measured using RP-UHPLC subunit analysis (ΔFcMod and ΔFabMod). In each case, the difference in relative peak area (Δrel%area) in comparison to the corresponding unstressed sample was determined.

To allow the comparison of the different SIAs and therefore effect of oxidative stress, the analytical data (Δrel%area) generated in this screening is normalized on a scale from 0 – 100. The lower limit (0) represents the method error of the corresponding method (SEC or RP-UHPLC) and the upper limit a pre-defined (arbitrarily chosen) worst case of the SIA. In the present study, the lower limit for ΔHMW is set to 0.4%, for ΔFcMod. and ΔFabMod a lower limit of 2% was defined.

The upper limit for all three SIAs was set to 25% increase compared to the unstressed control. These limits were established for other stress assays as part of high-throughput (HT) formulation screening in the past and will be similarly applied to the oxidation screening workflow. If a data point is below the lower limit or above the upper limit, the value is set to 0 or 100, respectively. The overall oxidation score for each oxidation stress assay performed in this screening (VIS, MCO and HP) was generated by summing up the normalized values of the individual SIAs. To obtain a comparable, general measure of oxidation susceptibility across molecules, the impact of the individual stress assays is combined in one final oxidation ranking. Therefore, the calculated oxidation scores for the stress assays were summed up to a final score, then divided by the number of assays (3). A score of 0 represents the lowest level of oxidation susceptibility and with increasing numbers the risk for oxidation of the molecule increases as well. The determination of the oxidation scores and the corresponding ranking of the formulations was conducted separately for each of the three mAbs.

4. Results & Discussion

4.1. Impact of buffer and pH

To evaluate the effect of buffer system and pH on the oxidation susceptibility, mAbs were formulated either in histidine buffer at pH 6 (His), succinate buffer at pH 6 (Succ) or citrate-phosphate buffer at pH 5, 6 or 7 (CP), then exposed to oxidative stress (detailed formulation compositions in supplementary data). As shown in Figure VI-1A, none of the tested formulations, including the non-formulated water control, showed formation of HMWs after hydrogen peroxide treatment in any of the tested mAbs. In contrast, peroxide-induced modifications of the Fc subunit were observed throughout the whole dataset (Figure VI-1B). Hydrogen peroxide represents a common oxidation risk for monoclonal antibody products, derived from degraded excipients in the formulation or as left over contamination after sterilization processes [9,12], which has been extensively described in literature. Multiple studies have already shown that HP primary targets the surface exposed methionine residues in the Fc region of mAbs [17–20]. We also observed similar Fc modification levels after hydrogen peroxide spiking in all three tested mAbs, supporting the assumption that the same targets are oxidized in all tested samples. In addition to the Fc located methionine residues, the NIST mAb contains an oxidation prone methionine residue in the Fab HC region, leading to Fab modification. All detected peroxide induced modifications detected in this data set were considered as independent of formulation buffer and pH, as all detected changes were within the method error range of the HT RP subunit analysis.

The effect of MCO on different antibody formulations was investigated using an iron and hydrogen peroxide oxidation system. The presence of metal ions resulted mainly in subunit modifications, especially of the Fc fragment (Figure VI-1B+C), whereas aggregation was a less pronounced consequence. Similarly to peroxide-based stress, for the majority of the tested samples, the formulation buffers and pH levels included in this screening had no effect on the extent of degradation. Still, in case of mAb2, which is the most MCO-prone mAb among the tested samples, an increase in HMW formation was detected in presence of histidine buffer (Figure VI-1A). Furthermore, the modification of the Fab subunit was also slightly increased compared to all other buffer systems in the screening. In contrast, the MCO induced aggregation seems to be reduced in citrate-phosphate buffer. Histidine and citrate are both known to be metal chelators [21,22]. However, although histidine has been described as an effective antioxidant [23], in cases of MCO the formation of histidine metal complexes has also been discussed to contribute to oxidation processes, for example by increasing hydroxyl radical formation [22,24]. Based on the results of this study, the formation of citrate-iron-complexes seem to have a protective effect compared to the other buffer systems, whereas the presence of histidine-iron-complexes most likely promotes metal

catalyzed oxidation processes, leading to increased oxidation and Fab modification. Interestingly, this effect was only observed for mAb 2. For both other mAbs, which are less prone to MCO in general, the histidine buffer was no additional risk and did not lead to increased aggregation or Fab modification compared to other buffer systems.

In contrast to the oxidation spiking studies, the effects of visible light exposure were significantly influenced by the formulation composition, especially the light induced aggregate formation, as shown in Figure VI-1A. Aggregation - as a consequence of UV or visible light exposure - is a common observation for monoclonal antibodies [25–27]. In this present data set, the highest aggregate formation after light exposure was detected in NIST mAb samples, whereas mAb2 was the least light sensitive mAb in this screening. Interestingly, even though the photosensitivity of the different mAbs varies noticeably, they all show the same trend regarding the oxidation susceptibility in different formulation buffers.

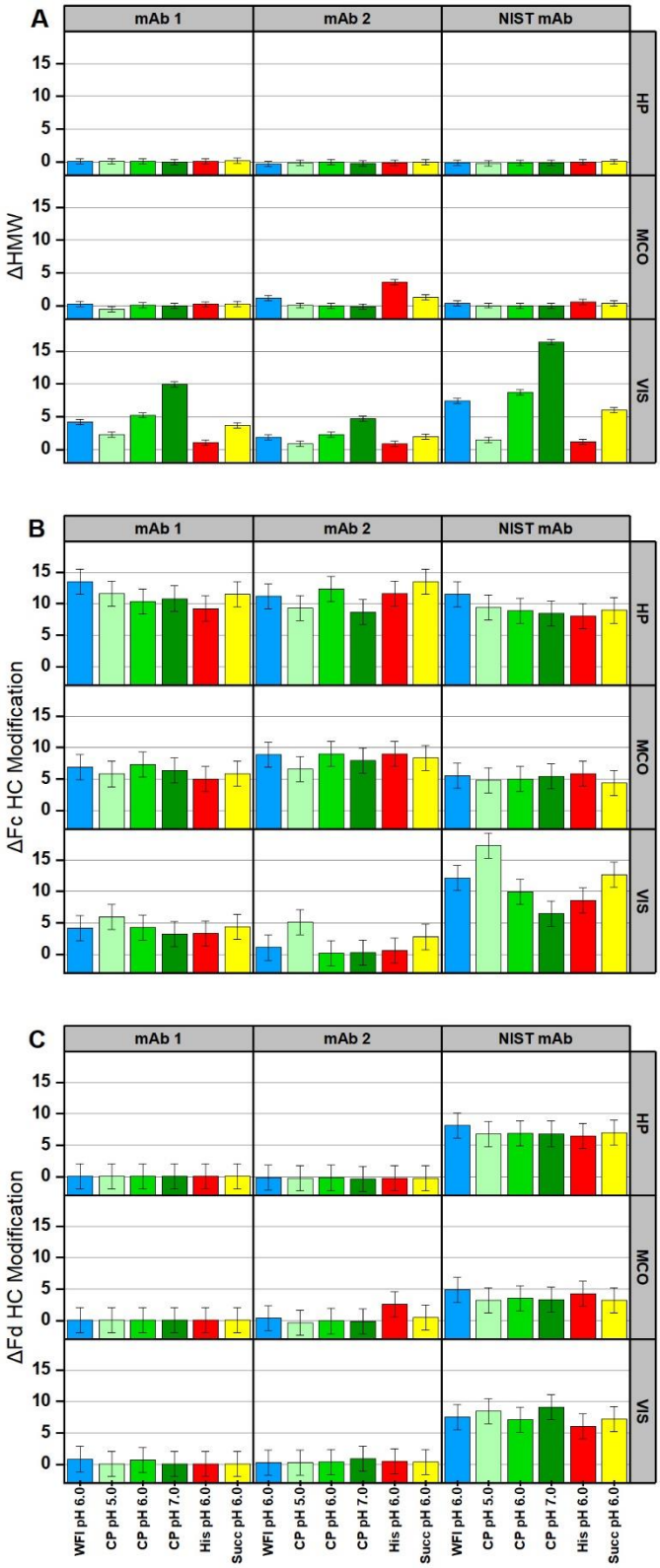

Figure VI-1: Impact of formulation buffer and pH on the increase in high molecular weight species (HMWs) (A), Fc HC (B), and Fd HC modification (C) after hydrogen peroxide spiking (HP), metal-catalyzed oxidation (MCO), or visible light exposure (VIS), relative to unstressed samples (Δ%). Error bars depict the method error of the SE-UHPLC (0.4%) and RP-UHPLC (2.0%) high-throughput methods.

Among all tested buffer systems, histidine buffer was the most effective one in protecting the mAbs from light induced aggregation. Apart from general destabilization of the protein structure, aggregation is also related to cross link formation of photo oxidized amino acid residues such as histidine [28–30]. In this context it has been reported that besides from protein-protein-crosslinks, cross link formation is also possible between photo oxidized buffer components and protein-bound histidine residues [31,32]. Interestingly, while photo oxidized histidine has been identified as a photosensitizer itself that potentially can initiate the photooxidation of proteins [33], under the selected light conditions of this screening workflow, the protecting capacity outweighs this effect. Most likely, the cross linking of oxidized histidine in the formulation buffer to potential cross-linking targets in the molecule prevents the formation of light induced protein-protein cross links and therefore reduces aggregation. This assumption is in line with the LC/MS results of light exposed NIST mAb (Figure VI-2), showing the formation of histidine adducts only in histidine formulated samples. Furthermore, those samples show the lowest level of histidine oxidation in general, suggesting additional scavenging capacity of free histidine.

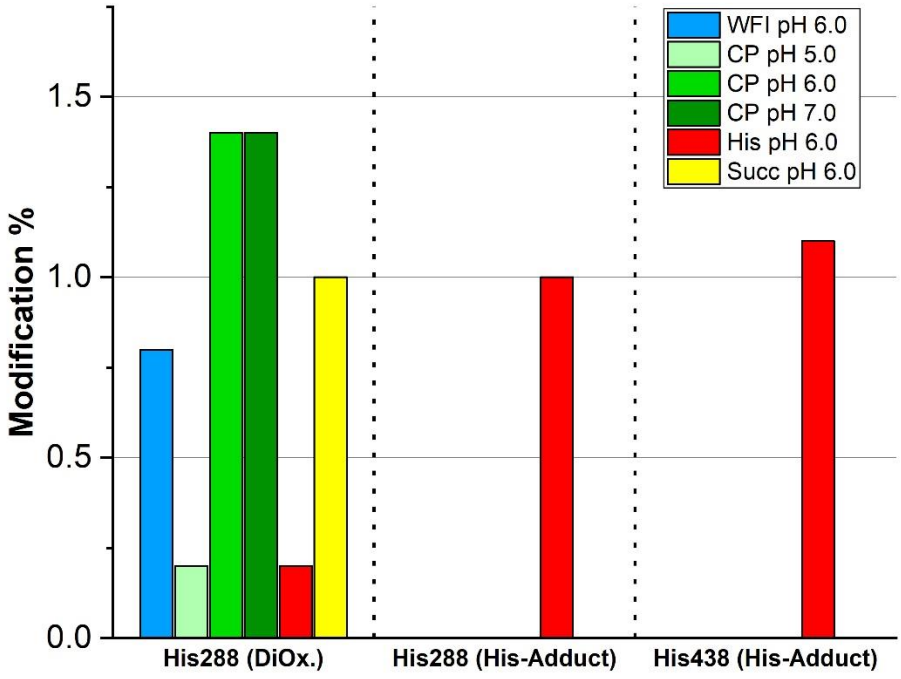

Figure VI-2: Impact of formulation buffer and pH on the level of histidine modifications detected in NIST mAb samples via LC/MS peptide mapping after exposure to 600 klux*h visible light.

In presence of succinate buffer or citrate phosphate buffer pH 6.0, the light-induced aggregation was comparable to the non-formulated control sample in water, no additional protective or photosensitizing effect was observed. However, the variation of pH in citrate phosphate buffer samples reveals that the light induced aggregation is also pH dependent. While samples formulated in citrate phosphate buffer pH 6.0 show a similar HMW content

as the non-formulated control, a decrease to pH 5.0 increases the photostability, whereas a higher pH of 7.0 lead to more aggregation in all mAbs. Similar observations were also described for UV light exposed Anti-streptavidin IgG1 mAb, showing an increase in nonreducible aggregates with increasing pH [27]. Furthermore, Liu et al. also reported a pH dependent aggregate formation under light exposure that indicates that the histidine cross linking in the IgG1 is favored at higher pH values [29].

Despite prior studies indicating that mAb2 has a lower photooxidation risk compared to other tested mAbs, its aggregation propensity is still affected by the formulation buffer, especially the formulation pH. Those results emphasize that apart from intrinsic molecule-derived factors several extrinsic factors such as formulation selection can have a severe impact on the photooxidation susceptibility of the drug product.

Contrary to light induced aggregation, the tested formulation parameters rarely affected the extent of Fc and Fab subunit modifications (Figure 1B+C). However, detected changes of the Fc fragment were pH dependent for all mAbs included in this screening. Interestingly, compared to light induced HMW formation an opposite pH trend was observed, leading to an increase in Fc modification with decreasing pH. The same trend was identified for all photo oxidized methionine residues (Fc and Fab located) in light exposed NIST mAb samples by LC/MS (Figure VI-3).

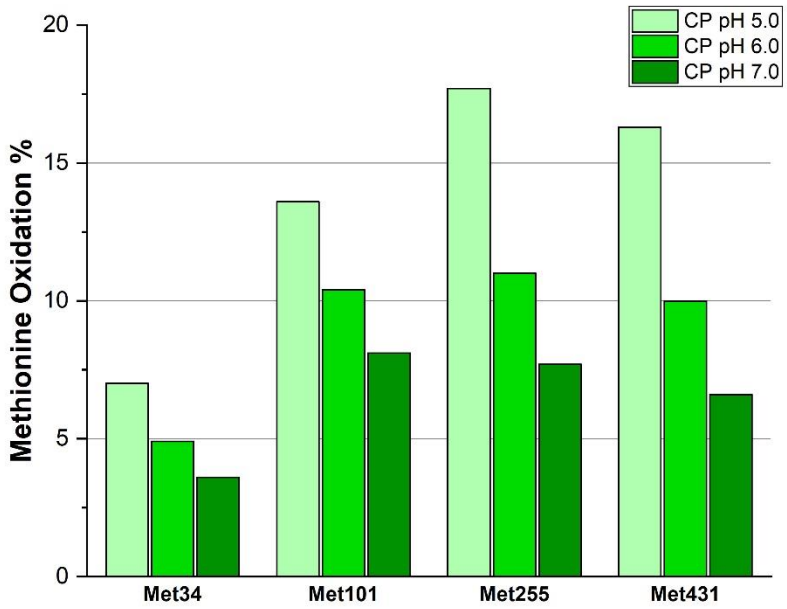

Figure VI-3: Impact of formulation pH on methionine oxidation of NIST mAbs samples detected via LC/MS peptide mapping after exposure to 600 klux*h visible light.

Since this effect seems to be specific for photooxidation and was not detected after HP or MCO treatment, those observation are most likely not linked to pH-dependent oxidation

susceptibility of the affected methionine residues, but a result of the photooxidation mechanisms itself. The light induced reactive oxygen species (ROS) formation and the oxidation capacity, as reviewed in detail by Hipper et al. [34], is characterized by high complexity and variability, depending on the environmental conditions. Presumably, formulation pH can also interfere with ROS reactions. However, the determination of ROS formation and activity would require further in-depth analysis and is therefore out of scope for this work.

4.2. Impact of protein concentration

Antibody samples were formulated at 50, 100 and 150 mg/ml to evaluate the impact of protein concentration on the oxidation susceptibility. Similar to the results for buffer and pH displayed in Figure 1, the effect of protein concentration on oxidation induced aggregation, Fc and Fab modification was antibody and stress dependent.

Based on the present data set, the extent of oxidation induced by hydrogen peroxide induced oxidation is completely independent of the protein concentration (data not shown).

Similar observations were made for the majority of MCO treated samples. Exceptions are histidine formulated samples. Histidine buffer, as described in the section above, can negatively affect the MCO stability of mAbs. In mAb2 and NIST mAb samples, an increase in Fab modification is observed with decreasing protein concentration (supplementary data – Table S4). Furthermore, the HMW formation is slightly increased in 50 mg/ml mAb2 histidine formulations compared to higher concentrated samples (data not shown). However, in all cases the detected differences barely exceed the error range of the corresponding method.

In case of light exposure, increasing protein concentration also promoted the formation of aggregates in mAb1 and NIST mAb samples (Figure VI-4). Additionally, the Fab subunit modification of NIST mAb samples was also increased at 150 mg/ml throughout all tested formulation buffers, as well as the Fc subunit modification in CP buffer at pH 5.0 (supplementary data – Table S5). In a photodegradation study by Hipper et al. investigating the same protein concentration levels, this observation was attributed to increased free radical formation due to higher concentrations of potentially protein-derived photosensitizer in the tested formulations [35]. An increase in reactive species would therefore promote oxidation of susceptible targets in the protein, as well as oxidation-induced cross linking and subsequent protein aggregation. In this context it is remarkable that in contrast to those observations, protein concentration has no impact on the formation

of light induced aggregates in mAb2 samples. Interestingly, Fc modification is even slightly increased at 50 mg/ml compared to the higher concentrations tested in this study (supplementary data – Table S5). This could indicate that the changes detected in mAb2 after light exposure might be caused by different degradation mechanisms compared to the more light sensitive mAb1 or NIST mAb.

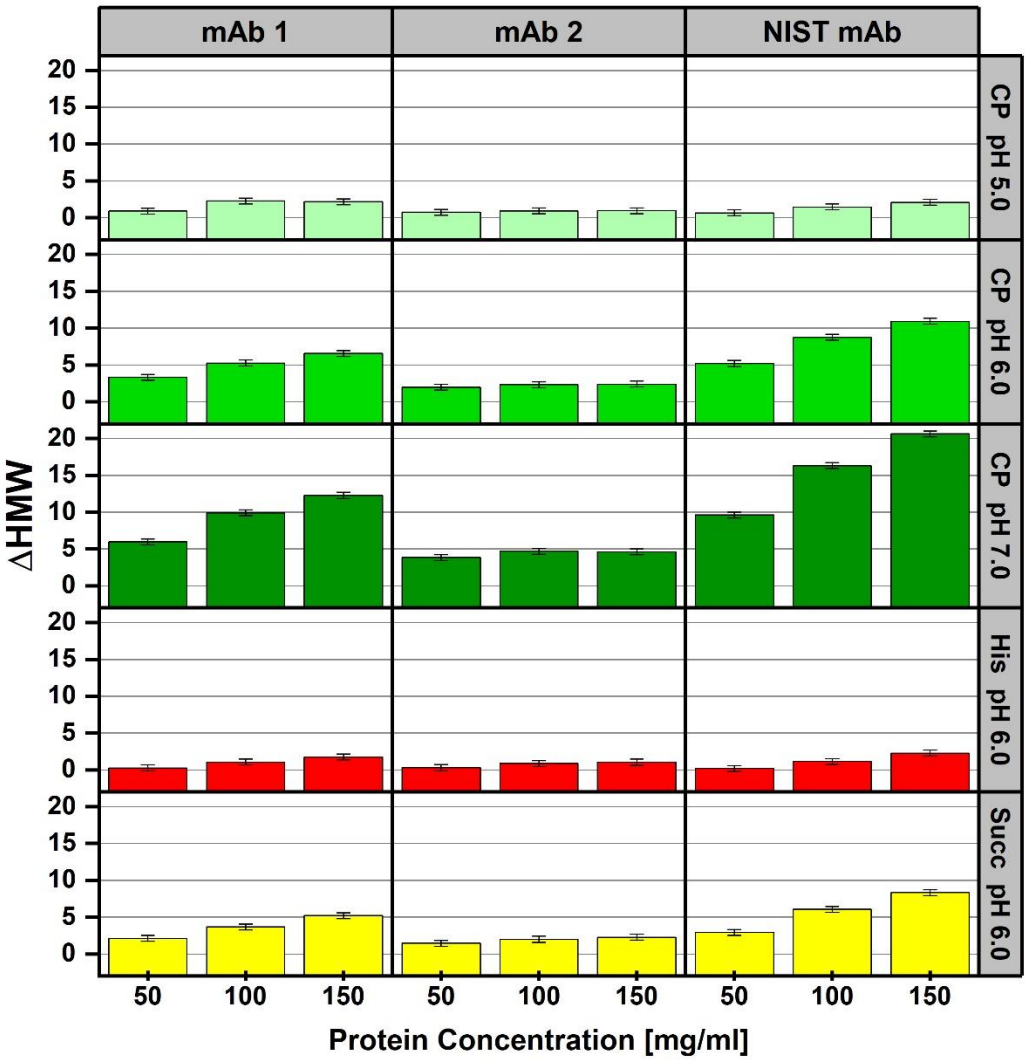

Figure VI-4: Impact of protein concentration on the level of high molecular weight (HMW) species formation following exposure to 600 klux*h of visible light relative to unstressed samples (Δ%). Error bars indicate the method error of 0.4% associated with the SE-UHPLC high-throughput method.

4.3. Impact of surfactant

To investigate the impact of surfactant on oxidation susceptibility, in this formulation screening samples were either formulated with polysorbate 80 (0.1 or 0.5 mg/ml), polysorbate 20 (0.5 mg/ml) or no additional surfactant. While polysorbate degradation has been identified to negatively impact the stability of biopharmaceuticals, for instance due to particle or aggregate formation [10–12], the aggregation and subunit modification analyzed in this data set was independent of the surfactant type and concentration. All detected changes were within the method error of the corresponding analytical method, therefore the impact of surfactant on the oxidation susceptibility was considered as not significant.

In addition to SEC and RP, AEX/RP-CAD analysis was performed to monitor the polysorbate 80 and 20 content after stress exposure.

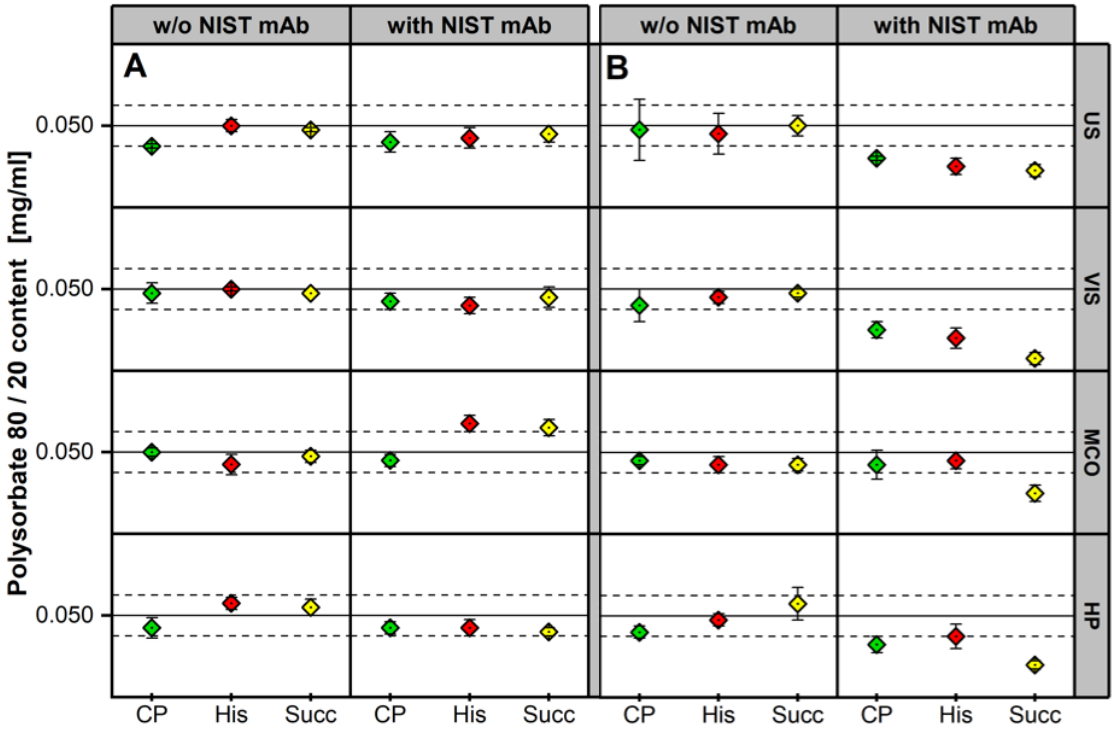

Figure VI-5: Polysorbate content analysis. Content of Polysorbate 80 (A) and Polysorbate 20 (B) in samples before (US) and after stress exposure (VIS, MCO, HP), both in the presence and absence of NIST mAb (10 mg/ml, after oxidation quenching). Error bars indicate the deviation between measurement replicates (n=2). The solid black line represents the target concentration level of 0.05 mg/mL of polysorbate 80 or 20 after dilution with quenching buffer, while the dotted lines depict the analytical method's error range of ±10.0%.

Surfactant content was measured in selected samples of the NIST mAb and corresponding buffer controls without any protein. As shown in Figure VI-5, none of the three stress assays lead to loss of polysorbate compared to the unstressed controls. Interestingly, even though the samples show a comparable level of polysorbate throughout the data set, the measured polysorbate content is slightly lower in samples containing NIST mAb compared to the

buffer controls, independent of the tested surfactant type. However, as this trend is identical for all three stress treatments and the unstressed controls, the lower levels of surfactant in samples containing protein is most likely not a consequence of oxidative stress but an effect caused by a systematic compounding deviation of the liquid handling system or an oxidation-independent degradation pathway. Overall, the surfactant concentration and type had no impact on the oxidation susceptibility of the tested mAbs, nor did the selected forced oxidation conditions result in detectable polysorbate degradation.

4.4. Impact of additional excipients

In a subsequent screening, additional excipients were added to selected NIST mAb formulations to evaluate their antioxidative capacity under the tested stress conditions. While the extent of peroxide induced oxidation was not affected by basic formulation parameters such as buffer and pH, the addition of free methionine reduced the extent of Fc and Fab modification in most tested samples (Figure VI-6B+C). As reported earlier, free methionine acts as a scavenger that is primarily oxidized, thus protecting the methionine residues in the mAb and neutralizing the effect of hydrogen peroxide [17,36]. Additionally, as shown in Figure VI-6C, a positive effect on the extent of Fab modification was observed in histidine samples formulated with metal chelators. Even at low concentrations, trace metal ions in the drug substance, for example leached from manufacturing materials, can trigger oxidation processes, especially in presence of hydrogen peroxide [37,38]. Complexation of trace metals by addition of metal chelators such as EDTA or DTPA could therefore reduce the risk of metal catalyzed oxidation after hydrogen peroxide spiking [5–7].

Similar observations were made for MCO stressed samples in this screening such as histidine formulated NIST mAb samples stressed in presence of EDTA and DTPA showed a reduction in HMW formation and Fab subunit modification (Figure VI-6D+F). Interestingly, the addition of arginine also reduced Fab modification and HMW formation in histidine buffer. Furthermore, due to its oxidation scavenging capacity, free methionine was identified as a beneficial excipient to reduce Fc and Fab subunit modifications (Figure VI-6E+F). In succinate formulated samples none of the tested excipients were effective. As the MCO susceptibility of the NIST mAb was comparatively small in this study, the overall possibility to identify potential antioxidative effects in the excipient screening is limited.

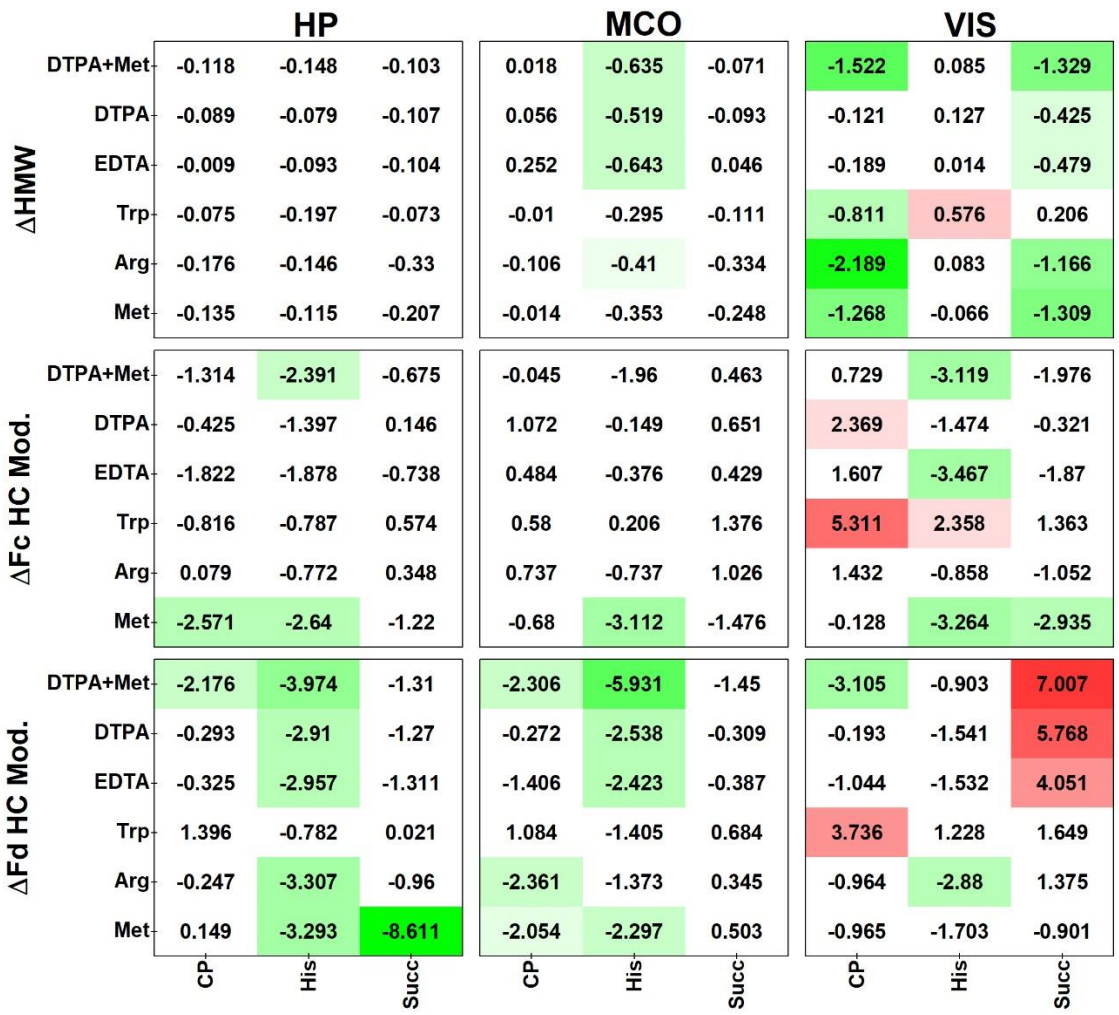

Figure VI-6: Effect of antioxidants on NIST mAb oxidation. This figure illustrates the impact of antioxidative excipients on the formation of high molecular weight (HMW) species and modifications of the Fc heavy chain (Fc HC) and Fd heavy chain (Fd HC) fragment following hydrogen peroxide spiking (HP), metal-catalyzed oxidation (MCO), or visible light exposure (VIS). The figure displays the relative change in modification levels (Δ%) indicated by color: green represents a decrease, while red represents an increase, compared to identically formulated samples without antioxidative excipients, exposed to the same stress conditions. Changes are only highlighted in color if they exceed the method error thresholds: 0.4% for HMW and 2.0% for Fc and Fd HC modifications.

The photooxidation susceptibility of the NIST was considerably influenced by the presence of additional excipients. Similarly to HP and MCO, the addition of free methionine positively affected the photostability, reducing aggregation and Fc subunit modification (Figure VI-6G+H). Shown in Figure VI-6G, a positive impact on HMW formation was also observed in samples formulated with arginine. In contrast, the presence of free tryptophan resulted in the opposite effect, increasing degradation in multiple tested samples. While methionine and tryptophan residues are also both known targets for photooxidation in proteins [3,28,39], a protective effect was only observed for free methionine. In a photodegradation study using comparable excipients, similar observations were described, while the presence of additional methionine protects the mAb from aggregation and significantly reduces the loss

of stability and FcRn binding, samples containing free tryptophan showed severe photodegradation [26]. It is hypothesized that the presence of additional tryptophan and the corresponding oxidation products further promotes ROS formation and therefore increases damage of oxidation prone targets in the molecule [26,39].

Interestingly, the referred study also reported that the presence of arginine had no additional protective effect on the mAb [26], whereas in our data set light exposed samples formulated with arginine show a reduction in HMW formation (Figure VI-6G). While the protective effect of free methionine is predominantly caused by its oxidation scavenging capacity, arginine is not directly considered as an antioxidant. Arginine is preferably used in protein formulations to increase solubility, lower the viscosity and reduce protein-protein interactions, consequently leading to overall stabilization of the product [40]. This stabilizing effect most likely also reduces aggregation in light exposed proteins without direct interaction with ROS [16].

The effect of metal chelators was highly dependent on the formulation buffer, as reflected by the results shown in Figure 6G-I. For instance, while the addition of chelators seems to positively affect Fc modification in histidine samples, in CP buffer the samples show the opposite effect. Furthermore, the Fc modification is drastically increased in succinate formulated samples in presence of EDTA and DTPA, whereas no negative effect was found in histidine or CP formulations. However, reduction of HMW formation in metal chelator containing samples was only detected in succinate buffer.

In general, the effects of additional antioxidative excipients tested in this study were highly dependent on stress type, other formulation components and the individual oxidation susceptibility of the NIST mAb.

4.5. Evaluation of formulation impact in high throughout data sets – oxidation ranking

The impact of formulation on oxidative degradation is known to be different for individual mAbs, depending on their unique susceptibility towards a specific kind of oxidative stress and the corresponding exposure risk in their life cycle, emphasizing the need for a comprehensive evaluation of potential liabilities. For full characterization, analysis on peptide level remains the go-to strategy. However, despite the establishment of automated LC-MS peptide mapping workflows in recent years, data evaluation is often more complex and time-consuming compared to high-throughput (HT) analytical methods. Moreover, when dealing with large HT datasets in formulation development, such extensive data

analysis is often unnecessary. Many formulations can already be excluded based on simpler and more easily detectable read-outs.

In this study, we combined a high-throughput oxidation screening workflow with UV-based chromatographic detection and a scoring-based ranking system for data evaluation. The oxidation scoring system facilitates rapid assessment of various formulation combinations by ranking them based on their calculated oxidation risk scores, thereby providing an efficient means to evaluate oxidation liabilities and protective effects.

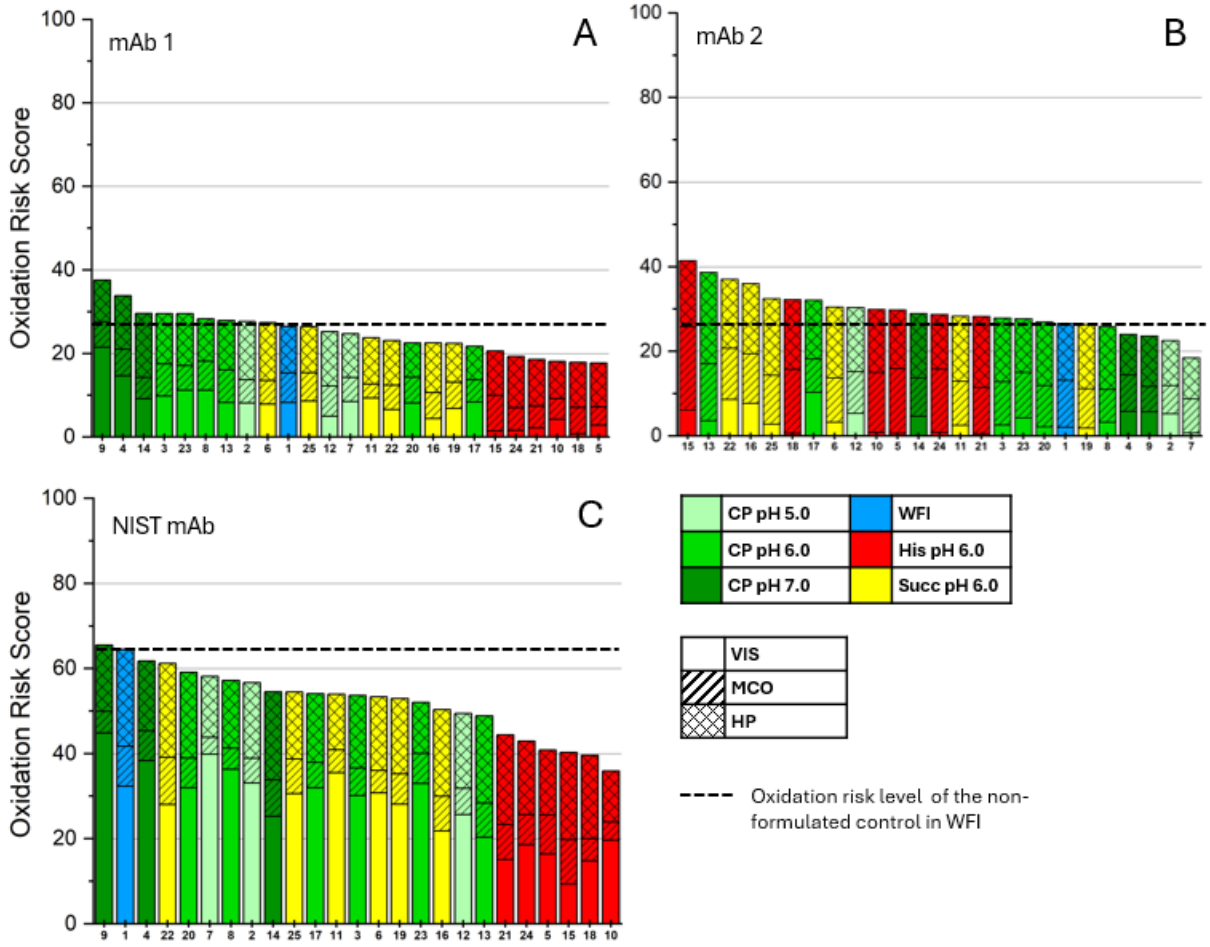

Figure VI-7: Overall oxidation risk score ranking. Ranking of different formulations for each tested mAb, based on the calculated individual risk levels of each oxidation stress assay (indicated by different patterns). The dotted line represents the oxidation risk level of the non-formulated control in WFI, providing a benchmark for comparison across the formulated samples

Figure VI-7 shows the individual rankings for all mAbs tested in the first part of this study. As in this data set, buffer and pH were identified as the most relevant formulation parameters in terms of oxidation susceptibility, each color displayed in the figures representing a different buffer system.

As expected, in a site-by-site comparison the NIST mAb shows a higher risk for oxidation compared to the therapeutic mAbs. The strongest liability was found for the non-formulated

control sample in WFI, whereas addition of a formulation buffer and pH adjustment considerably improved the oxidation stability. In contrast, formulation adjustment barely had an effect for mAb2. Moreover, compared to the non-formulated control, most formulation approaches increased the oxidation risk score for the mAb. Overall, for the NIST mAb and mAb1 histidine-based formulations are the best selection in terms of oxidation risk in this study, for mAb2 citrate-phosphate based approaches are the preferred selection. Those patterns are mainly driven by the unique susceptibility towards different oxidation stresses. NIST mAb and mAb1 show a higher sensitivity towards photooxidation, therefore the protective effects of histidine buffer have a remarkable impact on the overall score. Mb 2 on the contrary is more prone to MCO, making histidine a less preferable buffer selection.

It should be noted that the outcome of the oxidation scoring is strongly influenced by the stability indicating attribute used for evaluation. In this study oxidation monitoring focused on aggregation and Fc and Fab modifications, as those SIAs can be effectively detected in high throughput workflows [15]. However, the consequences of oxidation in biopharmaceuticals are extremely diverse. Therefore, specific selection of analytical methods and specification of lower and upper limits based on the purpose of the screening and prior molecule knowledge are a prerequisite for reliable scoring results.

5. Conclusion

Oxidation of biotherapeutics is a complex degradation pathway influenced by various intrinsic and extrinsic factors. This study highlights how formulation excipients can either increase a molecule's oxidation liability or mitigate degradation, with the formulation buffer and pH being key factors. The extent of degradation is highly influenced by the individual protein's susceptibility and the type of oxidative stress, emphasizing the need for thorough oxidation risk assessment during formulation development.

The high-throughput (HT) oxidation screening approach presented requires minimal sample amounts and allows for parallel testing of multiple stress conditions, providing a time-efficient evaluation of formulation impacts on oxidation behavior. Coupled with an HT-compatible ranking system, the effects of various formulation parameters on individual monoclonal antibodies (mAbs) can be readily identified.

In the present feasibility study, the workflow enabled the identification of each tested mAb's specific oxidation susceptibilities and simultaneously detected formulation liabilities and potential compositions that mitigate oxidation risks, all through HT compatible UV-based analytical readouts. Consequently, this approach facilitates the strategic selection of promising samples and supports the efficient optimization of formulations to reduce oxidation risks within development workflows of biopharmaceuticals.

6. References

1. Li S, Schöneich C, Borchardt RT. Chemical instability of protein pharmaceuticals: Mechanisms of oxidation and strategies for stabilization. *Biotechnol Bioeng*. 1995;48(5):490-500. doi:10.1002/bit.260480511

2. Gupta S, Jiskoot W, Schöneich C, Rathore AS. Oxidation and Deamidation of Monoclonal Antibody Products: Potential Impact on Stability, Biological Activity, and Efficacy. *J Pharm Sci*. 2021;111(4):903-918. doi:10.1016/j.xphs.2021.11.024

3. Torosantucci R, Schöneich C, Jiskoot W. Oxidation of Therapeutic Proteins and Peptides: Structural and Biological Consequences. *Pharm Res*. 2014;31(3):541-553. doi:10.1007/s11095-013-1199-9

4. Grassi L, Cabrele C. Susceptibility of protein therapeutics to spontaneous chemical modifications by oxidation, cyclization, and elimination reactions. *Amino Acids*. 2019;51(10-12):1409-1431. doi:10.1007/s00726-019-02787-2

5. Strickley RG, Lambert WJ. A review of Formulations of Commercially Available Antibodies. *J Pharm Sci*. 2021;110(7):2590-2608.e56. doi:10.1016/j.xphs.2021.03.017

6. Parkins DA, Lashmar UT, Parkins DA, Lashmar UT. The formulation of biopharmaceutical products. *Pharm Sci Technol Today*. 2000;3(4):129-137. doi:10.1016/s1461-5347(00)00248-0

7. Rayaprolu BM, Strawser JJ, Anyarambhatla G. Excipients in parenteral formulations: selection considerations and effective utilization with small molecules and biologics. *Drug Dev Ind Pharm*. 2018;44(10):1565-1571. doi:10.1080/03639045.2018.1483392

8. Weber J, Buske J, Mäder K, Garidel P, Diederichs T. Oxidation of polysorbates – An underestimated degradation pathway? *Int J Pharm: X*. 2023;6:100202. doi:10.1016/j.ijpx.2023.100202

9. Kerwin BA. Polysorbates 20 and 80 used in the formulation of protein biotherapeutics: Structure and degradation pathways. *J Pharm Sci*. 2008;97(8):2924-2935. doi:10.1002/jps.21190

10. Markus T, Lumer J, Stasavage R, Ruffner DB, Philips LA, Cheong FC. Monitoring polysorbate 80 degradation in protein solutions using Total Holographic Characterization. *Int J Pharm*. 2024;652:123843. doi:10.1016/j.ijpharm.2024.123843

11. Doshi N, Fish R, Padilla K, Yadav S. Evaluation of Super Refined™ Polysorbate 20 With Respect to Polysorbate Degradation, Particle Formation and Protein Stability. *J Pharm Sci*. 2020;109(10):2986-2995. doi:10.1016/j.xphs.2020.06.030

12. Ha E, Wang W, Wang YJ. Peroxide formation in polysorbate 80 and protein stability. *J Pharm Sci*. 2002;91(10):2252-2264. doi:10.1002/jps.10216

13. Zhang Y, Schöneich C. Visible Light Induces Site-Specific Oxidative Heavy Chain Fragmentation of a Monoclonal Antibody (IgG1) Mediated by an Iron(III)-Containing Histidine Buffer. *Mol Pharm*. 2023;20(1):650-662. doi:10.1021/acs.molpharmaceut.2c00840

14. Siedler M, Eichling S, Huelsmeyer M, Angstenberger J. Formulation Development for Biologics Utilizing Lab Automation and In Vivo Performance Models. In: Jameel" ["Feroz, Skoug" "John W, Nesbitt"] "Robert R, eds. *Development of Biopharmaceutical Drug-Device Products*. AAPS Advances in the Pharmaceutical Sciences Series, vol 35. Springer; 2020:299-341. https://doi.org/10.1007/978-3-030-31415-6_13

15. Fischer P, Merkel OM, Siedler M, Huelsmeyer M. Development of a high throughput oxidation profiling strategy for monoclonal antibody products. *Eur J Pharm Biopharm*. 2024;199:114301. doi:10.1016/j.ejpb.2024.114301

16. Maity H, O'Dell C, Srivastava A, Goldstein J. Effects of Arginine on Photostability and Thermal Stability of IgG1 Monoclonal Antibodies. *Curr Pharm Biotechnol*. 2009;10(8):761-766. doi:10.2174/138920109789978711

17. folzer E, diepold K, bomans K, et al. Selective Oxidation of Methionine and Tryptophan Residues in a Therapeutic IgG1 Molecule. *J Pharm Sci*. 2015;104(9):2824-2831. doi:10.1002/jps.24509

18. Stracke J, Emrich T, Rueger P, et al. A novel approach to investigate the effect of methionine oxidation on pharmacokinetic properties of therapeutic antibodies. *mAbs*. 2014;6(5):1229-1242. doi:10.4161/mabs.29601

19. Pan H, Chen K, Chu L, Kinderman F, Apostol I, Huang G. Methionine oxidation in human IgG2 Fc decreases binding affinities to protein A and FcRn. *Protein Sci*. 2009;18(2):424-433. doi:10.1002/pro.45

20. Loew C, Knoblich C, Fichtl J, et al. Analytical protein A chromatography as a quantitative tool for the screening of methionine oxidation in monoclonal antibodies. *J Pharm Sci*. 2012;101(11):4248-4257. doi:10.1002/jps.23286

21. Glusker JP. Citrate conformation and chelation: enzymic implications. *Acc Chem Res*. 1980;13(10):345-352. doi:10.1021/ar50154a002

22. Zbacnik TJ, Holcomb RE, Katayama DS, et al. Role of Buffers in Protein Formulations. *J Pharm Sci*. 2017;106(3):713-733. doi:10.1016/j.xphs.2016.11.014

23. Wade AM, Tucker HN. Antioxidant characteristics of L-histidine 11The work described in this manuscript was partially sponsored and funded by Cytos Pharmaceuticals, LLC. *J Nutr Biochem*. 1998;9(6):308-315. doi:10.1016/s0955-2863(98)00022-9

24. Lv JY, Ingle RG, Wu H, Liu C, Fang WJ. Histidine as a versatile excipient in the protein-based biopharmaceutical formulations. *Int J Pharm*. 2024;662:124472. doi:10.1016/j.ijpharm.2024.124472

25. Sreedhara A, Yin J, Joyce M, et al. Effect of ambient light on IgG1 monoclonal antibodies during drug product processing and development. *Eur J Pharm Biopharm*. 2016;100:38-46. doi:10.1016/j.ejpb.2015.12.003

26. Shah DD, Zhang J, Maity H, Mallela KMG. Effect of photo-degradation on the structure, stability, aggregation, and function of an IgG1 monoclonal antibody. *Int J Pharm*. 2018;547(1-2):438-449. doi:10.1016/j.ijpharm.2018.06.007

27. Mason BD, Schöneich C, Kerwin BA. Effect of pH and Light on Aggregation and Conformation of an IgG1 mAb. *Mol Pharm*. 2012;9(4):774-790. doi:10.1021/mp2004719

28. Pattison DI, Rahmanto AS, Davies MJ. Photo-oxidation of proteins. *Photochem Photobiol Sci*. 2012;11(1):38-53. doi:10.1039/c1pp05164d

29. Liu M, Zhang Z, Cheetham J, Ren D, Zhou ZS. Discovery and Characterization of a Photo-Oxidative Histidine-Histidine Cross-Link in IgG1 Antibody Utilizing 18O-Labeling and Mass Spectrometry. *Anal Chem*. 2014;86(10):4940-4948. doi:10.1021/ac500334k

30. Lei M, Carcelen T, Walters BT, et al. Structure-Based Correlation of Light-Induced Histidine Reactivity in A Model Protein. *Anal Chem*. 2017;89(13):7225-7231. doi:10.1021/acs.analchem.7b01457

31. Lei M, Quan C, Wang YJ, Kao YH, Schöneich C. Light-Induced Covalent Buffer Adducts to Histidine in a Model Protein. *Pharm Res*. 2018;35(3):67. doi:10.1007/s11095-017-2339-4

32. Powell T, Knight MJ, Wood A, O'Hara J, Burkitt W. Photoinduced cross-linking of formulation buffer amino acids to monoclonal antibodies. *Eur J Pharm Biopharm*. 2021;160:35-41. doi:10.1016/j.ejpb.2021.01.011

33. Stroop SD, Conca DM, Lundgard RP, Renz ME, Peabody LM, Leigh SD. Photosensitizers form in histidine buffer and mediate the photodegradation of a monoclonal antibody. *J Pharm Sci*. 2011;100(12):5142-5155. doi:10.1002/jps.22714

34. Hipper E, Blech M, Hinderberger D, Garidel P, Kaiser W. Photo-Oxidation of Therapeutic Protein Formulations: From Radical Formation to Analytical Techniques. *Pharmaceutics*. 2022;14(1):72. doi:10.3390/pharmaceutics14010072

35. Hipper E, Lehmann F, Kaiser W, et al. Protein photodegradation in the visible range? Insights into protein photooxidation with respect to protein concentration. *Int J Pharm: X*. 2023;5:100155. doi:10.1016/j.ijpx.2022.100155

36. Ji JA, Zhang B, Cheng W, Wang YJ. Methionine, tryptophan, and histidine oxidation in a model protein, PTH: Mechanisms and stabilization. *J Pharm Sci*. 2009;98(12):4485-4500. doi:10.1002/jps.21746

37. Schöneich C. Advanced Oxidation Processes in Pharmaceutical Formulations : Photo-Fenton Degradation of Peptides and Proteins. *International Journal of Molecular Sciences*. Published online 2022.

38. Glover ZK, Wecksler A, Aryal B, et al. Physicochemical and biological impact of metal-catalyzed oxidation of IgG1 monoclonal antibodies and antibody-drug conjugates via reactive oxygen species. *mAbs*. 2022;14(1):2122957. doi:10.1080/19420862.2022.2122957

39. Schöneich C. Photo-Degradation of Therapeutic Proteins: Mechanistic Aspects. *Pharm Res*. 2020;37(3):45. doi:10.1007/s11095-020-2763-8

40. Ren S. Effects of arginine in therapeutic protein formulations: a decade review and perspectives. *Antib Ther*. 2023;6(4):265-276. doi:10.1093/abt/tbad022

7. Supplementary data

Table S1: Experimental design of sample set 1 of the formulation screening

	Sample ID	Protein Conc. [mg/ml]	Formulation buffer	Formulation buffer [mM]	pH	Stabilizer	Stabilizer [mg/ml]	Surfactant	Surfactant [mg/ml]
Sample Set 1	1	100	WFI	n/a	6	n/a	0	n/a	0
	2	100	CP	15	5	Tre	70	PS80	0.5
	3	100	CP	15	6	Tre	70	PS80	0.5
	4	100	CP	15	7	Tre	70	PS80	0.5
	5	100	His	15	6	Tre	70	PS80	0.5
	6	100	Succ	15	6	Tre	70	PS80	0.5
	7	150	CP	15	5	Tre	70	PS80	0.5
	8	150	CP	15	6	Tre	70	PS80	0.5
	9	150	CP	15	7	Tre	70	PS80	0.5
	10	150	His	15	6	Tre	70	PS80	0.5
	11	150	Succ	15	6	Tre	70	PS80	0.5
	12	50	CP	15	5	Tre	70	PS80	0.5
	13	50	CP	15	6	Tre	70	PS80	0.5
	14	50	CP	15	7	Tre	70	PS80	0.5
	15	50	His	15	6	Tre	70	PS80	0.5
	16	50	Succ	15	6	Tre	70	PS80	0.5
	17	100	CP	15	6	Tre	70	PS80	0.1
	18	100	His	15	6	Tre	70	PS80	0.1
	19	100	Succ	15	6	Tre	70	PS80	0.1
	20	100	CP	15	6	Tre	70	PS80	0
	21	100	His	15	6	Tre	70	PS80	0
	22	100	Succ	15	6	Tre	70	PS80	0
	23	100	CP	15	6	Tre	70	PS20	0.5
	24	100	His	15	6	Tre	70	PS20	0.5
	25	100	Succ	15	6	Tre	70	PS20	0.5
Buffer Controls	26	0	CP	15	6	Tre	70	PS80	0.5
	27	0	His	15	6	Tre	70	PS80	0.5
	28	0	Succ	15	6	Tre	70	PS80	0.5
	29	0	CP	15	6	Tre	70	PS20	0.5
	30	0	His	15	6	Tre	70	PS20	0.5
	31	0	Succ	15	6	Tre	70	PS20	0.5

Table S2: Experimental design of sample set 2 of the formulation screening including antioxidative excipients.

	Sample ID	Protein Conc. [mg/ml]	Formulation buffer	Formulation buffer [mM]	pH	Stabilizer	Stabilizer [mg/ml]	Surfactant	Surfactant [mg/ml]	Met [mg/ml]	Arg [mg/ml]	Trp [mg/ml]	EDTA [mM]	DTPA [mM]
	1	100	WFI	n/a	6	Tre	70	PS 80	0.5	0	0	0	0	0
	2	100	CP	15	6	Tre	70	PS 80	0.5	0	0	0	0	0
	3	100	CP	15	6	Tre	70	PS 80	0.5	1.5	0	0	0	0
	4	100	CP	15	6	Tre	70	PS 80	0.5	0	10	0	0	0
	5	100	CP	15	6	Tre	70	PS 80	0.5	0	0	1.5	0	0
	6	100	CP	15	6	Tre	70	PS 80	0.5	0	0	0	0.8	0
	7	100	CP	15	6	Tre	70	PS 80	0.5	0	0	0	0	0.8
	8	100	CP	15	6	Tre	70	PS 80	0.5	1.5	0	0	0	0.8
	9	100	His	15	6	Tre	70	PS 80	0.5	0	0	0	0	0
	10	100	His	15	6	Tre	70	PS 80	0.5	1.5	0	0	0	0
Sample Set 2	11	100	His	15	6	Tre	70	PS 80	0.5	0	10	0	0	0
	12	100	His	15	6	Tre	70	PS 80	0.5	0	0	1.5	0	0
	13	100	His	15	6	Tre	70	PS 80	0.5	0	0	0	0.8	0
	14	100	His	15	6	Tre	70	PS 80	0.5	0	0	0	0	0.8
	15	100	His	15	6	Tre	70	PS 80	0.5	1.5	0	0	0	0.8
	16	100	Succ	15	6	Tre	70	PS 80	0.5	0	0	0	0	0
	17	100	Succ	15	6	Tre	70	PS 80	0.5	1.5	0	0	0	0
	18	100	Succ	15	6	Tre	70	PS 80	0.5	0	10	0	0	0
	19	100	Succ	15	6	Tre	70	PS 80	0.5	0	0	1.5	0	0
	20	100	Succ	15	6	Tre	70	PS 80	0.5	0	0	0	0.8	0
	21	100	Succ	15	6	Tre	70	PS 80	0.5	0	0	0	0	0.8
	22	100	Succ	15	6	Tre	70	PS 80	0.5	1.5	0	0	0	0.8

Table S3: Stock solutions.

Stock	Concentration
mAb1 (pH 5.0)	214 mg/ml
mAb1 (pH 6.0)	228 mg/ml
mAb1 (pH 7.0)	217 mg/ml
mAb2 (pH 5.0)	203 mg/ml
mAb2 (pH 6.0)	205 mg/ml
mAb2 (pH 7.0)	204 mg/ml
NIST mAb (pH 5.0)	202 mg/ml
NIST mAb (pH 6.0)	207 mg/ml
NIST mAb (pH 7.0)	211 mg/ml
Citrate phosphate buffer (pH 5.0, 6.0 & 7.0)	500 mM
Histidine buffer (pH 6.0)	250 mM
Succinate buffer (pH 6.0)	925 mM
Trehalose	500 mg/ml
Polysorbate 80	25 mg/ml
Polysorbate 20	20 mg/ml
Methionine	50 mg/ml
Tryptophan	7 mg/ml
Arginine	35 mg/ml
EDTA	10 mM
DTPA	10 mM

Table S4: Effect of protein concentration on Fc HC and Fd HC modifications after MCO

Metal Catalyzed Oxidation		mAb1			mAb2			NIST mAb		
		50 mg/ml	100 mg/ml	150 mg/ml	50 mg/ml	100 mg/ml	150 mg/ml	50 mg/ml	100 mg/ml	150 mg/ml
Δ Fc HC Mod.	CP pH 5.0	7.007	5.8	5.992	8.79	6.587	7.529	4.77	4.799	4.177
	CP pH 6.0	7.404	7.273	6.827	11.3	9.035	7.341	5.373	4.965	4.591
	CP pH 7.0	5.513	6.401	6.204	8.253	7.93	6.128	5.854	5.468	4.41
	His pH 6.0	7.873	5.016	5.446	11.383	8.966	8.009	5.192	5.865	4.04
	Succ pH 6.0	6.282	5.889	4.318	9.617	8.346	8.222	5.681	4.4	4.001
Δ Fd HC Mod.	CP pH 5.0	0	0	0	-0.123	-0.395	-0.072	3.472	3.24	2.576
	CP pH 6.0	0	0	0	-0.005	-0.081	-0.24	4.165	3.527	2.825
	CP pH 7.0	0	0	0	-0.125	-0.16	-0.297	4.066	3.369	3.1
	His pH 6.0	0	0	0	4.213	2.593	2.2	6.002	4.265	2.869
	Succ pH 6.0	0	0	0	0.545	0.538	0.384	3.911	3.235	3.721

Table S5: Effect of protein concentration on Fc HC and Fd HC modifications after VIS

Visible Light Exposure		mAb1			mAb2			NIST mAb		
		50 mg/ml	100 mg/ml	150 mg/ml	50 mg/ml	100 mg/ml	150 mg/ml	50 mg/ml	100 mg/ml	150 mg/ml
Δ Fc HC Mod.	CP pH 5.0	4.974	5.908	6.219	5.387	5.159	1.85	14.572	17.335	20.286
	CP pH 6.0	4.975	4.237	3.978	3.007	0.189	2.397	8.048	9.907	10.401
	CP pH 7.0	3.124	3.226	5.732	0.983	0.323	-0.218	6.423	6.507	6.654
	His pH 6.0	2.991	3.347	3.675	6.252	0.598	1.47	5.933	8.578	8.593
	Succ pH 6.0	3.439	4.39	3.923	6.342	2.755	0.997	9.39	12.721	11.405
Δ Fd HC Mod.	CP pH 5.0	0	0	0	0.297	0.326	0.368	6.911	8.494	9.632
	CP pH 6.0	0	0.708	0.782	0.631	0.387	0.538	5.503	7.07	8.801
	CP pH 7.0	0	0	0	1.048	0.945	1.005	6.376	9.061	9.372
	His pH 6.0	0	0	0.496	0.613	0.534	0.428	4.504	6.04	7.227
	Succ pH 6.0	0	0	0.58	0.258	0.434	0.402	7.307	7.229	9.669

VII. SUMMARY OF THE THESIS

Oxidation is a common degradation pathway for therapeutic antibody products, necessitating continuous monitoring and risk mitigation to ensure product efficacy and safety. As extensively reported in literature, oxidation can be triggered by various factors throughout a protein's lifecycle, ranging from oxidative contaminants during manufacturing to light exposure during administration. The consequences of oxidation are diverse and significantly depend on the individual susceptibility of the therapeutic antibody. During product development, oxidation susceptibility is assessed through forced oxidation studies. These studies provide valuable insights into potential oxidation liabilities and degradation pathways. However, due to limited material availability during early development stages, the experimental setup is often restricted to a few samples and does not include relevant formulation parameters of the final product. This limitation can result in a less comprehensive understanding of oxidation susceptibility, potentially leaving some oxidation liabilities undiscovered.

In this context, AbbVie's High Throughput (HT) formulation screening line provides an ideal platform for efficient oxidation stress testing. The established workflow combines parallel testing of multiple product-relevant stresses with high-throughput analytical methods, all within a miniaturized setup that requires minimal sample consumption. Building on this existing platform, the aim of this thesis was to develop an HTS-compatible oxidation screening workflow, ready for integration into the current framework.

Given the specific requirements of the HTS workflow, including automation, miniaturization, and platformability, the initial chapters (III & IV) focused on identifying optimal oxidation conditions to generate a detectable level of stress within a minimal time frame. To create a comprehensive data set, six different oxidation stress assays were selected and optimized: peroxide spiking (H_2O_2 and tBHP), free-radical induced oxidation via AAPH spiking, metal-catalyzed oxidation initiated by iron ion spiking, and exposure to light in the visible and UV-A range. Furthermore, an HTS-compatible oxidation quenching strategy was established, using an excess of methionine to stop oxidation at a defined time point, thereby ensuring comparability across different data sets by generating identical oxidation conditions.

For oxidation detection, LC-MS peptide mapping is still regarded as the gold standard. However, since a mass spectrometry setup is not integrated into the existing high-throughput screening (HTS) workflow, the set of analytical methods was further refined to ensure reliable detection of oxidative stress across large sample sets, maintaining comparability across different molecules. A high-throughput version of an analytical Protein A chromatography method was developed, allowing for the identification of oxidation in Fc-located methionine residues with a 15-minute runtime per sample. Additionally, a reversed-phase (RP) subunit analysis workflow was established, also suitable for hinge-mutated mAbs. This method enables the detection and localization of oxidation within an HTS framework, providing a valuable expansion to the existing method repertoire. The outcome of these initial method development chapters lay the groundwork for a comprehensive oxidation screening. They provide an extensive workflow that incorporates the most relevant causes of oxidation in therapeutic proteins and offer a combination of analytical methods that enable fast detection and subunit localization of oxidative stress.

In Chapter V, this workflow was used as a starting point to define an efficient oxidation profiling strategy. Five different antibodies in an unformulated state were tested to assess their individual oxidation susceptibility. The results demonstrated that, although some trends could be identified for most mAbs, the extent of susceptibility to different oxidation stresses was highly antibody dependent. Each combination of antibody, stress assay, and analytical technique produced a unique result pattern. These findings underline the importance of combining multiple stresses and analytical techniques to detect all potential liabilities of a product. While the present oxidation profiling workflow provided a comprehensive picture of oxidation liabilities across different mAbs, maintaining the efficiency and minimal sample consumption of the HTS platform requires keeping the workflow as streamlined as possible, including only the most relevant stresses and analytical methods. Based on the findings in Chapter V, the following were identified as the most effective screening strategy: spiking with H_2O_2, exposure to visible light, and simulated metal-catalyzed oxidation via iron ion spiking, combined with RP-UHPLC subunit analysis, Size Exclusion Chromatography, and intrinsic tryptophan fluorescence emission spectroscopy.

In the final chapter, a feasibility study was conducted to evaluate the suitability of the oxidation screening workflow within a formulation development context. The study aimed to identify potential formulation liabilities and explore possibilities to mitigate oxidation risks through formulation adjustments. The results indicated that the impact of formulation on oxidation susceptibility is highly stress dependent. Photooxidation was significantly influenced by formulation parameters such as concentration, formulation buffer, and pH. Although chemical oxidation stresses were less affected by formulation components, the

selection of formulation still impacted the level of degradation, depending on the individual susceptibility of the tested mAb, either positively or negatively. To simplify the evaluation process, a scoring tool was developed. This tool utilizes data normalization to allow comparability between stress factors and stability indicating attributes, enabling the ranking of potential formulation combinations and evaluating of their performance in mitigating oxidation at a glance. This data evaluation approach is particularly useful for identifying the most promising formulation compositions and selecting them for further in-depth analysis (e.g., LC-MS peptide mapping) to enhance the information gathered. Additionally, the screening workflow was employed to explore potential antioxidants as a means of mitigating oxidation. Once again, the outcomes were highly stress-dependent but could be efficiently evaluated within the oxidation screening workflow. This study demonstrated that the established workflow, combined with an HTS-suitable data evaluation approach (such as the scoring tool presented in this chapter), offers a time-efficient alternative to traditional methods (i.e. forced degradation studies with LC-MS read-out) for identifying formulation liabilities and possibilities.

In conclusion, this work successfully developed a high-throughput compatible oxidation screening workflow, ready for integration into the existing automation line and formulation development process. The final screening strategy includes stress testing for visible light, metal-catalyzed oxidation, and hydrogen peroxide-induced oxidation, thereby covering the most relevant oxidation risks for therapeutic antibodies. Detection of oxidation is achieved using high-throughput chromatographic techniques, allowing for efficient detection and localization with minimal sample preparation. Combined with the scoring and ranking tool for data evaluation, the workflow can generate a comprehensive picture of oxidation liabilities and formulation mitigation possibilities with minimal sample and time consumption. Due to its flexibility, the workflow can be adjusted based on prior knowledge and material availability, for example, by reducing the number of stress assays or expanding the stress setup as needed.

The flowchart below (Figure VII-1) illustrates the final workflow established in this study, detailing each process step and including all optional steps.

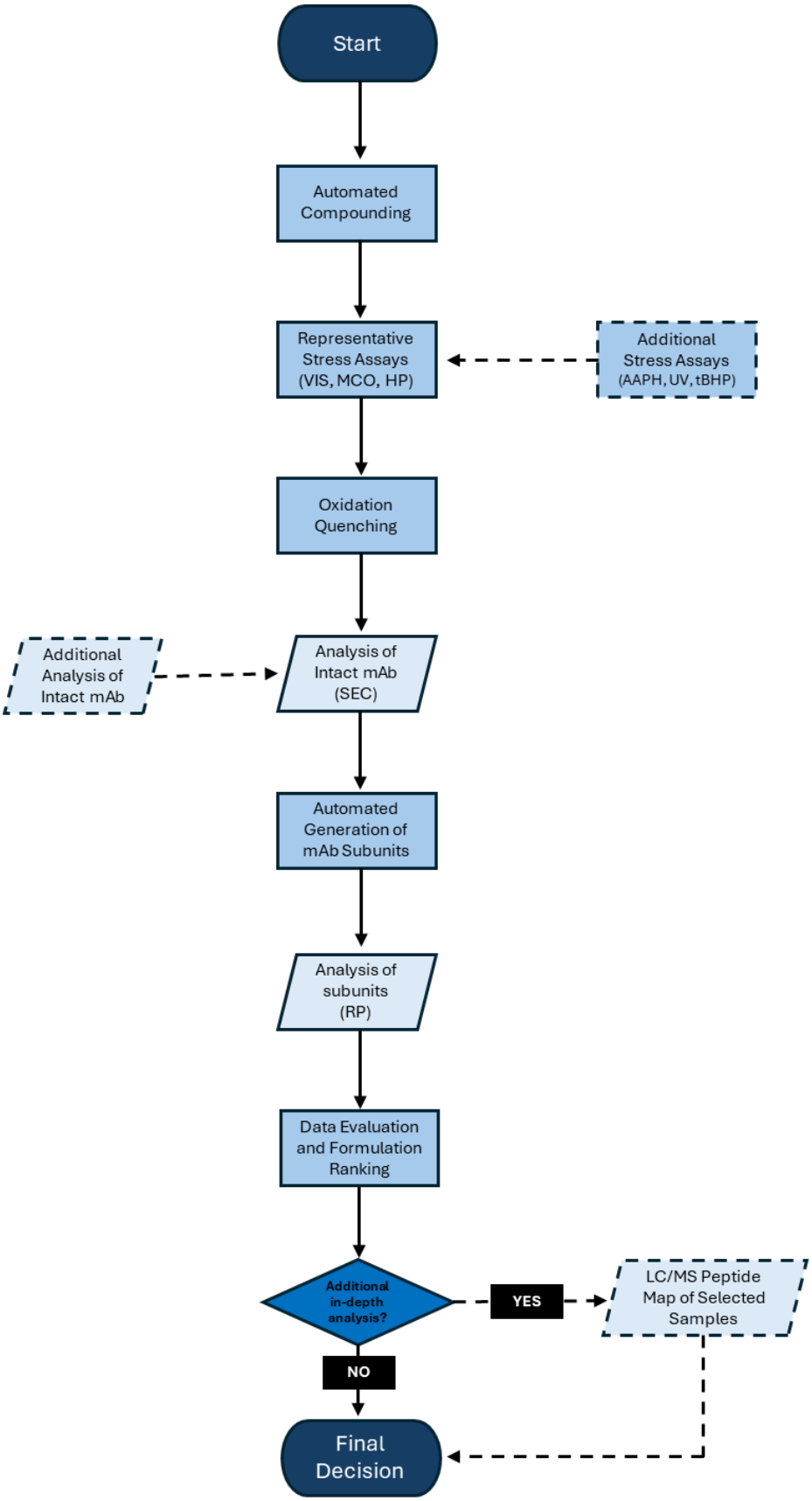

Figure VII-1: Flowchart of the final oxidation screening workflow. The figure shows each required process and analytical step (enclosed with solid lines) as well as optional steps for expanding the setup (enclosed with dotted lines).

As the market for biopharmaceutical products continues to develop and grow, it has to be noted that formulation development and stability evaluation are also becoming increasingly complex. In this context, the present screening workflow should be seen as a starting point for automated oxidation stress testing. Similar to all other HTS components, it should continuously evolve alongside development demands. Future improvements might include the ongoing development of analytical techniques that enhance the efficiency of degradation detection, or adjustments to the workflow to accommodate other molecule formats (e.g., antibody-drug conjugates) and formulation presentations (e.g., high-concentration formulations).

Overall, whether used as a stand-alone approach or integrated into a stability screening platform, the workflow established in this study, along with any future extensions and improvements, can actively support candidate selection and formulation development across various stages of biopharmaceutical development.